

Sheffield Hallam University

The investigation of some novel polysiloxane liquid crystal systems.

FOSTER, Kevin Anthony.

Available from the Sheffield Hallam University Research Archive (SHURA) at:

<http://shura.shu.ac.uk/19658/>

A Sheffield Hallam University thesis

This thesis is protected by copyright which belongs to the author.

The content must not be changed in any way or sold commercially in any format or medium without the formal permission of the author.

When referring to this work, full bibliographic details including the author, title, awarding institution and date of the thesis must be given.

Please visit <http://shura.shu.ac.uk/19658/> and <http://shura.shu.ac.uk/information.html> for further details about copyright and re-use permissions.

SHEFFIELD HALLAM UNIVERSITY LIBRARY
CITY CAMPUS POND STREET
SHEFFIELD S1 1WB

101 536 540 X



Bm 369332

Sheffield Hallam University

REFERENCE ONLY

ProQuest Number: 10694539

All rights reserved

INFORMATION TO ALL USERS

The quality of this reproduction is dependent upon the quality of the copy submitted.

In the unlikely event that the author did not send a complete manuscript and there are missing pages, these will be noted. Also, if material had to be removed, a note will indicate the deletion.



ProQuest 10694539

Published by ProQuest LLC (2017). Copyright of the Dissertation is held by the Author.

All rights reserved.

This work is protected against unauthorized copying under Title 17, United States Code
Microform Edition © ProQuest LLC.

ProQuest LLC.
789 East Eisenhower Parkway
P.O. Box 1346
Ann Arbor, MI 48106 – 1346

The Investigation of some Novel Polysiloxane

Liquid Crystal Systems

Kevin Anthony Foster

A thesis submitted in partial fulfilment

of the requirements of

Sheffield Hallam University

for the Degree of

Master of Philosophy

March 1997

Sheffield Hallam University

in collaboration with

DRA, Malvern

Acknowledgements.

I would like to thank Dr. D.G McDonnell of DRA, Malvern for his co-operation and input on this project, Dr. D.Simmonds and Dr. S. Spells for their technical help and guidance.

Abstract.

A range of liquid crystal units based on mainly phenyl benzoate esters have been synthesised and characterised. These have been attached to polysiloxane systems to form ring, linear and elastomeric polymer liquid crystals. The effect of system purity on the phase transitions of the ring materials was found to be crucial, and this has resulted in a phase diagram for a 'doped' ring system where the doped material exhibits liquid crystalline behaviour while the pure material does not. Properties of linear material were found generally to be consistent with data in the literature. Extremely low glass transition temperatures were not observed even though pure poly(hydrogenmethylsiloxane) is considerably more flexible than its hydrocarbon equivalent. Effects of degree of polymerisation and spacer length were as expected. Linear polymers were cross-linked to produce equivalent elastomeric materials. We have characterised a range of these systems and investigated the effect of deformation on the LC order within the elastomers through the use of FTIR. Phase transitions for the cross-linked systems were generally slightly lower than the analogous linear materials which is in agreement with data found in the literature. Partial substitution by cyano-terminated molecules enabled us to determine the peak ratios of Si-H/CN stretching frequencies on deformation. Small enhancements, approx 7%, of LC order parallel to the direction of stretching were observed. In addition, a novel 'ring' elastomer incorporating liquid crystal units has been produced. Cyclic materials were substituted with liquid crystal units and cross-

linked to yield elastomers with 25% and 37% mesogen density. Although elastomers were produced, no liquid crystal behaviour was observed. Glass transition temperatures in the region of $-100\text{ }^{\circ}\text{C}$ were observed. It is believed that by increasing mesogen density in these materials, elastomers with extremely low glass transition temperatures and liquid crystal properties could be achieved.

| | Contents | Page No. |
|--------|---|----------|
| 1 | Introduction. | 2 |
| 1.1.1. | The nematic state. | 4 |
| 1.1.2. | Chiral nematic phases. | 6 |
| 1.1.3. | Smectic phases | 8 |
| 1.1.4. | General transition order. | 11 |
| 1.1.5. | Non symmetric molecules. | 11 |
| 1.1.6 | Order parameter | 14 |
| 1.1.7. | Disc molecules. | 15 |
| 1.2. | Polymer liquid crystals. | 16 |
| 1.2.1 | Classification. | 16 |
| 1.2.2. | Side chain polymers. | 17 |
| 1.2.3. | The spacer concept. | 18 |
| 1.3. | Molecular engineering of polysiloxane liquid crystals. | 20 |
| 1.3.1. | Polysiloxanes : Structural types. | 20 |
| 1.3.2. | Structural types of polysiloxane liquid crystals. | 21 |
| 1.3.3. | Influence of molecular mass on phase behaviour. | 22 |
| 1.3.4. | Influence of spacer length on phase transitions. | 25 |

| | | |
|--------|--|----|
| 1.3.5. | Influence of mesogen length. | 27 |
| 1.3.6. | Influence of constitutional isomerism on phase transitions. | 28 |
| 1.3.7. | Influence of lateral placement of mesogens | 31 |
| 1.3.8. | Influence of dilution of side groups on phase behaviour. | 32 |
| 1.4. | Electro-optical effects in side chain polymers. | 35 |
| 1.5. | Cyclic polymers containing rod shaped mesogens. | 36 |
| 1.6. | Elastomers. | 39 |
| 1.6.1. | Rubber elasticity. | 39 |
| 1.6.2. | Polysiloxane liquid crystal elastomers. | 42 |
| 1.6.3. | Mechanical behaviour. | 44 |
| 1.6.4. | Director orientation by mechanical deformation. | 45 |
| 1.7. | Potential for liquid crystal polysiloxanes. | 48 |
| 2 | Strategy for synthesis. | 51 |
| 2.1 | Mechanistic aspects of polysiloxane | 51 |

| | | |
|----------|---|----|
| 2.1.1 | Preparation of linear poly(hydrogen methylsiloxane) | 51 |
| 2.1.2 | Coupling of mesogens to polymer backbone. | 53 |
| 2.3. | Characterisation of liquid crystal phases. | 57 |
| 2.3.1. | Optical microscopy. | 57 |
| 2.3.2. | Differential scanning calorimetry. | 60 |
| 2.4. | Synthesis. | 62 |
| 2.4.1. | Characterisation Techniques. | 62 |
| 2.4.2. | Stock reagents. | 62 |
| 2.4.2.1. | Tetrahydrofuran (THF). | 62 |
| 2.4.2.2. | Dichloromethane (DCM). | 63 |
| 2.4.3. | Target mesogen structures. | 63 |
| 2.4.4. | General procedure for the synthesis of p-alkenoxybenzoic acids p-hydroxybenzoic acid | 65 |
| 2.4.5. | General procedure for the synthesis of cyano-terminated mesogens. | 67 |
| 2.4.6. | Synthesis of p-methoxyphenyl-1,4- | 69 |

| | | |
|---------|--|----|
| | hydroxybenzoate. | |
| 2.4.7. | General procedure for the synthesis of methoxy-terminated mesogens. | 71 |
| 2.4.8. | Synthesis of 10-Undecenoyl chloride. | 73 |
| 2.4.9. | Synthesis of mesogens based on 10-Undecenoyl chloride. | 74 |
| 2.4.10. | Synthesis of cyano and methyl ester terminated mesogens. | 76 |
| 2.4.11. | Preparation of catalyst for polysiloxane synthesis. | 78 |
| 2.4.12. | Synthesis of divinyl terminated polysiloxanes. | 79 |
| 2.4.13. | Synthesis of poly(hydrogenmethyl- siloxanes). | 80 |
| 2.4.14. | Synthesis of ring systems. | 82 |
| 2.4.15. | Synthesis of linear polysiloxane liquid crystals. | 84 |
| 2.4.16. | Synthesis of polysiloxane elastomers. | 84 |
| 2.4.17. | Synthesis of ring elastomers. | 87 |
| 3. | Cyclic and linear systems. | 89 |
| 3.0 | Observations on cyclic and linear | 90 |

| | | |
|--------|--|-----|
| | systems. | |
| 3.1. | Cyclic polysiloxane systems. | 90 |
| 3.2. | Linear polysiloxane liquid crystals. | 105 |
| 4. | Observations on elastomeric material. | 118 |
| 4.1. | Polysiloxane elastomers. | 118 |
| 4.1.1. | Elastomers incorporating short spacers. | 126 |
| 4.1.2. | Effect of cross linking density on phase transitions. | 128 |
| 4.1.3. | Elastomers incorporating long spacers. | 130 |
| 4.2. | Novel networks. | 136 |
| 5. | Observations on deformation of elastomers. | 143 |
| 5.1. | Orientation by mechanical deformation. | 143 |
| 5.2. | Effects of heating undrawn samples. | 145 |
| 5.3. | Effect of stretching at constant temperature. | 145 |
| 5.4. | Absorbance measurements. | 146 |
| 5.5. | Partially substituted polysiloxanes. | 149 |

| | | |
|------|-----------------------------------|-----|
| 5.6. | Observations on sample thickness. | 154 |
| 6. | Summary. | 158 |
| 7. | References. | 163 |

1.Introduction

The first liquid crystalline observations are largely credited to Reinitzer (1) and Lehmann (2). In 1888 Reinitzer observed two apparent melting points for cholesteryl benzoate, 145°C and 179°C. Further work by Lehmann led to a publication in which he termed this material a 'liquid crystal', as between the two 'melting points' the material possessed low rigidity of fluidity (a liquid like property) and also optical anisotropy (a crystal like property). It is worth noting at this point that a similar class of compounds termed plastic crystals also exists. These materials are classed by their exhibition of positional order while the orientational order has disappeared or is strongly reduced. Conversely a liquid crystal is characterised by a degree(s) of orientational order while the positional order is reduced or completely absent. Today liquid crystals or mesophases are accepted as one of the five states of matter which occupy a position between ordered solids and isotropic (or random) liquids. As a consequence we might expect mesophases to exhibit properties characteristic of both. Molecules or atoms within crystalline solids exhibit long range 3D positional and orientational order with little mobility. In the liquid state there is no long range structure, but there is some short range structure with rapid molecular motion and mobility. In general, mesophases

contain a degree of fluidity coupled with long range orientational order (3). Liquid crystals can be further subclassified into thermotropic and lyotropic materials. In the former the term thermotropic arises since transitions result from changes in temperature. For traditional low molecular mass (LMM) liquid crystals length to breadth ratios of 4-8 and relative molecular masses of 200-500 are observed. Lyotropic behaviour is brought about by sufficiently high concentration solutions of rod-like molecules in an isotropic solvent. In lyotropic systems the 'rods' are typically larger than for thermotropic ones. Axial ratios greater than 15 are rarely found. So far we have seen that for a compound to exhibit a traditional low molar mass liquid crystal phase we require it to have a basic rod shape. In fact, liquid crystal phases are possible with polymers and disc-like molecules. These will be discussed later. By studying many compounds that exhibit liquid crystalline behaviour, two basic requirements for mesomorphic behaviour can be formulated (4):

(1) The compounds should have an anisotropic elongated form, as reflected in their length/width ratio.

(2) The compounds should have a relatively rigid polarisable part. Using these studies it is possible to deduce a set of building blocks that can be used to assemble a liquid crystal structure.

SUBSTITUENT-[-AROMATIC--LINKAGE-]_n-AROMATIC--SUBSTITUENT

The requirement for rigidity is met by choosing groups that contain multiple bonds for the linking units. Such units also have the advantage that they are capable of conjugating with the aromatic systems and can maintain the polarisability and birefringent properties of the molecules. Substituent units are generally used to tailor the molecule's phase type and behaviour. Here we may use anything from cyano units, which will provide a high induced dipole, through electronegativity effects, along the molecular axis, to alkyl units which can, if sufficiently long, disrupt the packing of the molecules due to many available statistical conformations. Structure/property relationships will be discussed more fully later.

1.1.1 The nematic state. (Fig 1) (5)

The simplest LC state is the nematic state in which the molecules are aligned with their molecular axes roughly parallel, this direction being defined locally as the director, \underline{n} . There is no correlation between the centres of gravities of the molecules and the molecules can flow easily over one another, so that the viscosities are of the same order of magnitude as the isotropic phase. For nearly all the known molecules that exhibit nematic phases, the nematic phase is uniaxial. That is, there exists rotational symmetry around the director. This axis has no polarity even though the constituent molecules may exhibit polarity.

Hence \underline{n} and $-\underline{n}$ are equivalent. A transition from isotropic to nematic involves a first order phase transition for which the enthalpy change, ΔH , and density change, $\Delta \rho$, can be measured. Thermodynamic theory (6) tells us that the entropy change, ΔS , can be calculated from the enthalpy change using the formula;

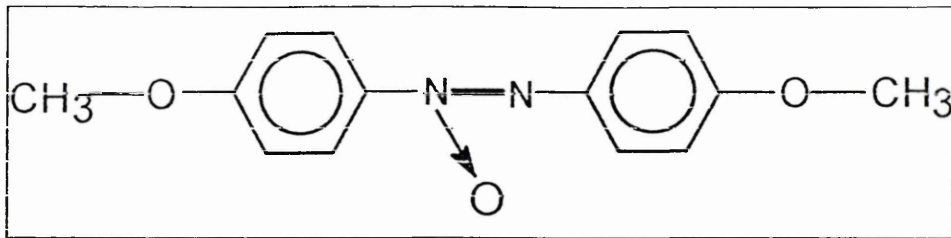
$$\Delta G = \Delta H - T \Delta S$$

where ΔG is the Gibbs free energy, which is zero at the transition, and T is the temperature. Hence the entropy change is given by;

$$\Delta S = \Delta H/T$$

Typically, values of between 0 and $10 \text{ J K}^{-1} \text{ mole}^{-1}$ are observed for nematic systems passing through the nematic to isotropic transition. Typically, organic materials that exhibit solid to liquid transitions have entropy changes around $100 \text{ J K}^{-1} \text{ mole}^{-1}$. Therefore the nematic phase contains only a small amount of order.

Fig 1. A typical nematic molecule



K 118 N 135.5 I

The notation above describes the phase behaviour the system exhibits on heating from the crystalline phase. Hence K 118 N represents the temperature at which the molecules pass from the crystalline phase to the nematic phase while N 135.5 I represents the temperature at which the system passes from the nematic phase to the isotropic phase. The superscript of * is used to indicate a chiral nematic phase. Other notations include S to represent smectic phases. A subscript is used to indicate the type, i.e. S_A represents a smectic A phase (these are described fully later). Temperatures are in $^{\circ}\text{C}$ unless otherwise stated.

1.1.2. Chiral Nematic phases.

These are a twisted version of the nematic phase due to the presence of chiral centres. A helical structure is observed within the phase which is

characterised by a pitch, P . As in optically active organic molecules, the pitch can be positive or negative depending on the sign of the chiral centre, i.e. if the chiral centre generates a clockwise rotation then the sign will be positive. If the pitch is in the region of the wavelength for visible light, then these materials will exhibit colours which may change with temperature due to a change in pitch (thermochromicity). Mixtures of materials with opposite chirality can result in a simple nematic compound where the pitch effectively becomes infinite. Nematic and chiral nematic materials are completely miscible and the addition of a small amount of an optically active compound changes a nematic phase into a chiral nematic phase.

Fig 2. A typical chiral nematic molecule.

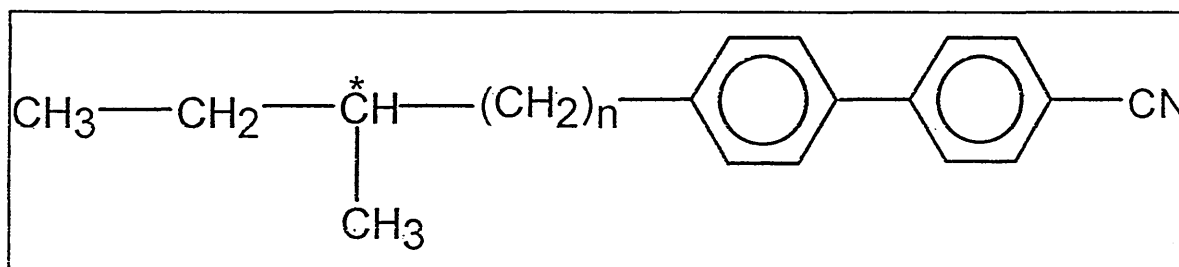
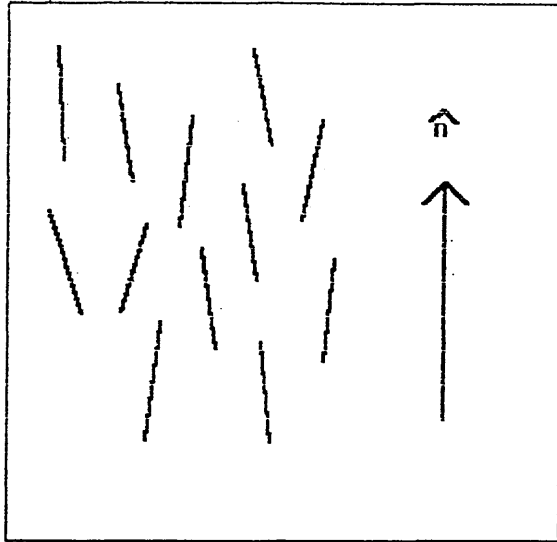
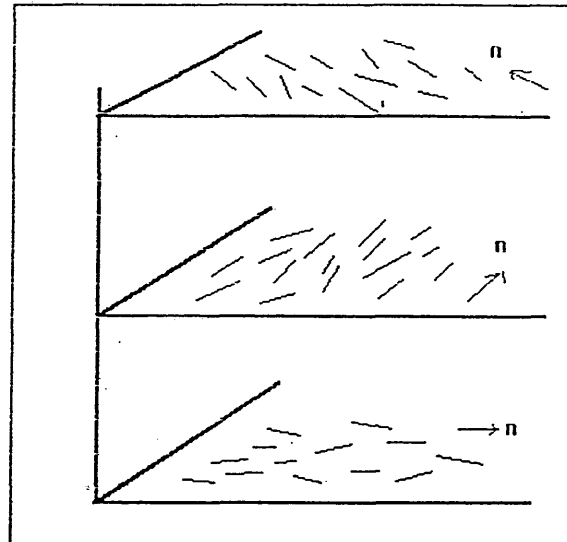


Fig 3. Nematic / Chiral nematic structures.



(a) Nematic



(b) Chiral nematic

1.1.3. Smectic phases.

More ordered mesophases, such as smectic mesophases, have an additional degree of order in that the molecules are also arranged in layers. Therefore, as well as the one dimensional orientational order present in nematics there is also a one dimensional density wave (7). The molecular centres are, on average, arranged in equidistant planes, leading to what is loosely called a layer structure. The simplest, smectic A, has no order within the layers so that there is no correlation between molecular axes other than the roughly parallel arrangement of the molecular axis. The layer thickness approximates, to within

5%, to the molecular length, the variations arising from fluctuations in the order or conformational changes in alkyl substituents. As in nematics, \underline{n} and $-\underline{n}$ are still equivalent. In simple terms the smectic C is a tilted version of the smectic A. However, the distinguishing feature is the optical biaxiality of the system. Further order is possible, so that for example, the smectic B phase adopts hexagonal clusters within the layers. Although these clusters possess a lattice like structure, the fluid character of the layers ensures that the distance between the centres of the clusters is not related to the lattice spacing. Thus we have a long range order of the orientation of clusters due to bond orientation order with positional order within the layers.

Fig 4. Typical Smectic A and B Molecules.

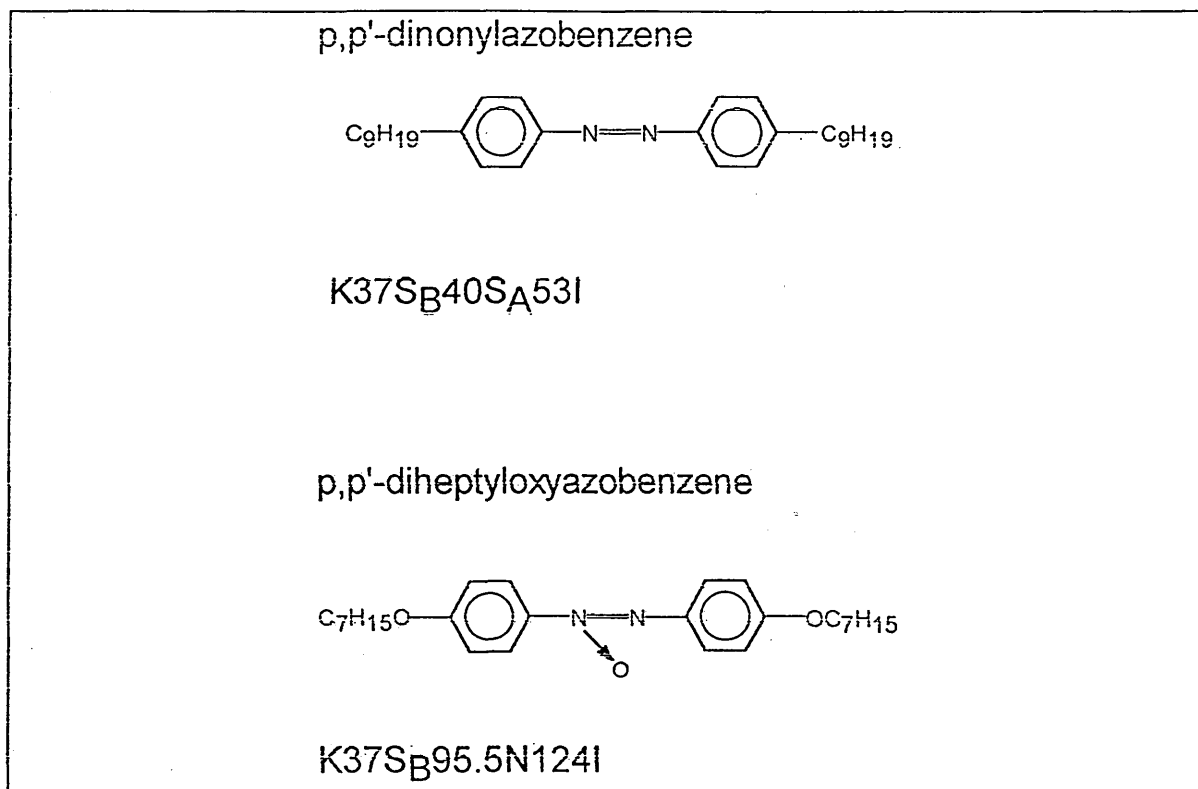
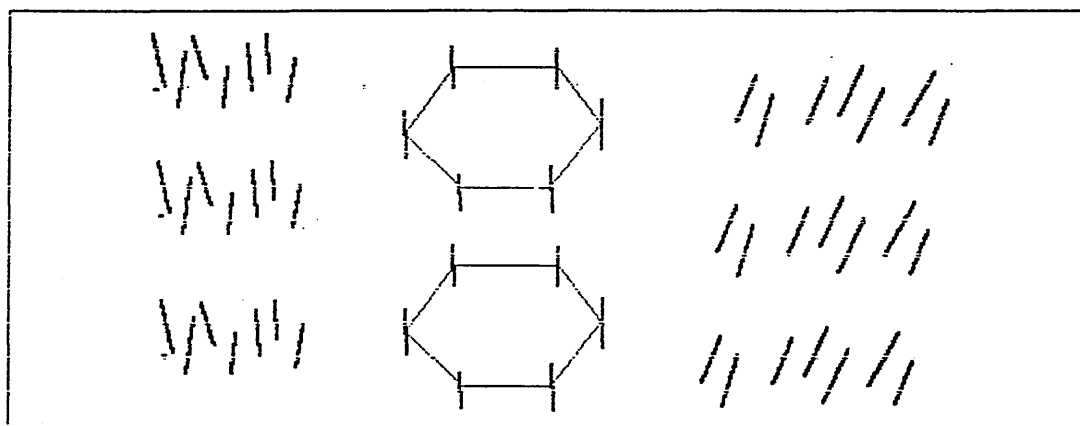


Fig 5. Smectic A, B and C structures.



Smectic A

Smectic B

Smectic C

1.1.4. General transition order.

Many molecules are found to exhibit a number of different liquid crystal states and comparison of these has led to a general order of the phase transitions observable during cooling in thermotropic liquid crystals.

ISO-LIQ, NEMATIC, SMECTIC A,C,HEX B,I,CRYST B,F,J,G,E,K,H

High temperature

Low temperature

1.1.5. Non symmetric molecules.

When the molecules possess a dipole moment it becomes possible to distinguish between the head and tail. Para cyano-substituted molecules, to be distinguished from ortho and meta types (see below) are an example for which a variety of smectic A phases have been observed. In such systems a number of orientations are possible. Firstly the molecules can minimise their dipolar interaction by an antiparallel dipole arrangement (Fig 7).

Fig 6. Arrangement of Ortho, Meta and Para substituents.

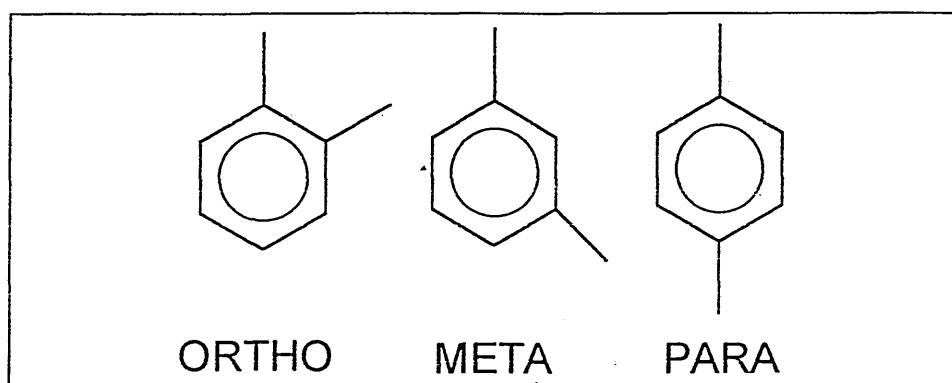
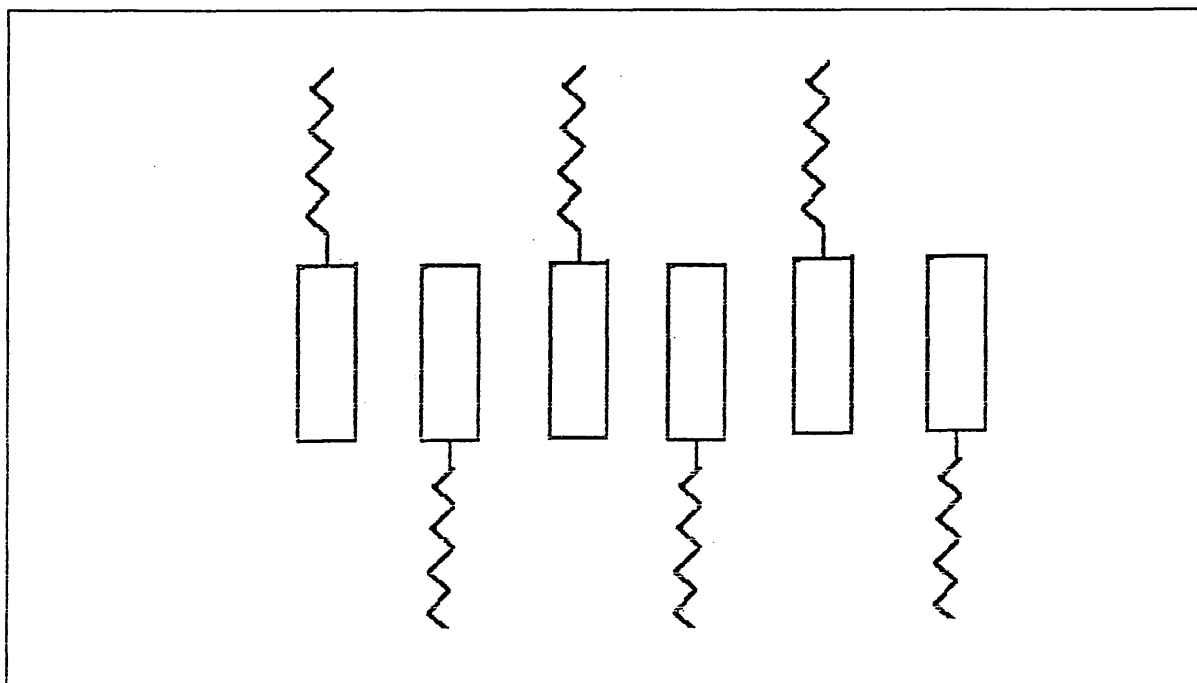
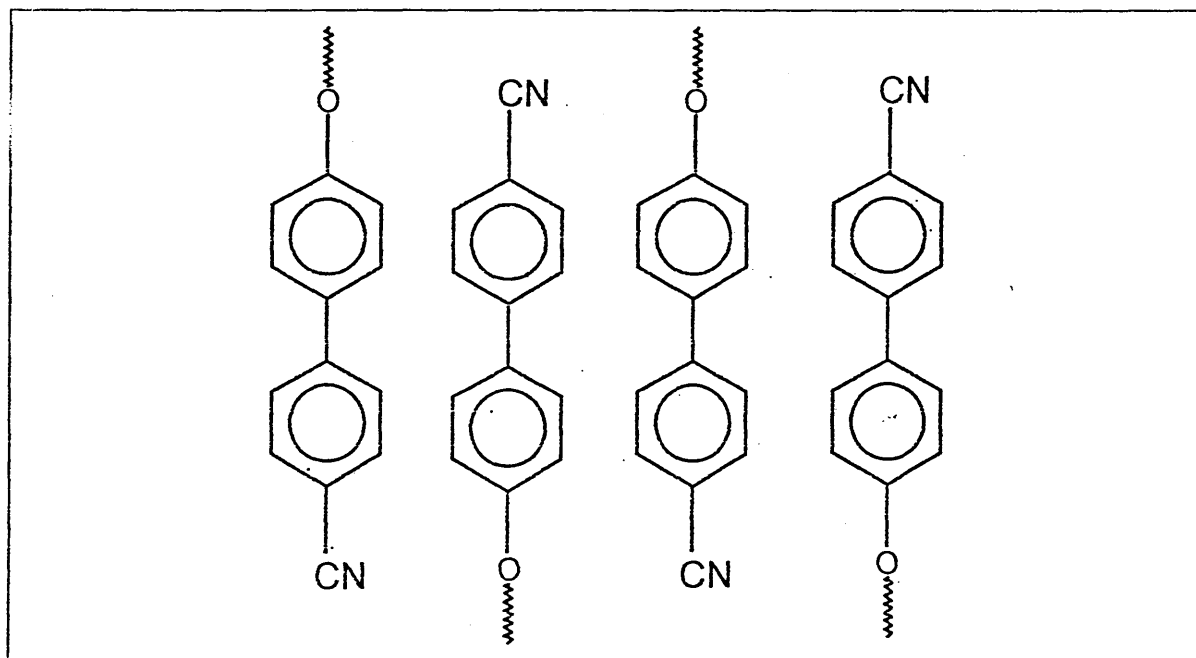


Fig 7. Antiparallel arrangement of mesogens.



As a result the layer thickness is now given by $d=a+2b$ where a is the length of the aromatic head and b is the length of the aliphatic chain. This type of interaction may be the origin of the 're-entrant nematic' phase (8).

Fig. 8. Antiparallel dipole correlation of CN terminated molecules.



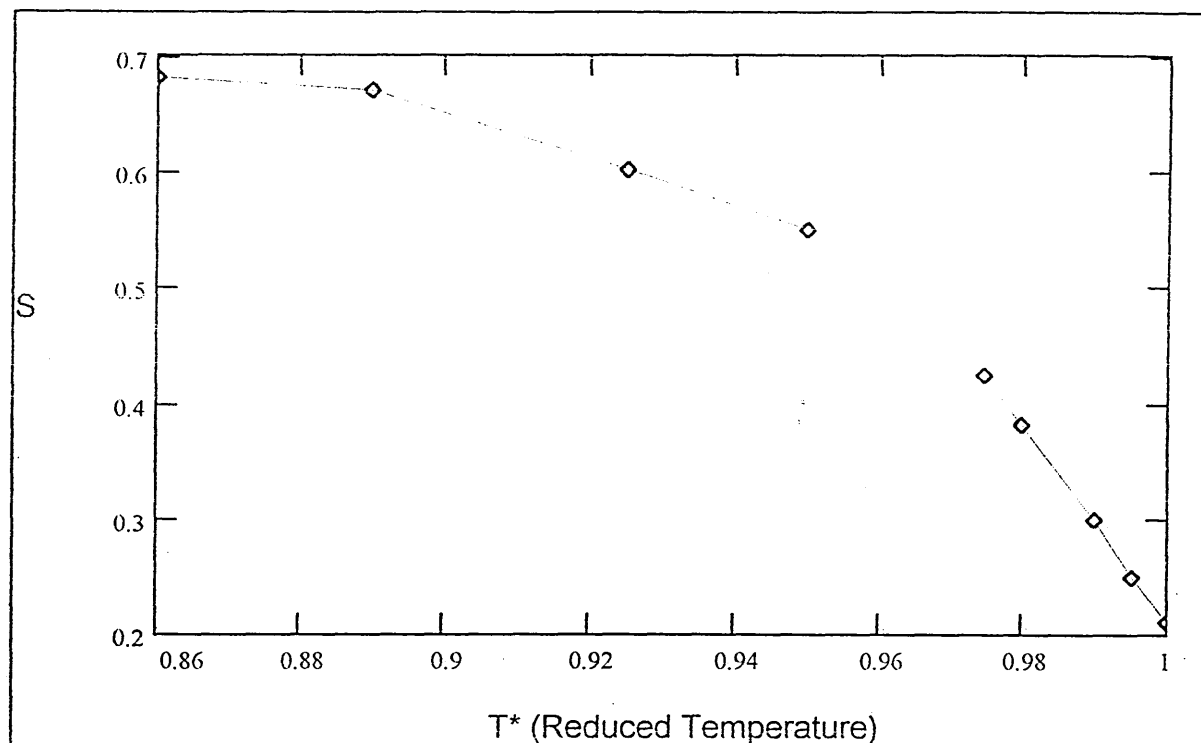
1.1.6. Order parameter.

A simple order parameter, S , describes the average orientational ordering of the molecules;

$$S = 0.5 \langle 3\cos^2 \theta - 1 \rangle$$

where θ is the angle a molecule makes with the director, \underline{n} , and S is the result of averaging over the macroscopic system. When a molecule can assume any angle relative to its neighbouring molecules with equal probability then the result of the above equation is zero and this represents the isotropic system. When all molecules are aligned exactly parallel then θ has a value of zero for all molecules and the result for the above equation is one. As a rule, liquid crystals have order parameters between 0.2 and 0.8. (9)

Fig 9. Typical order parameter diagram.



T^* is the actual temperature divided by the clearing temperature.

1.1.7. Disc molecules.

Molecules, such as those containing fused benzene rings, which are relatively flat and disc shaped, have been shown to exhibit mesophase behaviour (10,11,12). These materials also exhibit a variety of phases and form a new class of thermotropic liquid crystals. The thermotropic sequence of such systems is given below.

$$D_{hd}, D_{ho}, D_{rd}, D_t, N_D, N_D^*$$

Low temperature

High temperature

The simplest arrangement is the N_D or nematic-like arrangement of discs. In this phase all the discs are roughly in parallel planes but there is no correlation between the position of individual discs. Other phases involve the discs stacking in columns.

1.2. Polymer liquid crystals.

By analogy to low molar mass liquid crystals, these can be divided into thermotropic and lyotropic systems. The most extensively studied lyotropic polymer is poly- γ -benzyl-L-glutamate (13,14). However, we are primarily interested in thermotropic systems, in particular polysiloxanes.

1.2.1 Classification.

Polymeric liquid crystals can be subclassified into a number of divisions.

(1) Side chain liquid crystal polymers.

Here the liquid crystal behaviour is a result of liquid crystal units attached to a polymer backbone.

(2) Main chain liquid crystal polymers.

Here the liquid crystal behaviour is a result of LC monomers linked to form polymer chains. (15,16,17)

(3) Ring polymers.

Analogous to side chain systems. Here the chain terminals are connected to form a ring and the liquid crystal units are linked onto the side. Here we might expect to observe discotic phases so long as the system retains its rigidity.

(4) Cross linked systems.

Can be side or main chain systems that are connected by cross-linking units. Here we form a network and possibly an elastomeric liquid crystal system.

We have been interested in side chain polymers, particularly rings, linear polymers and cross-linked systems.

1.2.2. Side chain polymers.

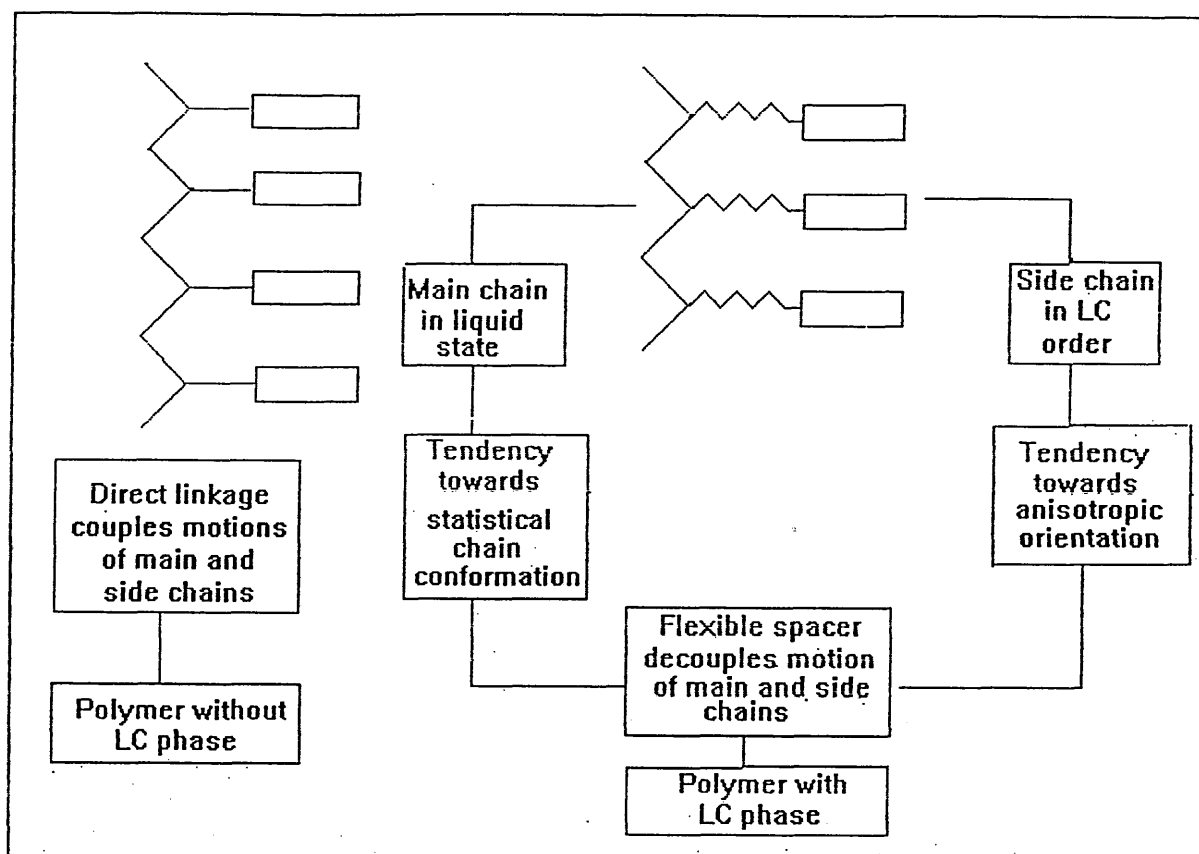
The idea of ordered polymer liquid crystal systems does not sit easily with traditional theories of polymers and liquid crystals. Polymer entropy is antagonistic to nematic order and a flexible polymer is expelled from a nematic solvent. Direct polymerisation of liquid crystal monomers into polymers is possible but not very successful. Blumstein (18) and Shibaev and Plate (19) provide reviews on this kind of work up to 1978. It is possible to polymerise monomers which exist in a well defined liquid crystal state. However, the resulting polymer loses the initial liquid crystal state. From nematic monomers, polymers result which exhibit either highly ordered smectic phases or a glassy

state at temperatures below those used for polymerisation. These polymers were either amorphous or showed a 'locked in' or 'memory effect' liquid crystal state which was permanently lost on heating above the phase transition temperature. Space filling models of such systems indicate that the result of such a polymerisation is a polymer which has a rigid main chain, thus explaining the high glass transition temperatures. Since nematic phases rely on a statistical distribution of centres of gravity of mesogens, which is not possible under these conditions, only amorphous or smectic phases are observed.

1.2.3. The spacer concept.

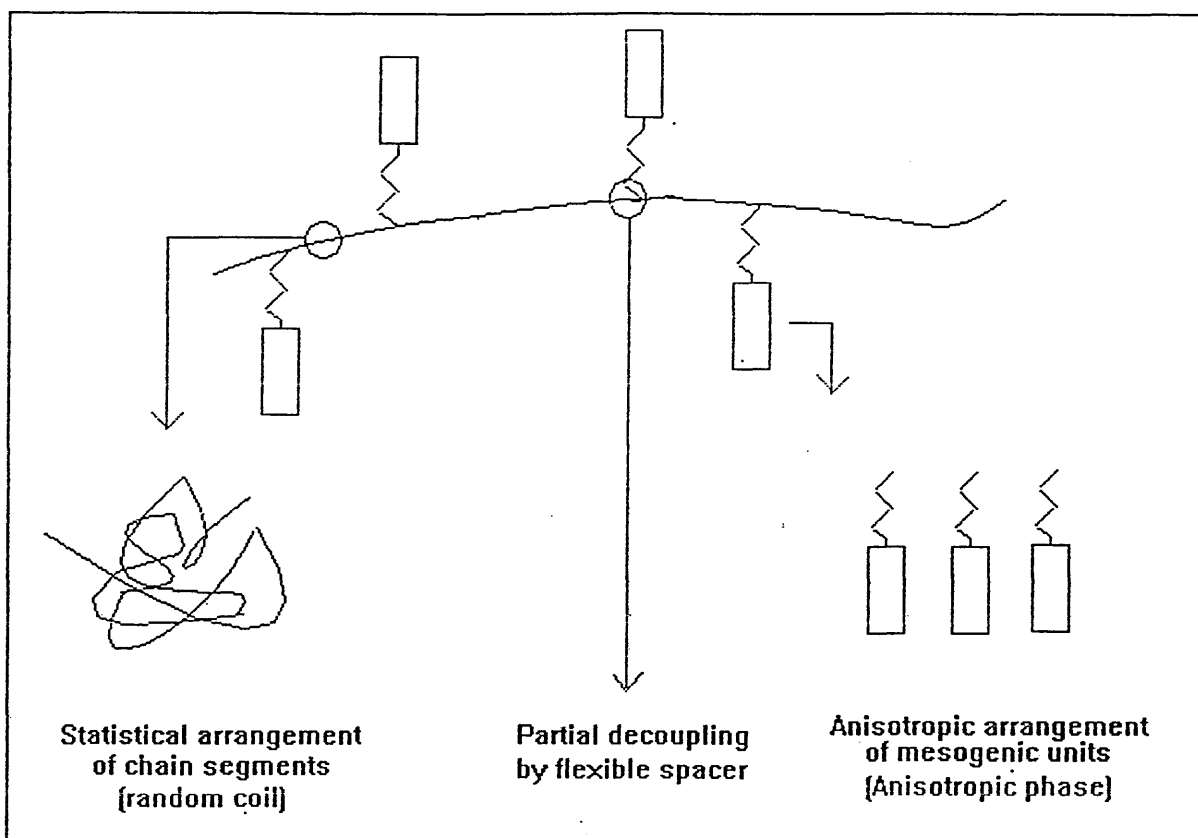
To balance the competition between the backbone random coil configuration and anisotropic side group alignment, Ringsdorf et al (117) proposed that the motions of the polymer main chain must be decoupled from the motions of the mesogenic side groups. This can be achieved via a flexible spacer. Using this approach, models predict that the side groups should be able to adopt ordered conformations even when the backbone adopts a random coil configuration. This approach assumes that the motions of the backbone and mesogenic side groups are completely independent and therefore the nature of the backbone should have no effect on the thermal stability or type of mesophase formed (see Fig.10). However, the nature of the backbone does affect the mesomorphic behaviour (20). This will be discussed more fully later.

Fig 10. Decoupling of mesogens and backbone.



We find that at least part of the spacer is anisotropically orientated together with the mesogen. Using the spacer concept a wide range of side chain LCPs have been synthesised and it is now accepted that only a partial decoupling of the mesogen and chain motions is achieved (see Fig. 11).

Fig 11. Partial decoupling by flexible spacers.



1.3. Molecular engineering of Polysiloxane liquid crystals.

1.3.1. Polysiloxanes : Structural types.

Achievement of good ordering of side chain liquid crystals is affected by the flexibility of the polymer backbone. In this respect polysiloxanes are promising because of the high flexibility of a backbone of alternating oxygen and silicon atoms. While it is true that the Si-O bond strength of 452 kJ mol^{-1} is high, compared to say that of Si-Si at 226 kJ mol^{-1} (21), thus giving good thermal stability, the rotational energy of the bond is low. Coupled with the wide

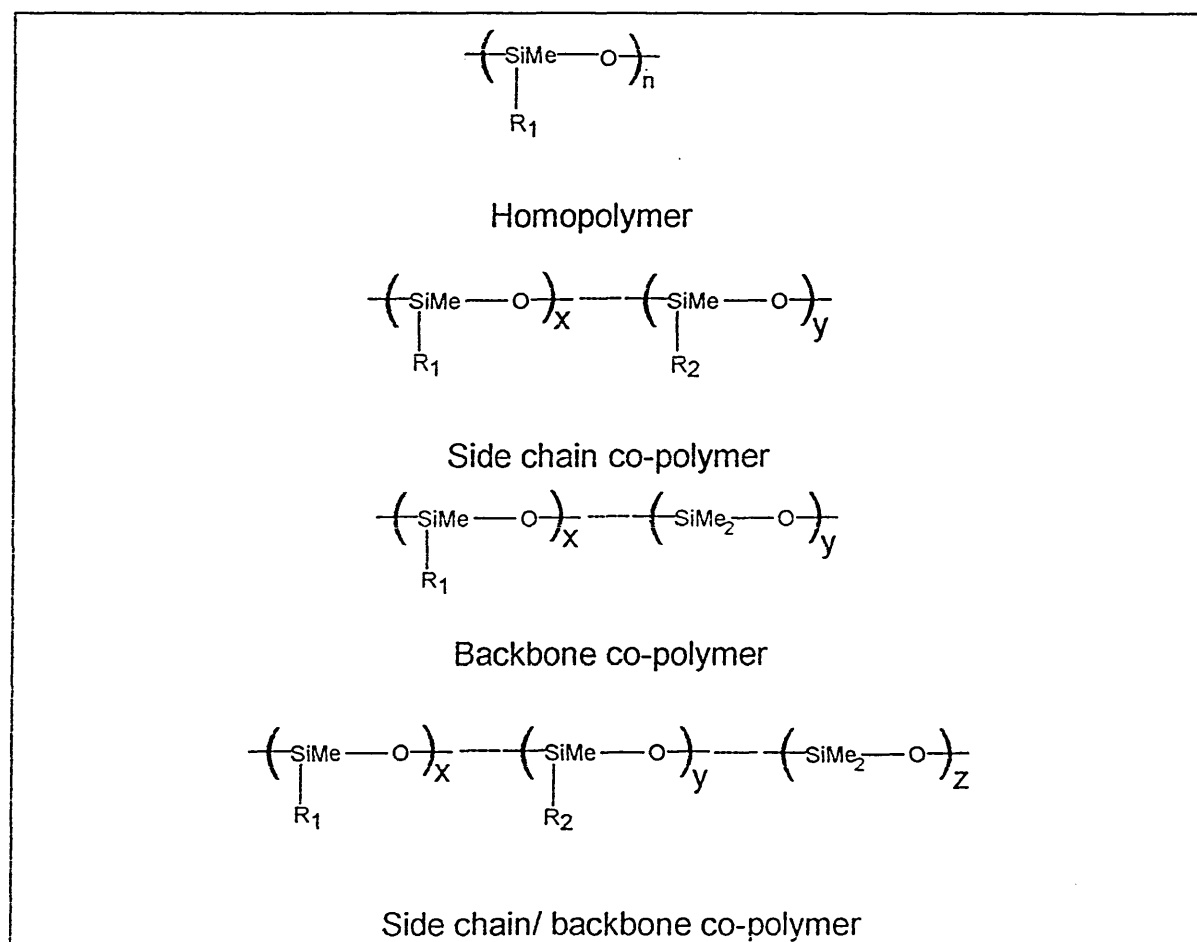
variations in the Si-O-Si bond angle, this results in low glass transition temperatures, i.e. pure poly(dimethylsiloxane) has a T_g of -127°C . Furthermore, rotational changes along the backbone are relatively easy and this should help the decoupling of the mesogens from the backbone (22).

1.3.2. Structural types of polysiloxane liquid crystals.

A number of structural types are possible. These are outlined in Fig.12 below.

Typical chain lengths are in the range 30 to 120.

Fig 12. Structural types of polysiloxane.



1.3.3. Influence of molecular mass on phase behaviour.

Initial work in this field suffered from the fact that many research groups did not publish polymer molecular mass data with the phase data. The fact that polymer molecular mass had an effect on phase transitions was not appreciated. Stevens et al (23) studied the effect using fractionated polysiloxanes. The data is shown in Fig. 13.

Fig 13. Influence of molecular mass on phase behaviour.

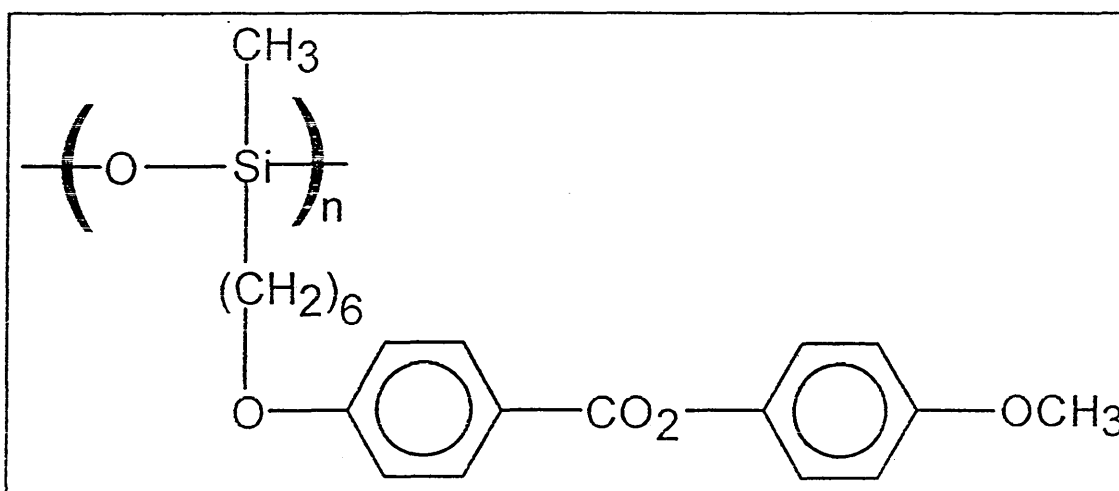
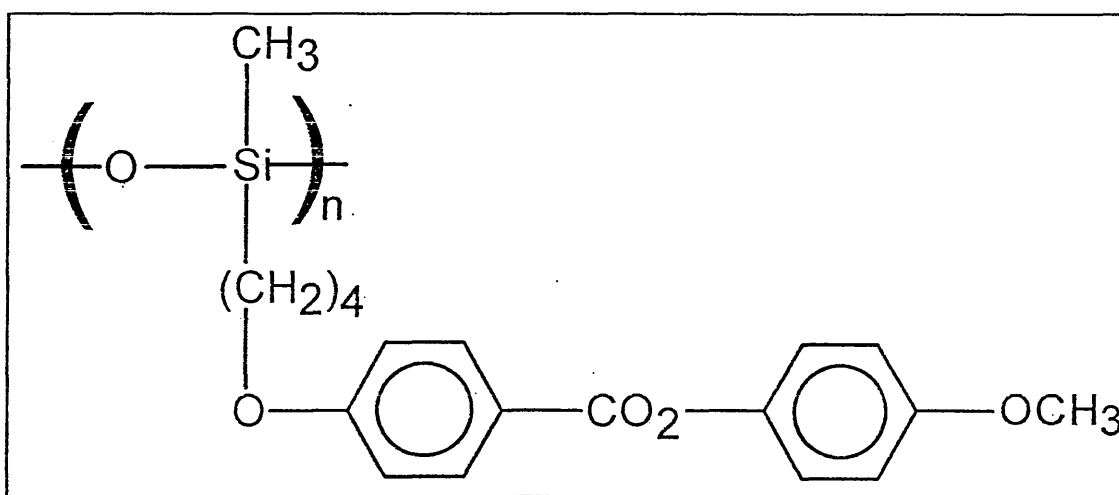
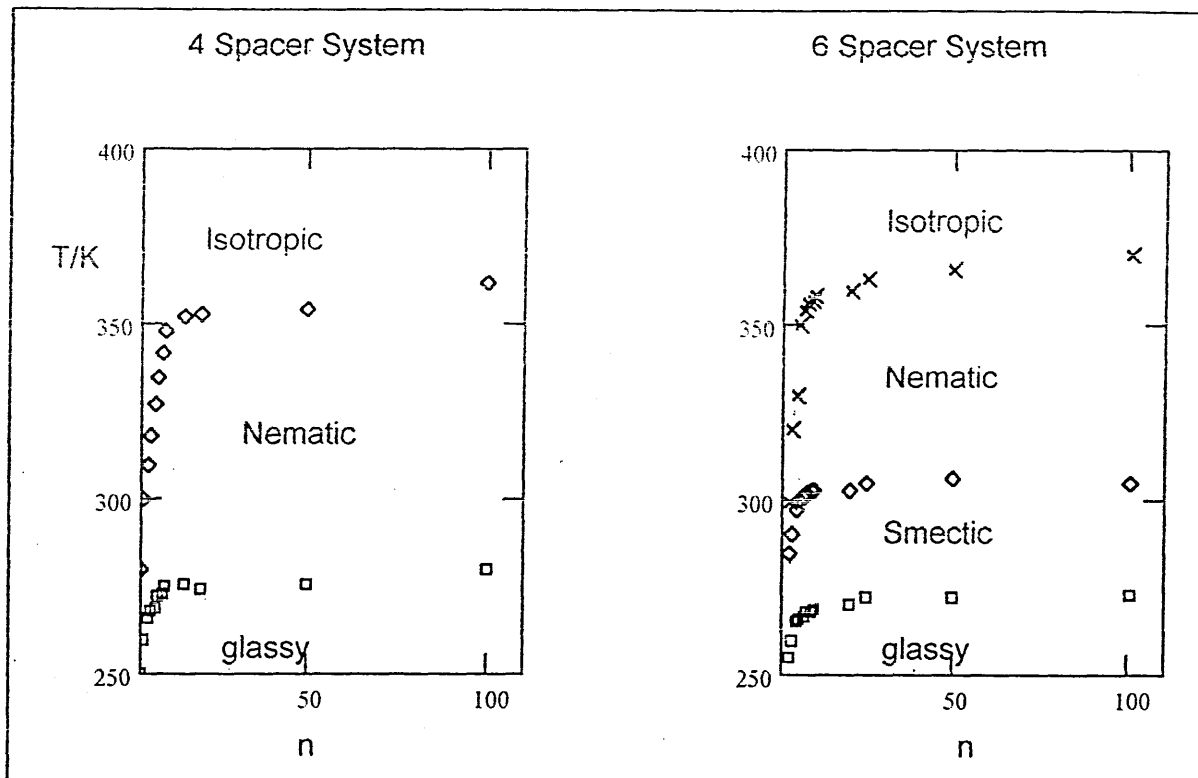


Fig 13 Ctd. Effect of degree of polymerisation on phase transition.



Note systems differ only in length of flexible spacer, but longer space induces additional transitions. See later.

A number of points arise. Initially we note that the tendency for side chain crystallisation to occur decreases from monomer onwards. There is a rapid increase in all transition temperatures up to a degree of polymerisation equal to 10 after which the transition temperature gradually levels off. It is generally accepted that an increase in molecular mass creates a denser packing of the mesogens and so reduces the specific volume at the phase transition. We must

also consider the polydispersity of the system. Ideally we would like a monodisperse sample ($M_w/M_n=1.00$) however, this ideal situation is unlikely to be achieved. Hawthorne (24) has studied the effect of polydispersity on such a system (Fig. 14).

Fig 14. Polymer studied by Hawthorne to investigate effect of polydispersity.

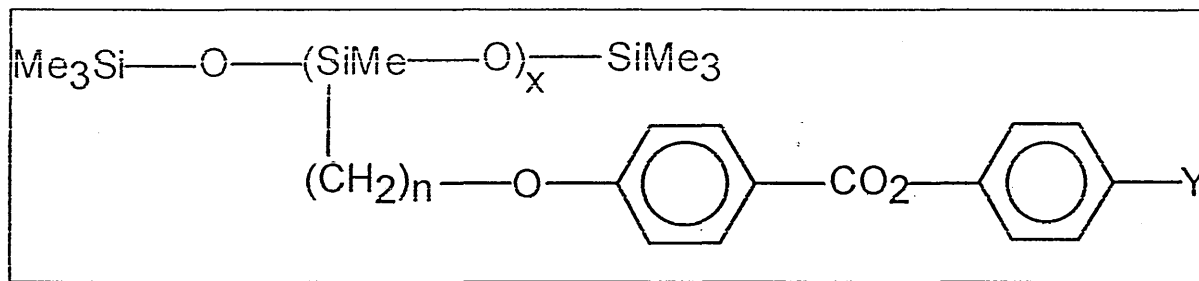


Table 1. Effect of polydispersity on phase transitions for system in fig.15.

M_w/M_n = Polydispersity T_g /°C = Glass transition temperature

T_{cl} /°C = Clearing temperature P_w /°C = Peak width

| Polymer | M_w/M_n | T_g /°C | T_{cl} /°C | P_w /°C |
|---------|-----------|-----------|--------------|-----------|
| n=3 | 15.5 | -2 | 73 | 26 |
| Y=OEt | | | | |
| | 1.9 | 5 | 79 | 20 |
| | 1.35 | 10 | 81 | 18 |
| n=6 | 15.5 | -12 | 117 | 25 |
| Y=CN | | | | |
| | 1.9 | -3 | 123 | 20 |
| | 1.15 | 2 | 128 | 16 |

Here the important indicator appears to be the peak width of a transition. The results demonstrate that as M_w/M_n approaches unity, the peak width of the transition decreases indicating a tendency towards sharper transitions with increased mesophase stability. The importance of such considerations becomes obvious when we consider the possibility that a single peak may actually consist of two unresolved peaks when small transition temperature ranges are involved.

1.3.4. Influence of spacer length on phase transitions.

The spacer length plays an important role in determining both the nature and thermal stability of the mesophase. As discussed earlier, a polymer with no spacer either exhibits a smectic phase or no liquid crystal phase. The introduction of a short flexible spacer allows the mesogens to adopt a nematic state while longer spacers cause the reappearance of the smectic phase.

Fig 15. Effect of spacer length on phase transitions.

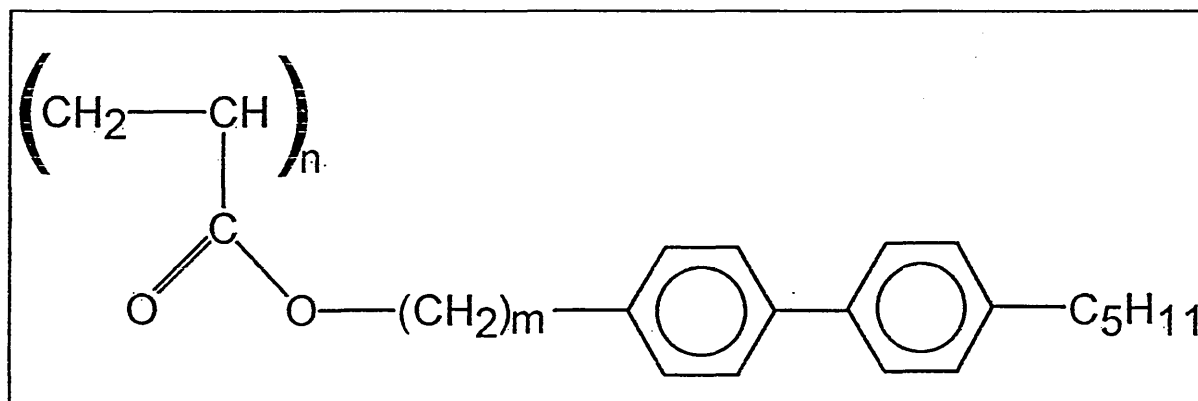
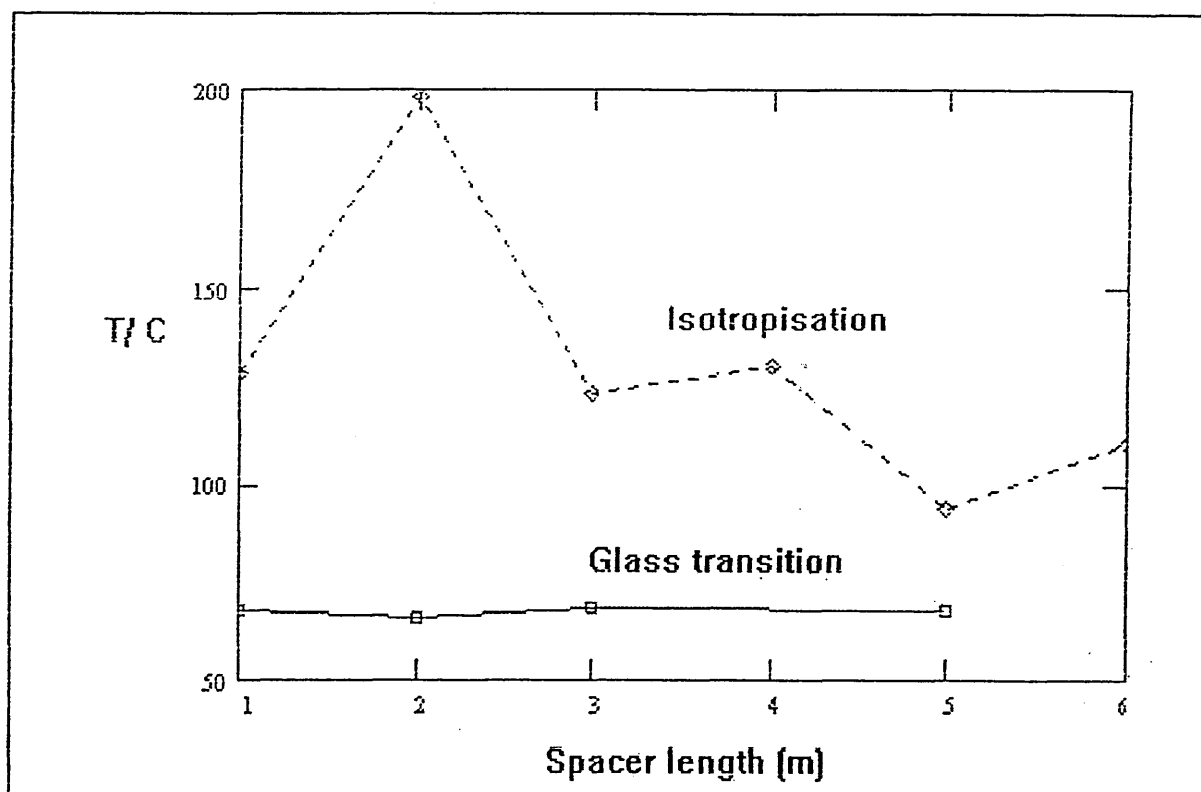


Fig 15. Ctd.



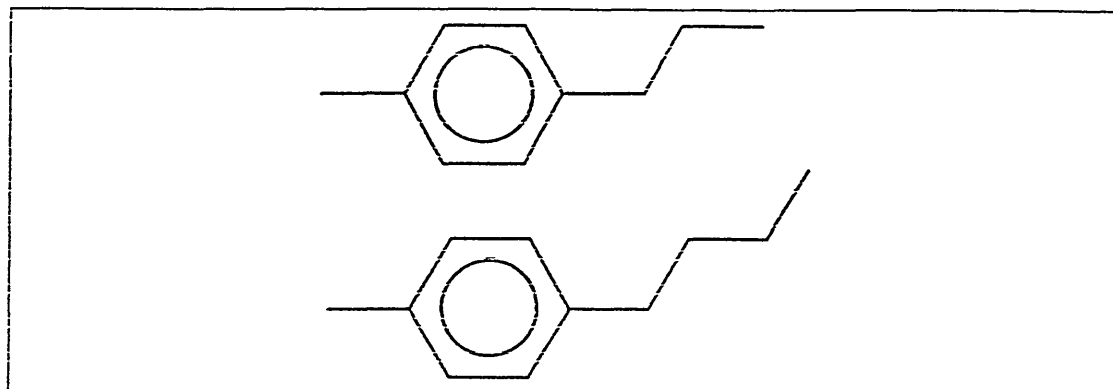
From figure 15, we can note two points. Initially we can see that the glass transition temperature remains effectively constant with respect to chain length. This is probably due to the increase in spacer length having very little effect on the overall polymer molecular mass. Secondly we can see a distinct odd-even effect in the isotropisation temperatures. Here we have to consider the architecture of the molecule as the spacer length increases. For this particular example, a spacer containing an even number of atoms places the mesogen perpendicular to the polymer chain which facilitates the formation of smectic

phases and increases the inter-atomic interaction between neighbouring mesogens. For odd spacer lengths we find the mesogens tilted with reduced interactions and hence lower transition temperatures. This tendency vanishes as the spacer length increases. Furthermore, Shibaev et al (25) has shown that when the spacer contains more than eight units, side chain crystallisation takes place independently of main chain conformation. It has been suggested that in these situations, on melting, the mesogens should show liquid crystal order with no interference from the polymer backbone and thus spacers of greater than eight units should be used in order to obtain 'complete decoupling'. However it is found that this type of polymer produces only smectic mesophases and thus the shorter, partially decoupling spacers are required to obtain the nematic phase.

1.3.5. Influence of mesogen length.

Analogously to low molar mass LCs, an increase in mesogen length leads to an increase in mesophase stability. A special case, where the mesogen contains an alkyl group in the para position of the core (fig. 16), must be considered. Again we must consider the odd-even effect. Gemmell et al (26) demonstrate this.

Fig 16. Influence of terminal alkyl groups.

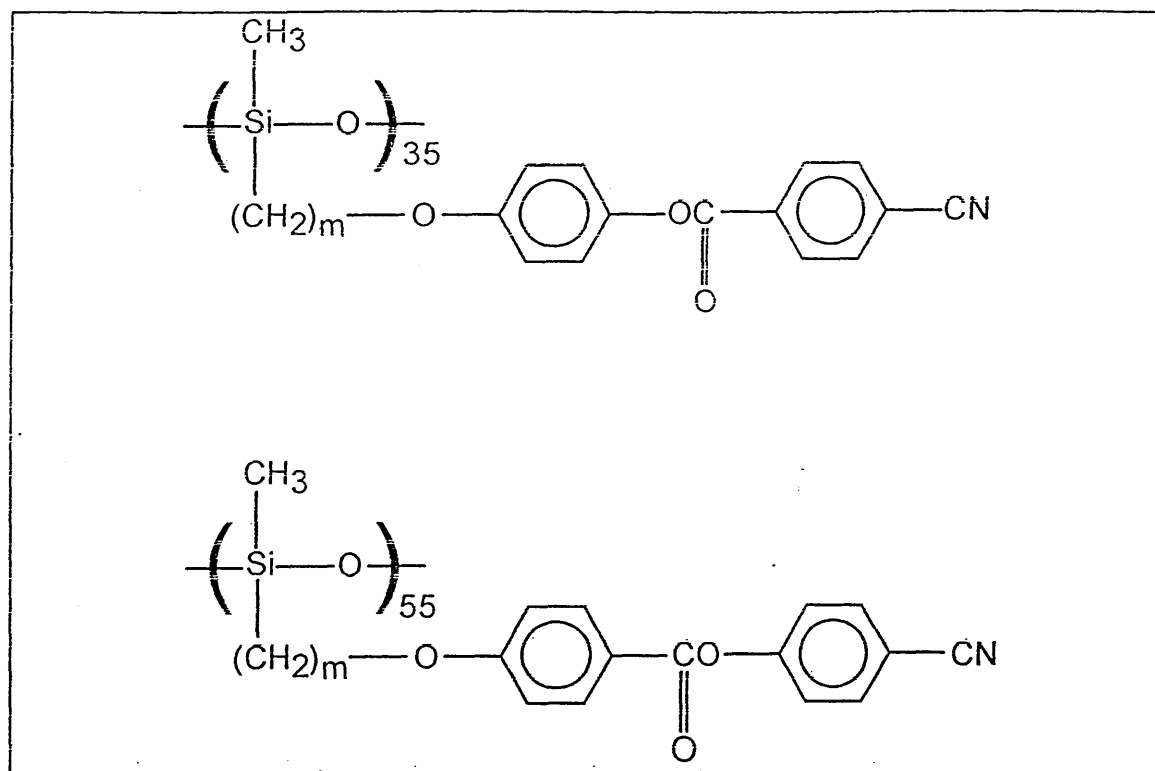


It can be seen that depending on the number of methylene units in the alkyl chain, the terminal methyl group will be placed either on or off axis, assuming an all trans arrangement of the alkyl chain. When placed on axis we expect the mesogens anisotropic behaviour to be improved and hence enhance mesophase stability.

1.3.6. Influence of constitutional isomerism on phase transitions.

Fig. 17 below demonstrates the effect of isomerism for various polysiloxanes with differing spacer lengths.

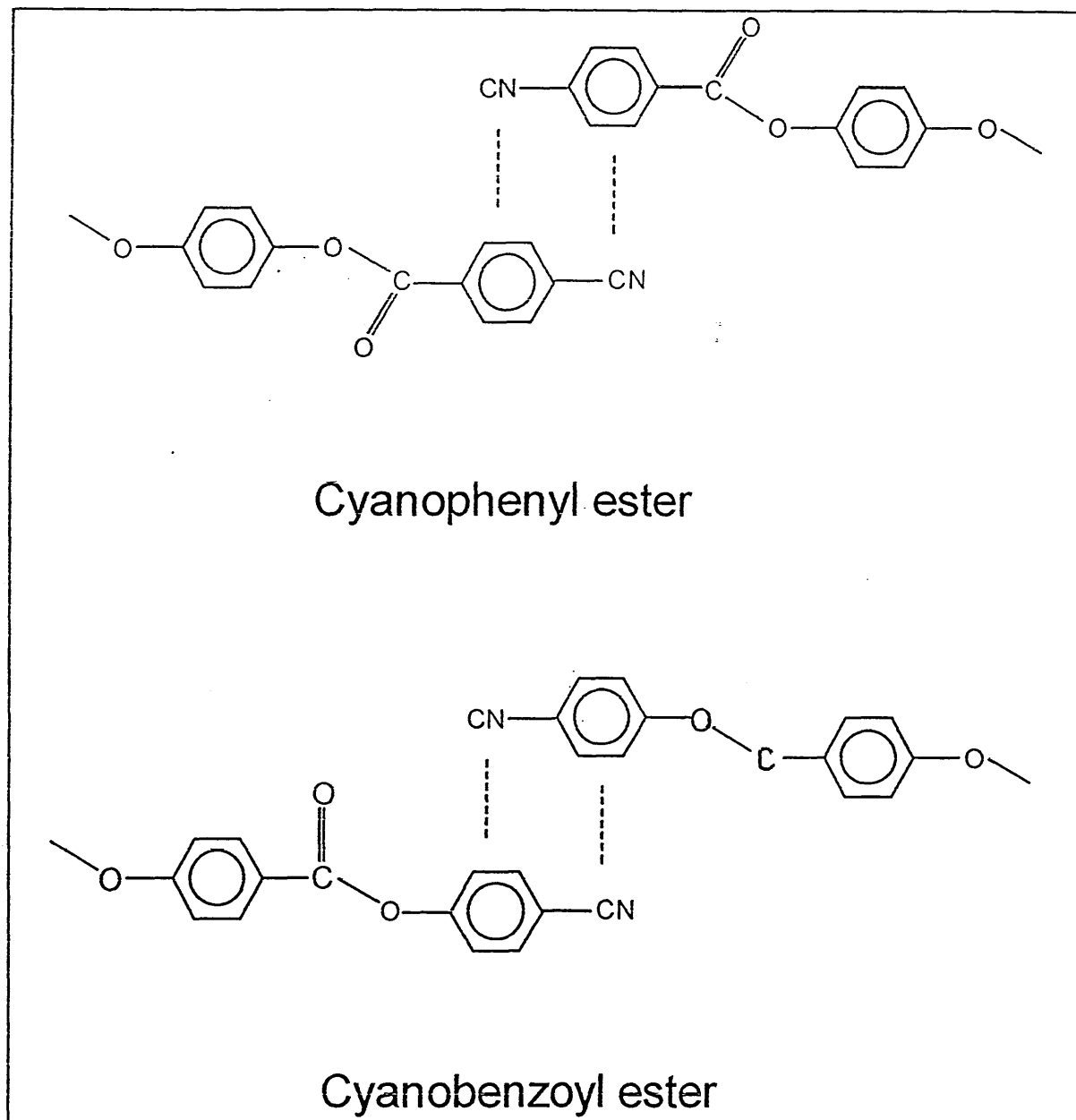
Fig 17. Influence of conformational isomerisation.



First we note that while the polymer molecular masses are different, they are well beyond the critical $\text{DP}=10$ value and hence should show little difference in phase behaviour due to this. The polymer containing the cyanobenzoyl ester unit has phase transitions much higher than that containing the cyanophenyl ester. The former also undergoes side chain crystallisation while the latter does not. The only way to explain this is that the cyanobenzoyl ester is less restricted in forming interdigitated layers than the cyanophenyl ester (See fig. 18).

Fig 18. Theoretical layer structures of cyanobenzoyl ester and cyanophenyl

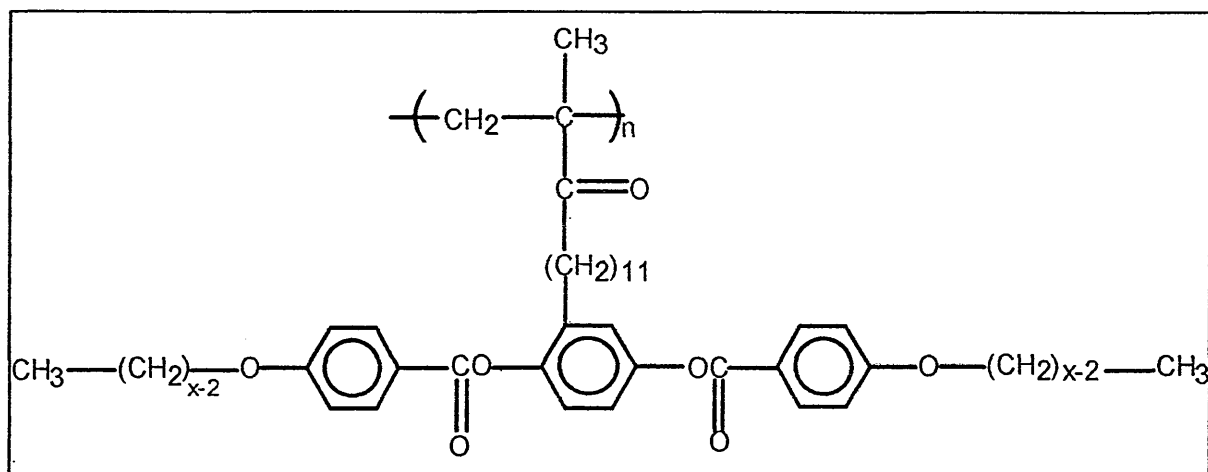
ester



1.3.7. Influence of lateral placement of mesogens.(27,28)

Keller (29) reports the synthesis of a polysiloxane with side groups attached laterally by a flexible spacer. Hassel et al have also reported a similar system which has biaxial properties (30) while Zhou et al have reported a system that uses very short linkages (31). Hassel studied the system shown in fig 29.

Fig 19. Laterally substituted mesogen studied by Hassel.

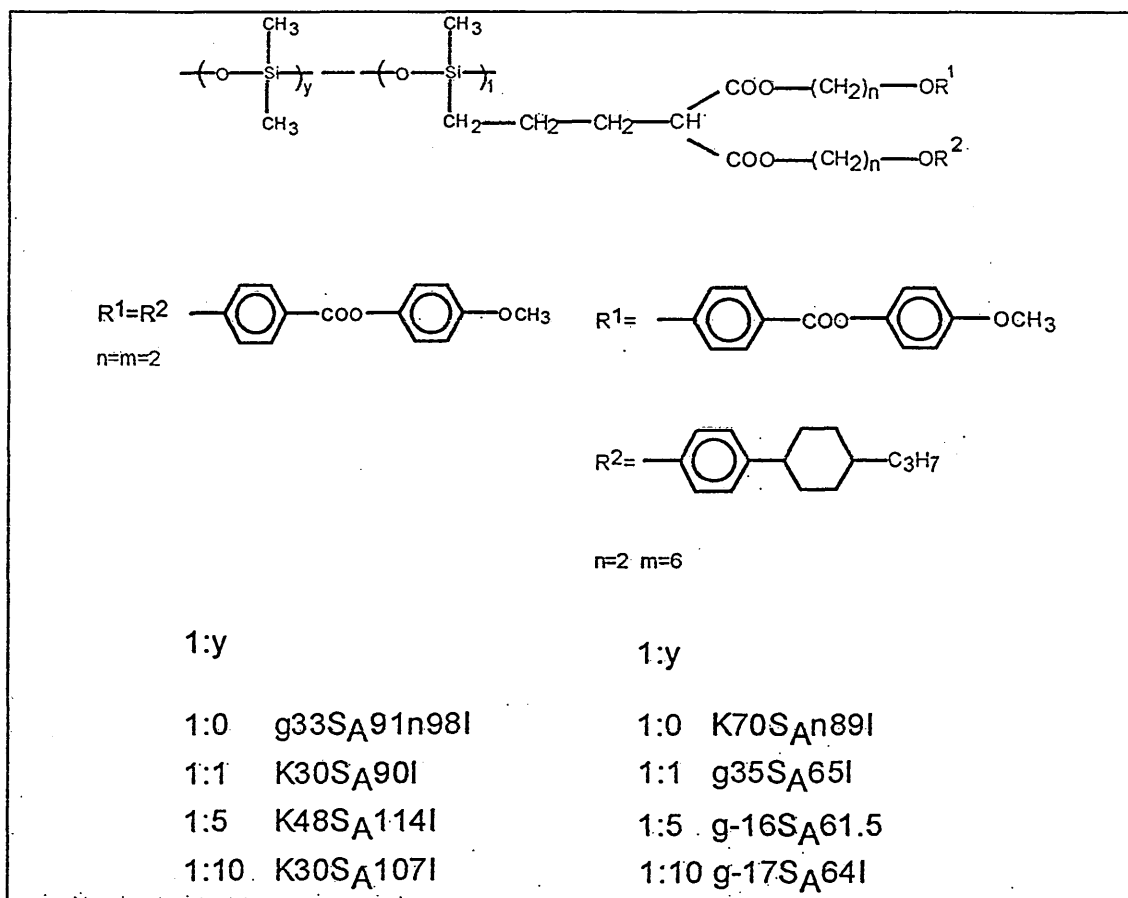


It was found that all polymers based on this mesogen were basically nematogenic. However, diamagnetic anisotropy measurements indicate a nematic to nematic transition. Here it is thought that the system is changing from a biaxial to a uniaxial system and while this is known for low molar mass liquid crystals, it is the first time this has been observed for a polymer system.

1.3.8. Influence of dilution of side groups on phase behaviour.

Diele et al (32) have investigated the effect of 'diluting' the side chain content of the polymer. They studied the effect of placing between one and ten dimethylsiloxane units between the side group being studied (see fig 20).

Fig 20. Effect of side group dilution.



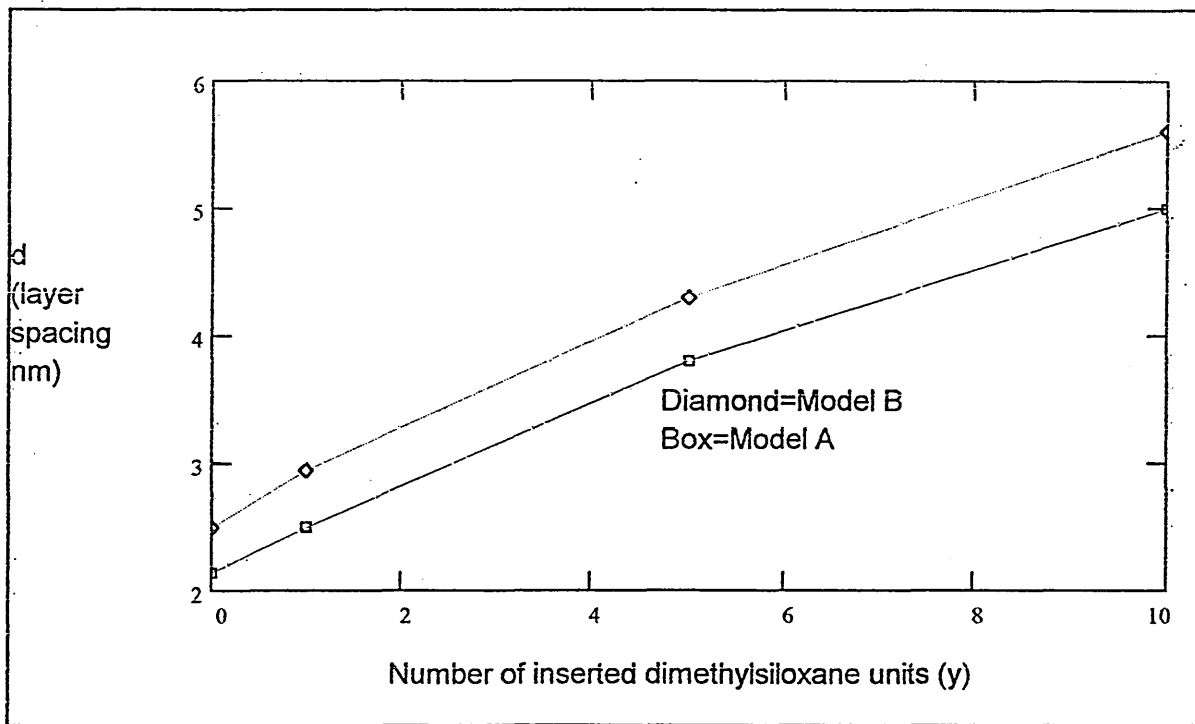
Model A

Model B

Only the non-diluted systems exhibit the nematic phase while all polymers exhibit a smectic A phase. It was also found that the layer spacing in the smectic phases was dependent on the extent of dilution with an approximately linear correlation between the two.

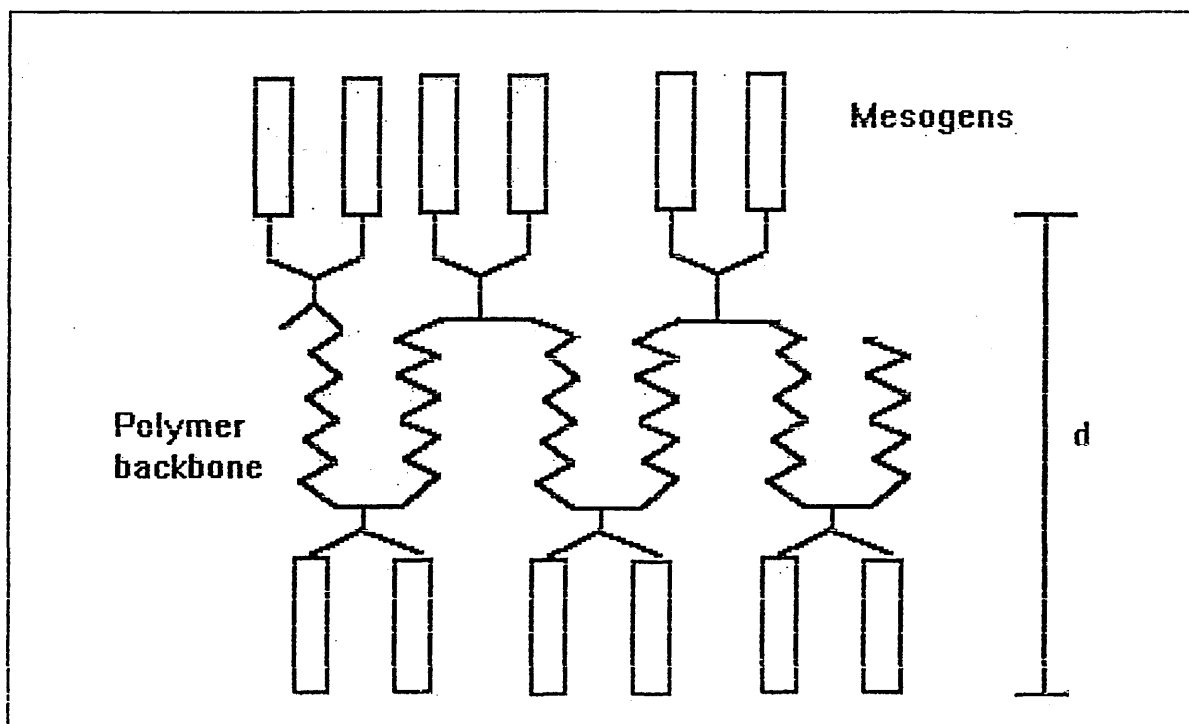
Fig 21. Dependence of layer spacing (d) on mesogen dilution for system in

fig. 20.



The only way that the variation in layer spacing (fig.21) can be explained is if the main chain participates in the layer formation. In the non-diluted systems, the agreement between the layer spacings and the side chain mesogen length indicates the layers are formed by the side chains. In the diluted systems, although the layer spacing increases, we must consider that the latter distances are effectively unchanged. This requires a biphasic model where the backbone is folded in the centre, thus allowing the mesogens to adopt the 'non-diluted positions'. (See fig.22).

Fig 22. Model of diluted system.



1.4. Electro-optical effects in side chain polymers.

1.4. Electro-optical effects in side chain polymers.

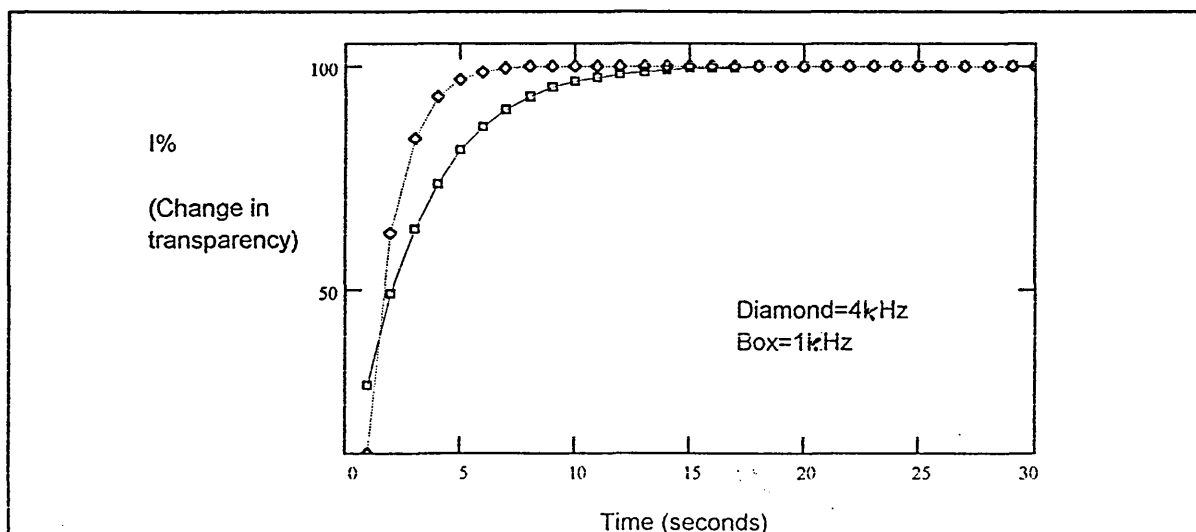
The ability of liquid crystals to orientate in an electric field is the basis of their use in display devices. For polymers, Talroze et al (33) have shown that in an electric field the side chains orientate in the direction of the field.

Studies of the kinetics of the process have yielded the equation:

$$1-\theta = e^{-kT^n}$$

Here θ is the degree of completeness of the process, T is the time and k and n are constants. k can be regarded as the rate constant for the orientation process and depends exponentially on time and field strength. The effect is demonstrated in fig.23 which demonstrates the polymers ability to orientate at two different frequencies.

Fig.23. Orientation of a typical LC side chain polymer in an electric field.

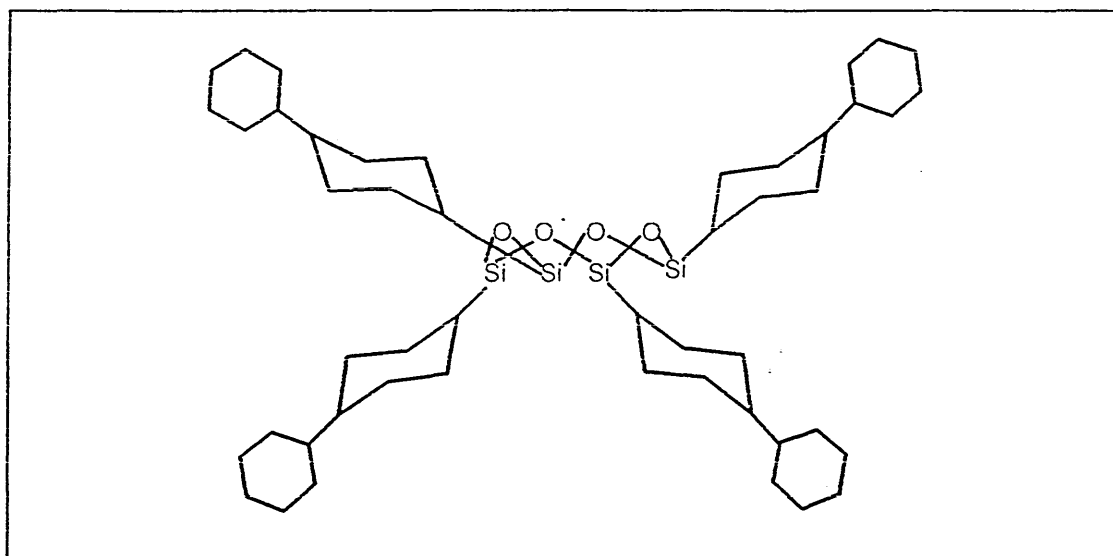


An important application here is in the field of non-linear optical materials which are characterised by a molecular non-centrosymmetry. By heating the system above its T_g and applying an electric field a net macroscopic order is introduced. For optically non-linear side groups possessing a permanent dipole a net polar ordering will be induced leading to non-centrosymmetric systems showing second and higher order effects, e.g. frequency doubling. Molecules without a permanent dipole lead to third and other odd order effects. The polymer is then cooled to below T_g while maintaining the field and the order remains frozen in. The bulk material now exhibits non linear optical properties and the potential for larger effects than those demonstrated by inorganic single crystals can be investigated.

1.5. Cyclic polymers containing rod shaped mesogens.(34,35,36)

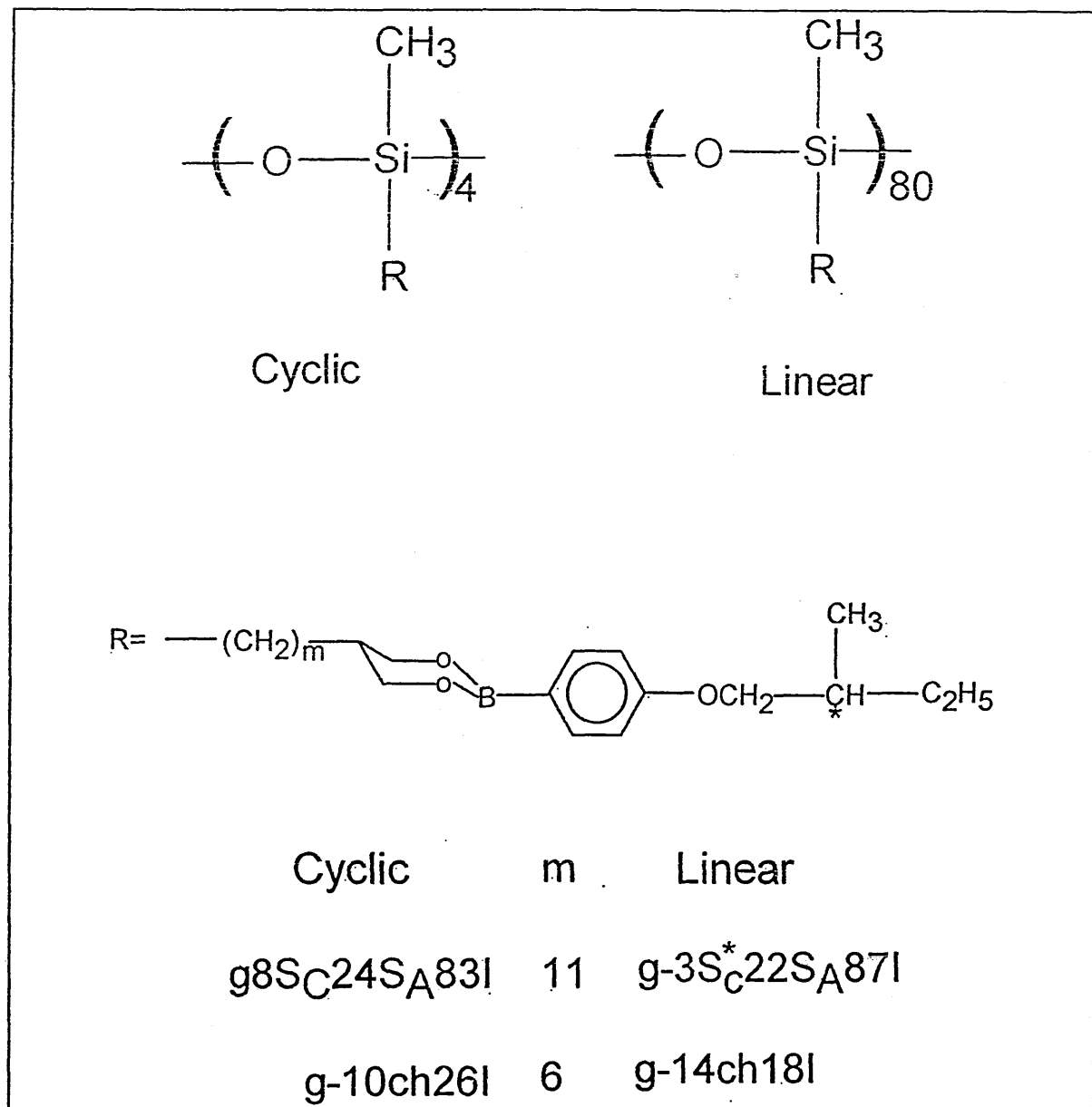
Studies of cyclic polysiloxane liquid crystals are quite rare. Everitt et al (37) used theoretical models to predict that 'disc shaped' molecules based on tetrahydrogenmethylcyclotetrasiloxane in which the hydrogen has been substituted by a mesogenic side chain would form discotic phases at low temperatures.

Fig 24. A typical modified cyclic polysiloxane.



Hahn and Percec (38) compared the phase transitions, for the same mesogenic side group, for a cyclic and linear polysiloxane. The results are indicated in fig.25.

Fig 25. Phase transitions of analogous cyclic and linear substituted polysiloxanes.



Considering the differences in degrees of polymerisation, it is

remarkable to note the similarity in phase behaviour. This has not been explained yet. The most comprehensive studies of cyclic LC polysiloxanes have been performed by Richards et al(39) and Kreuzer et al(40).

1.6. Elastomers.

1.6.1. Rubber elasticity.

Rubber-like behaviour is restricted to long chain molecules as only such systems have enough configurations to alter their end to end separation. It follows that the chain must not be rigid nor locked in the glassy state and to prevent chain slippage, the chain must be crosslinked at least every 100 units (41).

In elastomers the major effect of deformation is the stretching of the network chain which reduces the entropy (42,43,44). Therefore, when an elastomer held under permanent deformation is heated, shrinkage is observed, opposite to the effect observed for a metal strip, due to the elastomer's tendency to increase its entropy to a maximum. Molecular theories of elasticity are largely based on a Gaussian distribution for the end-to-end separation of the chains with the elastic force being largely entropically derived (45). Major assumptions are that the elastic response is entirely intramolecular, i.e. the response of n chains is n times the response of a single chain and that the strain induced displacements are affine.

Deformation ratios for elastomers are expressed as:

$$\alpha = \lambda^* / \lambda$$

where α is the extension ratio, λ^* is the extended length and λ is the original rest length.

Assuming that the mean square end to end distance is $\langle r^2 \rangle$ and values of the chains in the undeformed elastomer are essentially the same as for the uncrosslinked polymer we can deduce ;

$$\Delta F = (v\kappa T/2) * (\alpha_x^2 + \alpha_y^2 + \alpha_z^2 - 3)$$

For an affine elongation in the x axis we find;

$$\alpha_x = \alpha > 1 \quad \alpha_x = \alpha_z = \alpha^{0.5} < 1$$

The force is obtained by differentiation of F with respect to length and we can deduce the nominal stress as ;

$$*f = v\kappa T (\alpha - \alpha^2)$$

where $*f = f/A$, A being the undeformed cross sectional area. Commonly quoted is the reduced stress or modulus.

$$[*f] = *f / (\alpha - \alpha^2) = v\kappa T$$

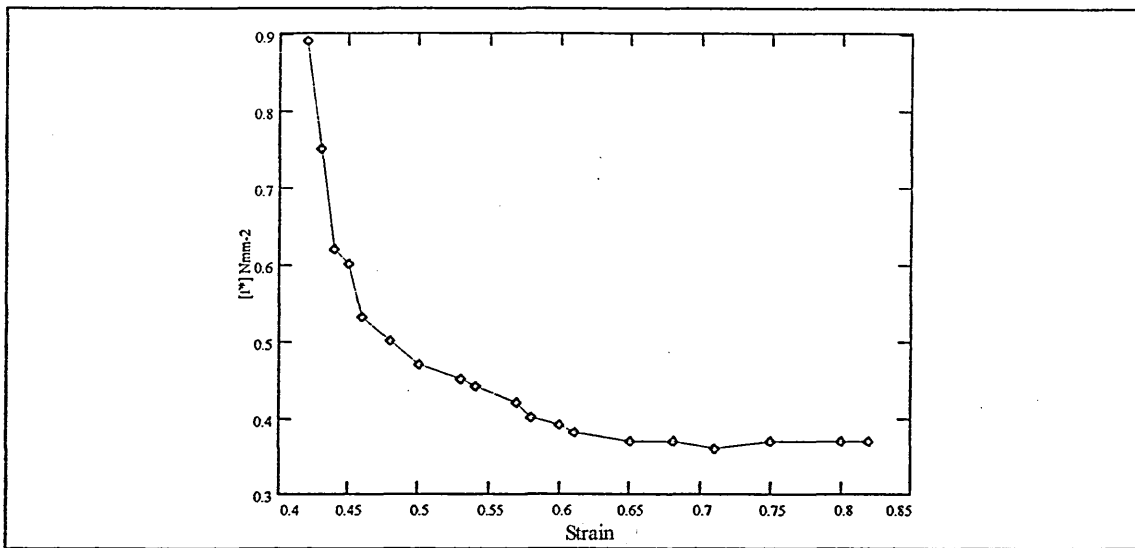
This is the elastic equation of state which demonstrates the stress is directly proportional to the temperature at constant α . $(\alpha - \alpha^2)$ is the strain function, where α^2 represents the compressive effects of near incompressibility of the network. The observed behaviour is often approximated by the semi-empirical

Mooney-Rivlin relationship (46,47):

$$[\sigma] = C_1 + C_2 * \alpha^{-1}$$

where C_1 and C_2 are constants. This is explained because network deformations are found to be non-affine. From the above equation we would expect a stress-strain plot to be linear. In fact, this is found to be only approximately true.

Fig 26. Stress-strain plot for PDMS.



Considering experimental results from figure 26, the rapid increase in force is attributed to limited extensibility of the chains as the strain is reapportioned within the network structure to avoid chain stretching to maximum length, until

no further reappportioning is possible. Theoretical work (48-53) suggests that the elongation of a network is not affine and that cross-link fluctuations diminish the modulus by a factor < 1 . For highly non-affine deformations, as exhibited by a phantom network, the chains are imagined to intersect each other.

1.6.2. Polysiloxane liquid crystal elastomers.

This represents a relatively new field within liquid crystal research. In 1981, Finkelmann et al (54,55,56) announced the synthesis of such a system based on a polysiloxane backbone. Cross-linked polymers are of interest due to their elasticity and ability to return to the original state after large deformations. If coupled with the anisotropic properties of liquid crystals, the potential for a new type of material is realised (57).

Due to the flexible linker (fig.27), which carries no mesogenic groups, the glass and liquid crystal transitions are lowered while the extent of the liquid crystal temperature range remains constant. Similarly to the case of linear polymers, short spacers lead to nematic phases while longer spacers yield smectic phases. Finkelmann observed that liquid crystal phases are produced at up to 10 mol% content of the cross-linking agent. Further increases lead to a drop in the liquid crystalline phase transition temperature due to the disturbing influence of the crosslinker. As far as can be established, no work has been

published on the effect of side-chain liquid crystal elastomers containing long spacers. The question here is whether side chain crystallisation will dominate over network properties. This will be addressed more fully in the Discussion section. At this point we note that a traditional elastomer undergoing a first order phase transition can be described by the Clausius-Clapeyron equation (58).

$$\Delta f / \Delta t = f / t - (\Delta H / T \Delta L)$$

Here ΔH is the enthalpy of transformation, Δf is the retractive force, ΔL is the change of sample length and $(\Delta f / \Delta T)$ is the slope of the co-existence line in the f - T diagram. On cooling, the elastomer becomes crystalline at the transition temperature, a first order process. Conversely on heating, the crystalline elastomer passes into the homogeneous liquid crystal state at the clearing point. Through thermoelastic measurements, the above equation can be used to determine the enthalpy of the isotropic to liquid crystal transformation.

The nature of liquid crystalline elastomers makes their physical properties of interest. Do they follow traditional network models? Characteristics such as mechanical, thermal and photoelastic behaviour are of particular interest.

1.6.3. Mechanical behaviour.

Treloar (59) described the elastic behaviour of networks by statistical theory. Thermodynamic variable changes due to deformation are linked solely to intramolecular phenomena. Thus we can relate stress to strain ratio in the following way.

$$\sigma = \nu \kappa T \frac{\langle r^2 \rangle}{\langle r^2 \rangle_0} (\lambda^2 - \lambda^{-1})$$

Here σ represents the stress; $(\lambda^2 - \lambda^{-1})$ represents the strain ratio; $\langle r^2 \rangle_0$ is the mean square end to end distance of unstrained free chains and $\langle r^2 \rangle$ is for cross-linked chains. This simple form has been developed to account for non-affine deformations (60) and chain entanglements (61). Liquid crystal elastomers are also subject to such factors. The factors contributing to the elastic properties in liquid crystal elastomers are direction-dependent due to the aligning potential of the side groups. In the isotropic state, stress-strain relationships can be derived (up to a point) using classical theories. However, in the liquid crystal state, we have to consider the coupling of the anisotropic properties to the network properties. Therefore we have to use anisotropic chain statistics to deal with an anisotropic contribution of network fluctuations and chain entanglements. deGennes (62) has shown that entanglement slippage is preferred parallel to a particular direction, while restricted in the perpendicular direction with the appearance of entanglements being related to the degree of

polymerisation of the elastomer. The elastic behaviour of liquid crystal networks is determined by conformational properties and hence retractive forces are entropic in origin. In the liquid crystal state conformational properties are also important. However, coupling of network anisotropy to the state of order of the liquid crystal phase probably contributes to the restoring forces.

1.6.4. Director orientation by mechanical deformation.

The director orientation can be determined by a number of methods such as X-ray investigations and possibly FTIR measurements (see later). In siloxane elastomers, the preferred orientation of the side groups depends on the spacer. Schatzle and Finkelmann (63) demonstrated the effect for the system shown in figure 27.

Fig 27. Schematic diagram of a polysiloxane elastomer.

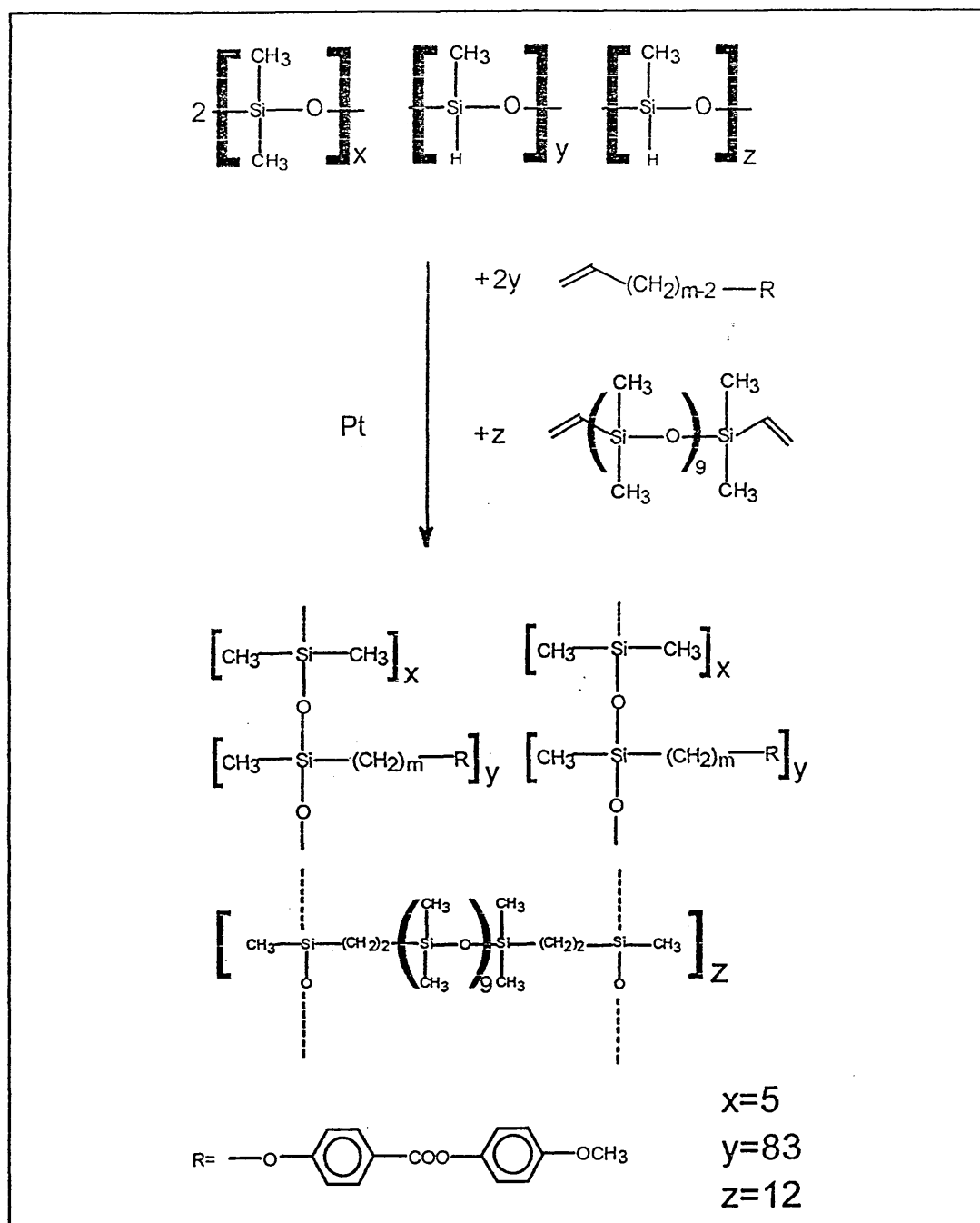
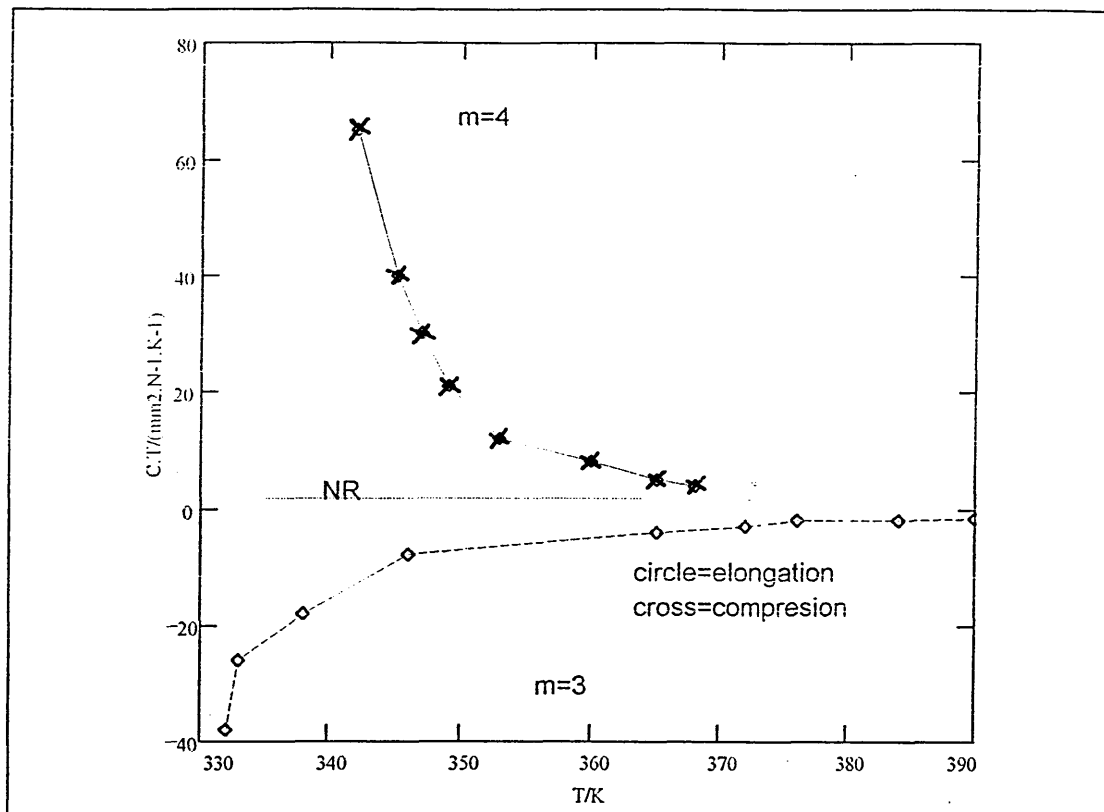


Fig 28. Plot of CT v T for LC elastomer in fig.27 and normal rubber.



Here C is the stress optical coefficient while T is the temperature. C is the quotient of the birefringence and the true stress and is proportional to the optical anisotropy of a chain segment. For natural rubber CT is constant. For the system studied by Schatzle and Finkelmann there are large deviations from this. Three spacer units allow perpendicular orientation while four allow parallel. Increasing spacer length reflects improved chain flexibility and it would be expected that a five spacer unit would also lead to parallel alignment. However, in this

case perpendicular alignment is observed. This could be a quirk of the odd-even effect and, if so, this would be expected the effect to tail off with increasing spacer length, but as yet the detailed mechanism of alignment is not understood. All lightly cross-linked liquid crystal polymers demonstrate elasticity. In the isotropic phase they behave like conventional rubbers. Similar results are found as the materials enter the nematic phase. Radius of gyration measurements show a slight anisotropy with the average being that of the isotropic phase. Transitions to the smectic A phase increase the anisotropy of the radius of gyration but the material retains its elasticity. When the network does not orientate spontaneously in the liquid crystal state, it is found that strains as small as 20% are enough to induce liquid crystal monodomains. Similar strains induced in the material in the isotropic state yield a value of the order parameter several orders of magnitude smaller. This corresponds to the situation in non-LC elastomers where strains of up to 1000% are required to induce network orientation.

1.7. Potential for Liquid crystal polysiloxanes.

Investigations on polysiloxane liquid crystals are still young but already a number of uses have been demonstrated. Optical computers require materials which exhibit non-linear optical effects, lithium niobate being an

example. However, organic materials with extended pi-electron systems and non-centrosymmetric crystal structures can have good non-linear optical properties and can switch faster. The major problem of needing the material in a crystalline state is overcome by using the polymer in the glassy state with suitable side chains locked in. The idea of locking the liquid crystal structure within the polymer has other uses. This can potentially be used for data storage (64,65,66). Local heating by a laser takes the polymer above its glass transition temperature. The side chain orientation can then be modified by electric or magnetic fields. As the laser beam moves on, the polymer reverts to its glassy state and the information is stored through the retained order. Obvious advantages of this are that data storage at a molecular level becomes feasible, provided the beam size can be controlled effectively. However, there are still some doubts as to the effectiveness of the long term data storage potential for such systems.

Chapter 2

Strategy for synthesis

Characterisation

Synthetic methods

2. Strategy for synthesis.

The ultimate aim of the project was to synthesise and characterise a liquid crystal elastomer based on a polysiloxane backbone. To achieve this, various mesogens were prepared and characterised. Selected mesogens were then substituted onto linear and cyclic polysiloxane backbones and these products were also characterised before the final elastomeric materials were produced.

Earlier work by Cockett (67) had studied the effect of attaching known mesogens to cyclic siloxane systems. Work carried out by Everitt et al (37) on the modelling of such systems suggested their potential to exhibit discotic phases. Cockett found no evidence of liquid crystalline behaviour in the systems he studied. With the cyclic siloxane readily available it was decided to repeat and expand on this work. This would provide familiarity with the synthesis of the mesogens and indicate any potential problems with the hydrosilylation coupling reaction. Once satisfactory results from the ring systems were obtained, work was then started on a range of linear polymers based on those of Finkelmann et al (68) and novel systems. The final step involved cross-linking the linear species to produce elastomers (53).

2.1. Mechanistic aspects of polysiloxane chemistry.

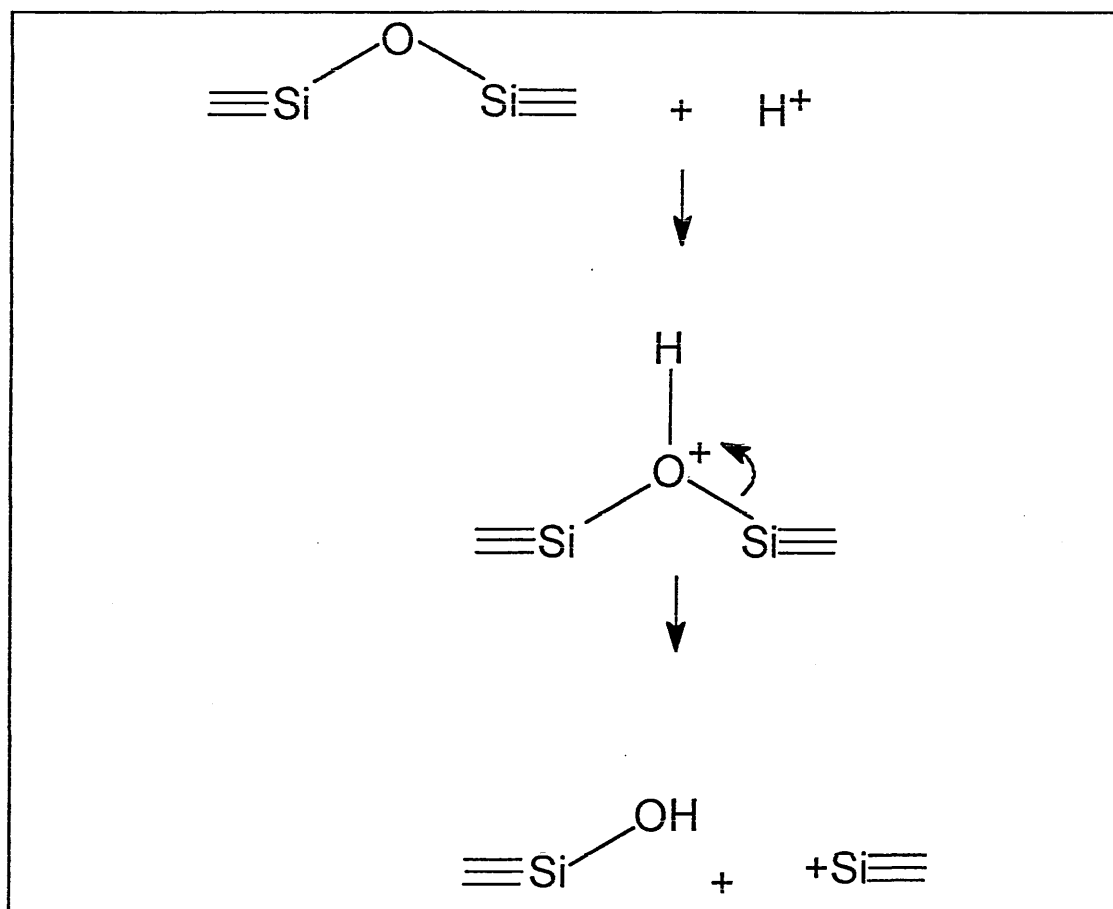
2.1.1. Preparation of linear poly(hydrogenmethylsiloxane)

Polysiloxanes of a 'determined length' can be made by cationic polymerisation

of a cyclic siloxane precursor (tetrahydrogenmethylcyclotetrasiloxane, DH4
heof a cyclic siloxane precursor (tetrahydrogenmethylcyclotetrasiloxane, DH4
denoted HMD hereafter).

This ring opening reaction (69-72) is an equilibrium or redistribution
process because the breaking and reformation of the siloxane bonds takes place
effectively at random.

Fig 29. Ring opening process.



A variety of interchange reactions can take place and hence the precursors are not converted quantitatively to high RMM material. During the course of the reaction the mixture consists of linear and cyclic materials. Since the formation of cyclic material requires a backbiting process, which is statistically unfavourable, only small ring structures are formed. Cyclic material can be removed by vacuum distillation. Using this approach we can synthesise linear poly(hydrogenmethylsiloxanes) of comparable mass to those commercially available ones. The degree of polymerisation (DP) is given by:

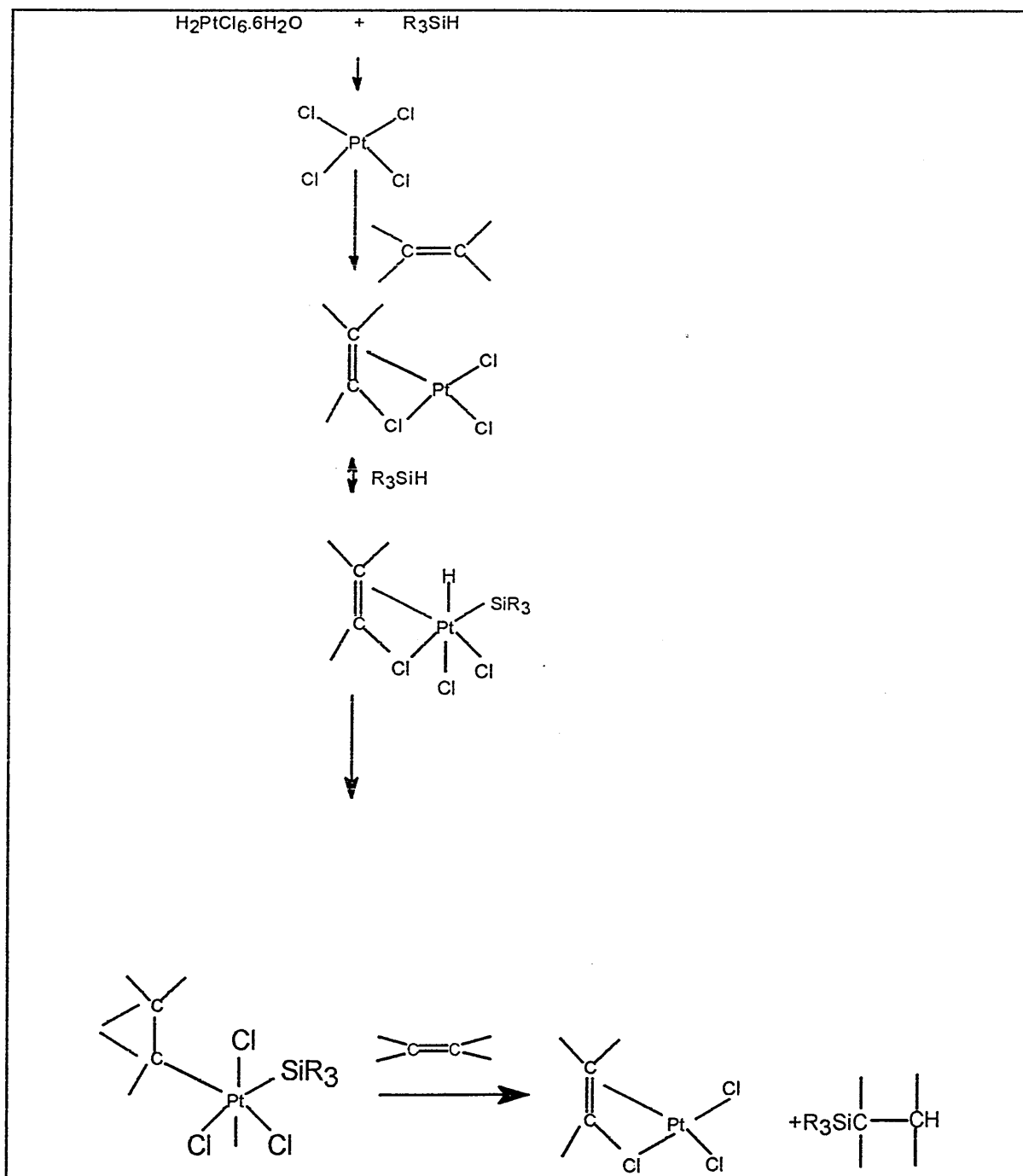
$$DP = \frac{\text{Moles of DH4} \times 4}{\text{moles of HMD}}$$

Obviously there will be a spread of chain lengths that are not indicated by such an equation. However, this can be narrowed down by distillation and gel permeation chromatography. Divinyl-terminated cross-linking agents can be prepared in much the same way. Here we have the advantage that the average RMM can be determined by end group analysis using $^1\text{H-nmr}$.

2.1.2. Coupling of mesogens to polymer backbone.

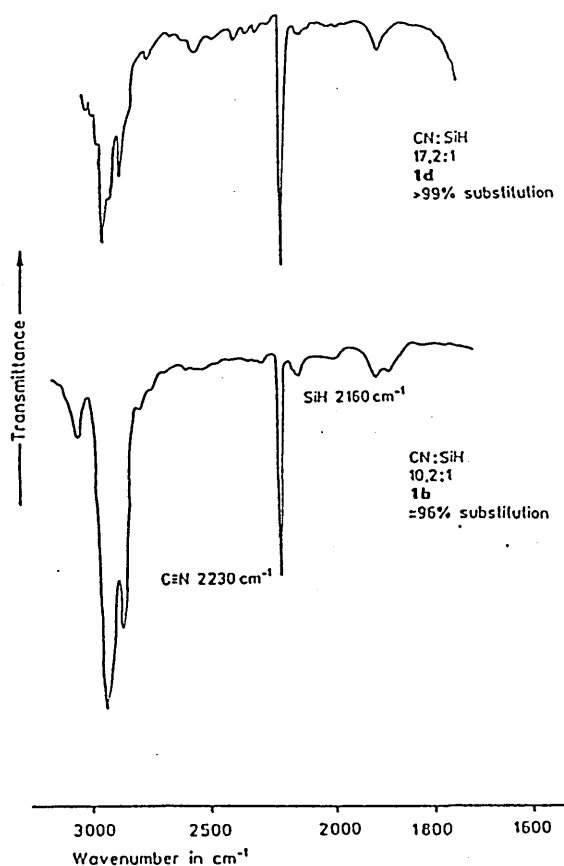
This reaction utilises the hydrosilylation process (73-76) which can be carried out by irradiation, thermally, or in the presence of a catalyst.

Fig 30. The catalytic hydrosilylation process.



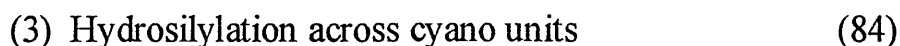
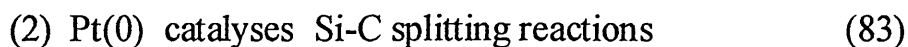
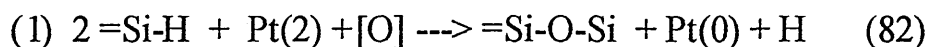
It can be seen from Fig.30 that the process utilises an alkene-terminated mesogen, whereby the sp^2 hybridised carbon atoms in the double bond are converted to sp^3 hybridised via a hydrogen transfer process. The most commonly favoured process is the catalytic approach using, for example, hexachloroplatinic acid ($H_2PtCl_6 \cdot xH_2O$) prepared in a solvent, commonly dry THF or propan-2-ol. The progress of the reaction is easily monitored using infrared spectroscopy and observing the gradual loss of the Si-H stretch at 2160 cm^{-1} (77) (see Fig.31).

Fig 31: Reaction progress monitored by IR.



Apfel et al (78) have recommended the use of 1H -nmr in preference to

IR. However, this technique requires the instrument to either resolve the almost identical shifts for Si-H and CH₂=CHR or detect the 10% excess alkene at 100% reaction. Thus the residual peak intensity for the alkene will be 9.1% of its original intensity and to detect the differences between 95% and 100% reaction would mean working at the limits of the instrumental capability. Early attempts at hydrosilylation gave only sporadic success. Products varied in colour, often being off-white or black rather than the pure white, or contained impurities associated with side reactions. The most commonly prepared catalyst is Spiers catalyst. This consists of hexachloroplatinic acid in propan-2-ol. Freshly prepared solutions are found to function as expected as the platinum is present in the +4 state and this is the species that performs the catalysis (79-81). In older solutions the platinum is gradually reduced to both Pt(2) and Pt(0). Both of these catalyse the reaction but also induce side reactions such as:



Evidence demonstrating that propan-2-ol used in the catalyst is gradually oxidised to propanone was produced by Pukhnarevich et al (118) whereby it was shown that gradually the Pt(IV) had been reduced to the Pt(II) state. The dark appearance of some polymers is attributed to the Pt(2) being reduced to Pt metal.

The method for removal of excess alkene is determined by the nature of the product. Elastomeric material is swollen in a suitable solvent, e.g. toluene, for a number of days followed by careful deswelling in methanol. Linear material is purified by precipitation using a polar solvent such as methanol. Traditionally, the number of precipitations was arbitrary and one or two were considered as acceptable. However, recent studies show that a minimum of eight to ten precipitations are required to completely remove the excess mesogen. Such operations generally reduce the phase transition peak width, as observed by DSC, and increase the melting transition temperature. Nestor et al ⁽⁷⁶⁾ demonstrated that different groups producing 'identical' polymers could report transition temperatures differing by as much as 10°C. Cyclic material is generally purified by gel permeation chromatography. With such materials we have a consistent point emerging from the data. That is, that the purity is essential for an accurate characterisation of any polymeric liquid crystal material.

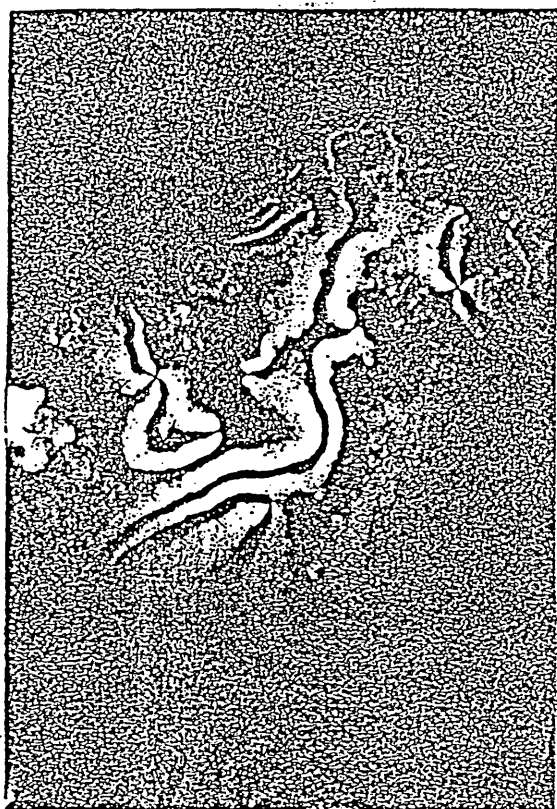
2.3. Characterisation of liquid crystal phases.

2.3.1. Optical microscopy.

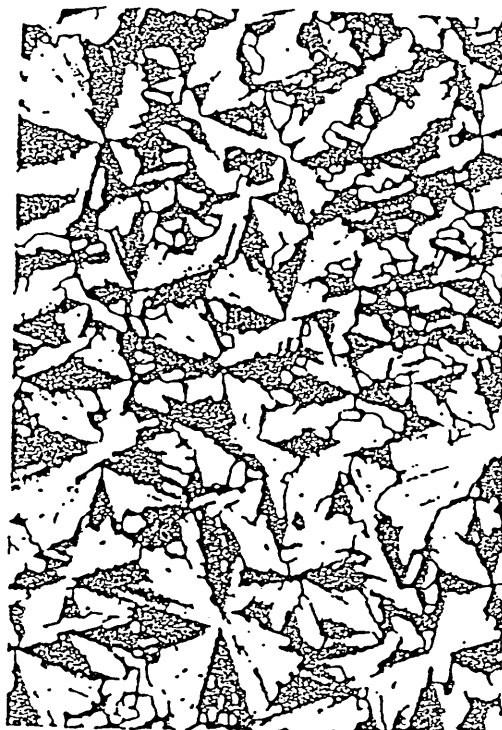
Using a polarising microscope with a heated stage, it is possible to observe characteristic textures of the different mesophases. Isotropic liquids, with randomly orientated molecules, yield a black image through crossed polarisers.

Introduction of ordering into the system allows the molecules to refract the light into characteristic birefringent textures which can be observed changing during transitions on heating or cooling. This technique allows the observation of typical textures such as nematic Schlieren or focal conic textures (the latter from smectic phases).

Fig 32. Typical LC textures.



(a) Nematic schlieren



(b) Smectic A focal conic

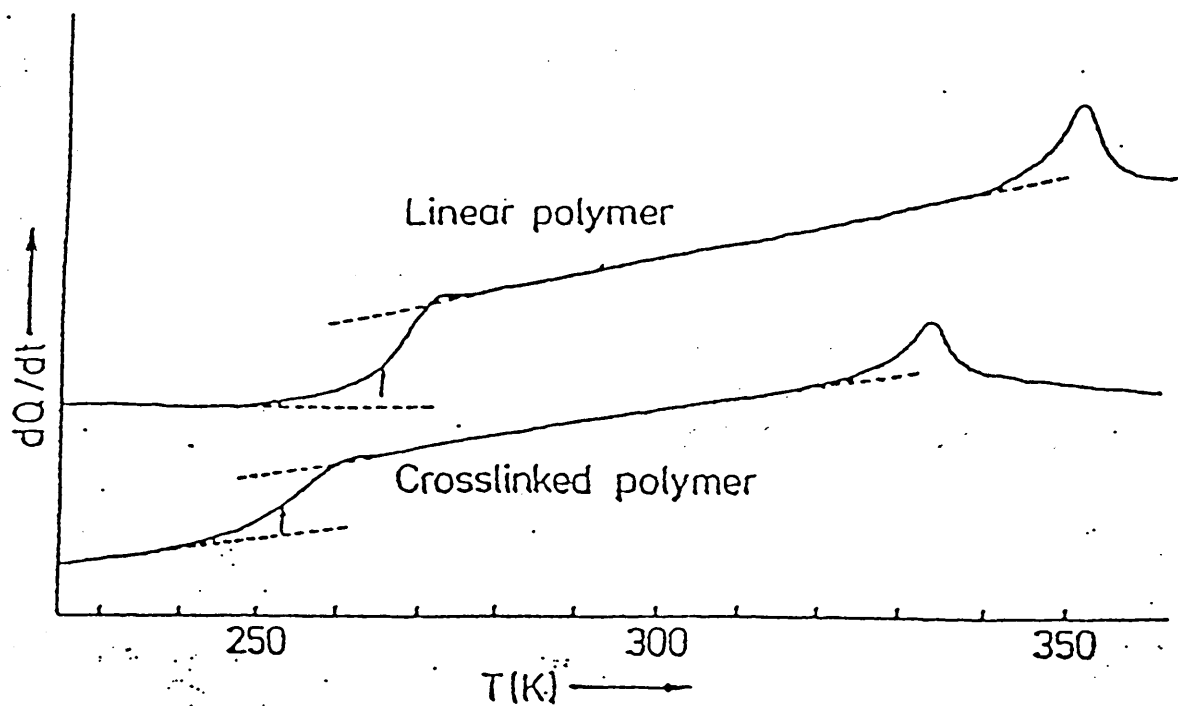
This technique can be coupled with miscibility investigations. When two phases have a different symmetry, i.e. uniaxial or biaxial, they will not mix. By mixing an unknown with a compound of known phase behaviour and

observing their mixing behaviour under the microscope it may be possible to determine the phase types of the unknown. Phases with identical symmetry may undergo complete mixing to yield a single texture. Different symmetries will produce a boundary separating the respective textures. It should be noted that observations of phase changes have to be carefully controlled. Many liquid crystal materials are subject to defects analogous to crystalline materials. Due to the polymorphic behaviour of liquid crystals, defects in one phase may be transmitted to another. That is, textures observed exhibit characteristics of the previous phase. Hence if we observe an LC phase as a result of heating from the crystal phase, we could observe defects that may be associated with the crystal rather than the texture of the liquid crystal phase. For this reason, observation of phase changes during cooling are used to classify phases. In this way the risk of large defects obscuring the texture of the phase is reduced. The observations were carried out using a Vickers microscope equipped with twin polarisers. To raise the mesogens to their isotropic temperature, a heated stage was built. An observation hole was drilled through a copper plate. A 12 V block heater was attached to one end, while a Pt resistance thermometer was attached to the other. The voltage signal obtained from this was converted to a temperature reading using a conversion chart supplied by RS components.

2.3.2. Differential Scanning Calorimetry (DSC).

Nematic to isotropic transitions are on the whole first order with heats of transition of about 500 J mole^{-1} which are easily detected by DSC. Transitions between mesophases can be second order and have much smaller heats of transition. The DSC technique is usually used to determine mesophase temperature ranges and enthalpies of transition and is not used to determine phase type.

Fig 33. Typical DSC curve.



Experiments were carried out using a Mettler TA 2000 instrument equipped with a liquid nitrogen cooling system. Samples of about 5 to 20 mg were used in sealed aluminium pans. The system was purged with nitrogen gas, and heating/cooling rates were 10 K min^{-1} .

2.4. Synthesis.

2.4.1. Characterisation techniques.

Infra-red spectra were recorded using a Galaxy 6021 FTIR spectrometer equipped with a liquid nitrogen cooled mercury cadmium telluride detector. ¹H-nuclear magnetic resonance spectra were recorded using a Bruker 80 MHz instrument. Melting point and elemental analysis were performed by Medac Ltd.

2.4.2. Stock reagents.

All chemicals were supplied by Aldrich and used as supplied without further purification, apart from siloxane compounds which were supplied by Petrarch Systems, Germany. Solvents were used as supplied apart from the following.

2.4.2.1. Tetrahydrofuran (THF).

This solvent absorbs water very readily and so must be dried as required and used immediately. Stock supplies were kept over sodium wire. When required the THF was transferred to a still equipped with a nitrogen purge system. A few grams of potassium pieces were added along with a few grams of benzophenone and the system was set to reflux. When the THF was dry the solution turned a dark blue colour. If no colour was observed after refluxing for about an hour further benzophenone was added. If colour still failed to appear further potassium was added with care. When dryness had been achieved the addition

of just a small amount of either substance produced a deep blue colour around the potassium chips.

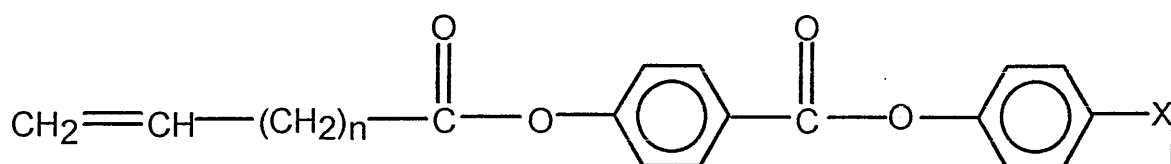
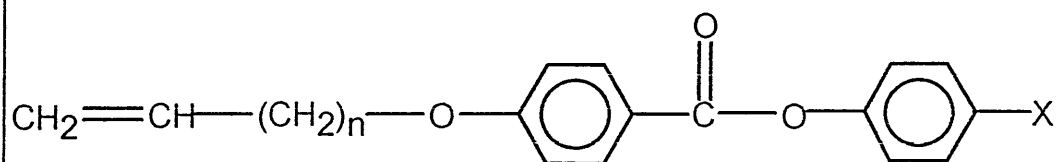
2.4.2.2. Dichloromethane (DCM).

Generally this was used as supplied. However due to expense, and the contamination of some supplies with grease, a still was set up to clean up new supplies and recycle used DCM.

2.4.3. Target mesogen structures.

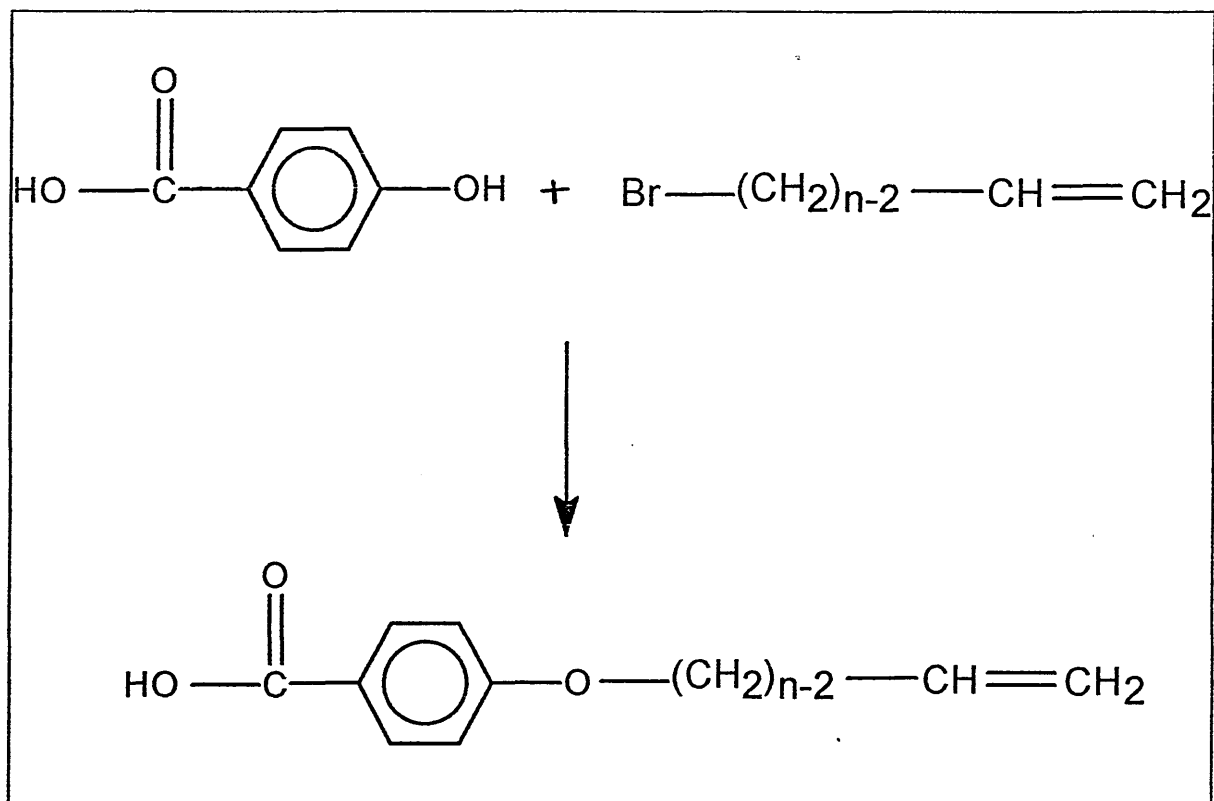
The figure overleaf (Fig.34) indicates the range of mesogens that were to be investigated. All were vinyl terminated to allow coupling to a poly(hydrogenmethylsiloxane) backbone. The phenyl benzoate esters with $n=1,2$ and 3 were chosen as they have been extensively used by other researchers and provided a reference point from which to work. The second group was also based on phenylbenzoate esters coupled to 10-undecenoic acid to yield mesogens with longer spacer units which hopefully would improve the decoupling of the mesogen from the polymer.

Fig 34. Target mesogen structures.



2.4.4. General procedure for the synthesis of p-alkenoxybenzoic acids from p-hydroxybenzoic acid

Scheme 1. Coupling of p-hydroxybenzoic acid to Haloalkene.



p-Hydroxybenzoic acid (10.0 g, 0.0724 moles) was dissolved in ethanol (100 ml) and potassium hydroxide solution (8.124 g, 0.1448 moles in 8 ml of water) and a few crystals of potassium iodide were added. The solution was brought

to reflux and the haloalkene (0.0724 moles) was added slowly. After refluxing for 12 hours the solution was cooled, diluted with water and acidified. The crude product was collected by vacuum filtration and recrystallised from ethanol.

Syntheses were carried out using allyl chloride, 4-bromo-1-butene and 5-bromo-1-pentene. Yields were 55, 30 and 20% respectively.

¹H-Nmr.

Allyl: 7.5(q) , 5.0(t) , 4.5(d)

Butene: 7.5(q) , 5.0(t) , 4.0(t)

Pentene: 7.5(q) , 5.0(t) , 4.0(t) , 1.8(m)

Elemental analysis.

Allyl: Calculated C = 67.40% H= 5.65%

Obtained C = 67.23% H= 5.73%

Butene: Calculated C = 68.73% H= 6.29%

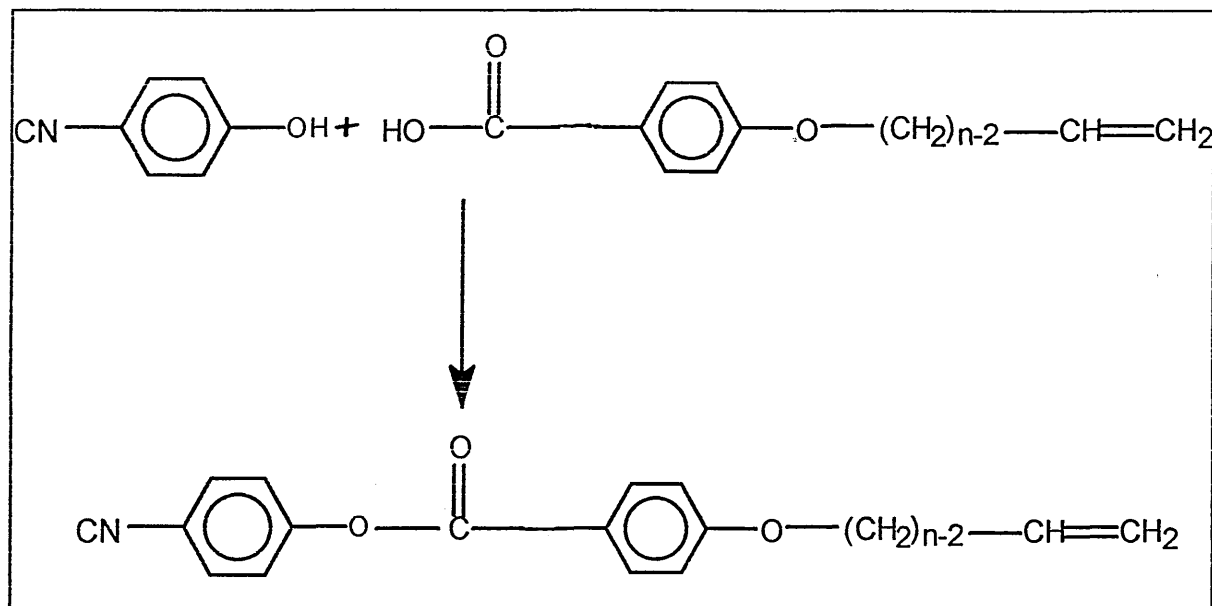
Obtained C = 68.01% H= 6.68%

Pentene: Calculated C = 69.88% H= 6.84%

Obtained C = 69.46% H= 6.52%

2.4.5. General procedure for the synthesis of cyano terminated mesogens.

Scheme 2. Coupling of alkenoxybenzoic acid to cyanophenol.



An alkenoxybenzoic acid (0.0112 moles) was stirred with thionyl chloride (0.0168 moles) and two drops of N,N-dimethylformamide at room temperature for 30 minutes. The excess thionyl chloride was removed under reduced pressure and the crude acid chloride dissolved in dry THF. p-Cyanophenol (0.0112 moles) was dissolved in dry THF (50 ml). Triethylamine (1.25 g, 0.0123 moles) was added and the solution was cooled to below 5 °C. The acid chloride solution was added dropwise during four hours while maintaining the

temperature below 5 °C. After dilution with dichloromethane (200 ml) the solution was washed three times with water and dried over magnesium sulphate. The solvent was removed under reduced pressure and the pure product was obtained by column chromatography using the system silica gel/dichloromethane. Yields of white solid product were 45-55%.

IR (cm⁻¹)

| | |
|---------|---|
| Allyl | 3 100, 2900, 2200, 1730, 16 10, 1460-1380, 1300-1070,990, 840 |
| Butene | 3080, 2940, 22 15, 1730, 16 10, 1520, 1280, 1180, 925, 760 |
| Pentene | 3070, 2960, 2220, 1740, 16 10, 1520, 1270, 1175, 920, 765 |

¹H Nmr.

Allyl: 7.3(m) , 5.0(t) , 4.4(d)

Butene: 7.3(m) , 5.0(t) , 4.1(d)

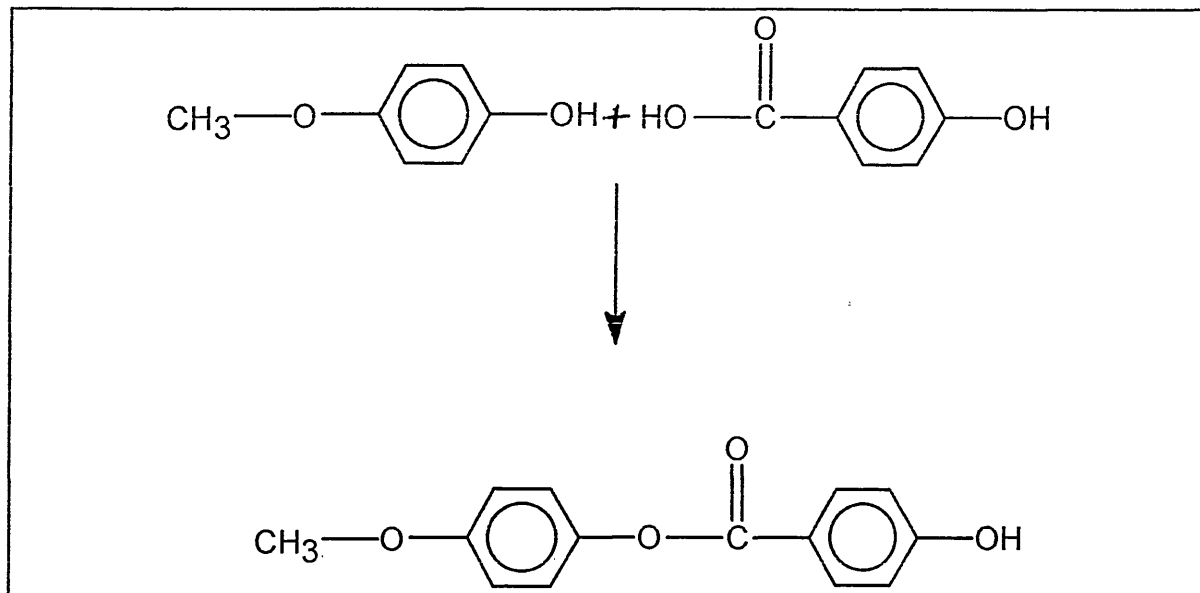
Pentene: 7.3(m) , 5.0(t) , 4.1(t) , 2.0(m)

Elemental analysis.

| | |
|----------|--|
| Allyl: | Calculated C = 73.10% , H = 4.69% , N =5.02% |
| | Obtained C = 71.78% , H = 5.54% , N =4.42% |
| Butene: | Calculated C = 73.70% , H = 5.15% , N =4.77% |
| | Obtained C = 74.72% , H = 5.64% , N =4.70% |
| Pentene: | Calculated C = 74.25% , H = 5.57% , N =4.56% |
| | Obtained C = 74.12% , H = 5.92% , N =4.35% |

2.4.6. Synthesis of p-methoxyphenyl-1,4-hydroxybenzoate.

Scheme 3. Coupling of p-hydroxybenzoic acid to p-methoxyphenol.



A mixture of p-hydroxybenzoic acid (4.9 g, 0.036 moles) and p-methoxyphenol (4.96 g, 0.04 moles) in toluene (20 ml) containing concentrated sulphuric acid (10 drops) was refluxed for six days. Water was removed using a Dean Stark trap and the reaction was monitored by TLC (70% petroleum spirits / 30% ethyl acetate). The cooled mixture was filtered and the crude product dissolved in diethyl ether (250 ml), washed with saturated sodium bicarbonate and dried over anhydrous magnesium sulphate. The ether was reduced in volume to 100 ml and hexane added to yield a white solid.

Yield = 6.8 g / 79 %.

¹H Nmr.

7.1(m) , 3.1(s)

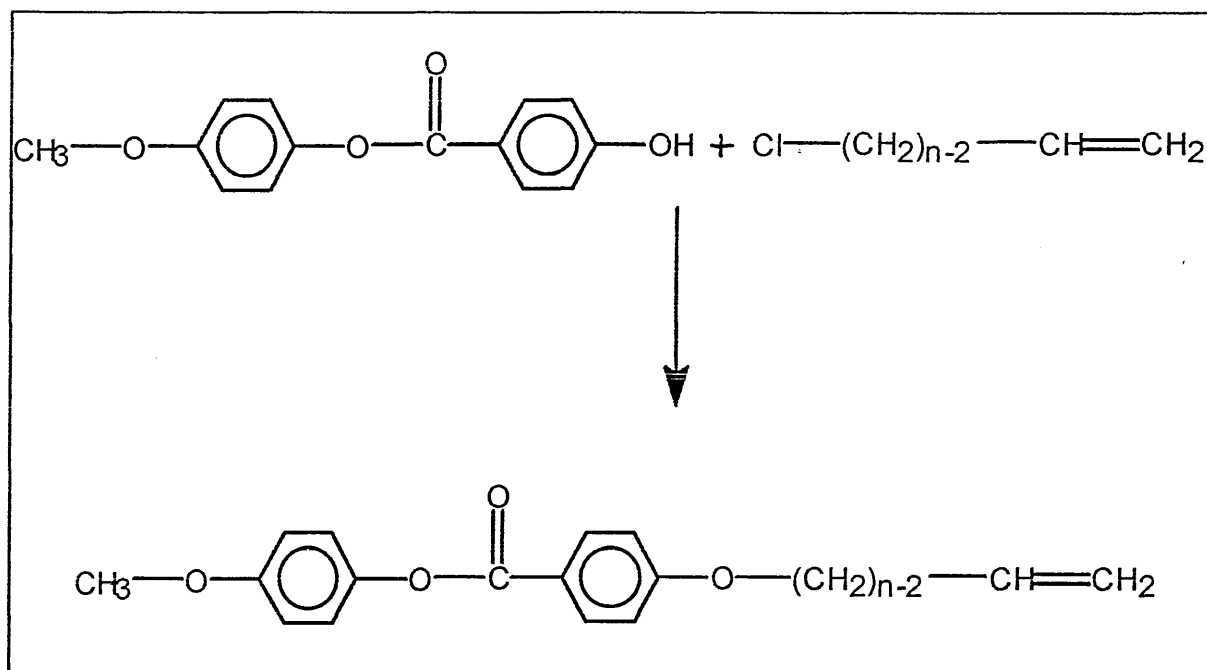
Elemental analysis.

Calculated C = 68.84% , H = 4.95%

Obtained C = 69.50% , H = 5.20%

2.4.7. General procedure for the synthesis of methoxy-terminated mesogens.

Scheme 4. Coupling of 4-methoxyphenyl-4-hydroxybenzoate to the haloalkenes.



A haloalkene (0.028 moles) was added to a mixture of 4-methoxyphenyl 4-hydroxybenzoate (6.8 g, 0.028 moles) and potassium carbonate (5.4 g, 0.028 moles) in dry acetone under dry nitrogen. The mixture was refluxed for 48 hours with TLC monitor (90% petroleum spirit / 10 % ethyl acetate). The potassium salts were filtered off and acetone was removed under reduced pressure. The pure product was obtained by column chromatography using the system

silica gel / 90% petroleum spirits / 10% ethyl acetate. Syntheses were carried out using allyl chloride, 4-bromo-1-butene and 5-bromo-1-pentene. Yields of white solid were about 70%.

IR (cm⁻¹)

C3 3079, 2954, 1733, 1607, 1459-1363, 1269-1072, 940, 872-761

C5 3080, 2960, 1730, 1615, 1520, 1290, 1180, 980, 845

¹H-Nmr.

Allyl: 7.1(m) , 5.3(t) , 4.3(d)

Butene: 7.1(m) , 5.3(t) , 4.0(t)

Pentene: 7.1(m) , 5.3(t) , 4.0(t) , 2.0(m)

Elemental analysis.

Allyl: Calculated C = 71.82% , H = 5.67%

Obtained C = 71.38% , H = 6.13%

Butene: Calculated C = 72.47% , H = 6.08%

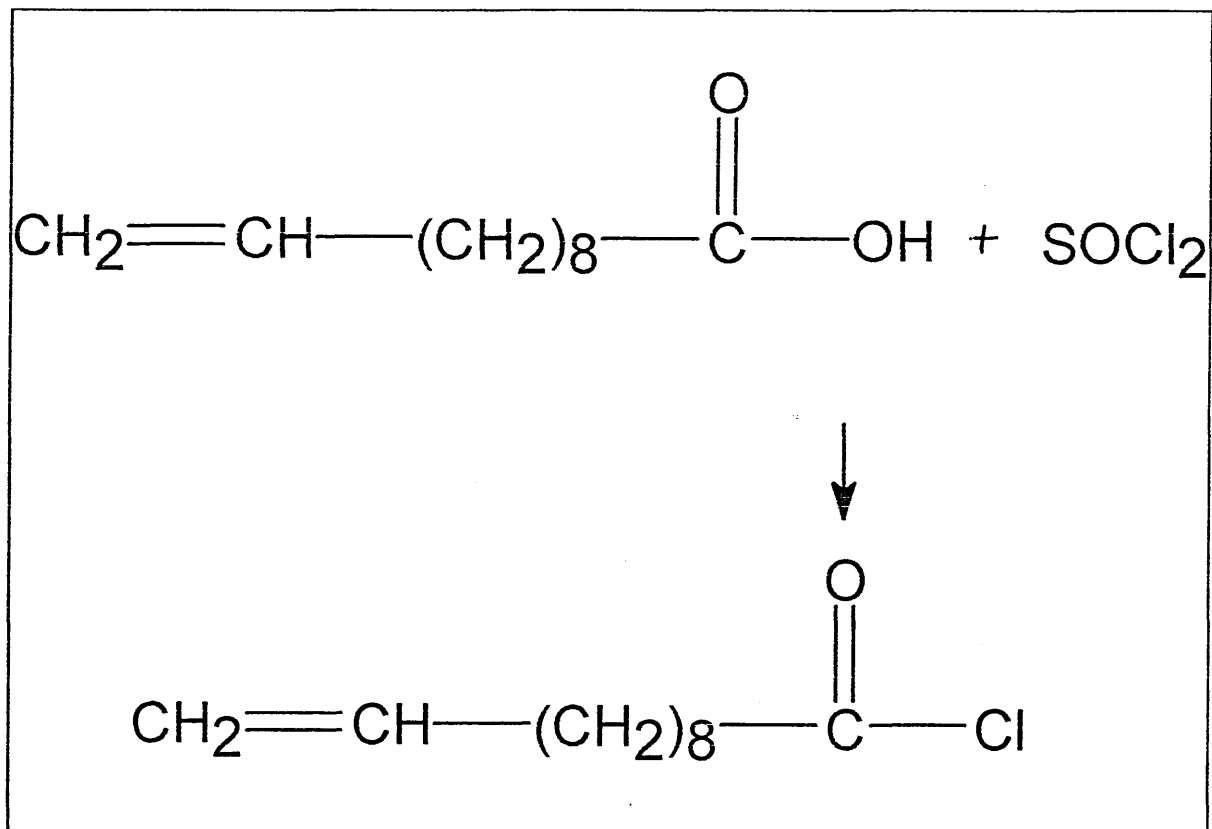
Obtained C = 71.07% , H = 6.00%

Pentene: Calculated C = 73.05% , H = 6.45%

Obtained C = 73.28% , H = 7.28%

2.4.8. Synthesis of 10-undecenoyl chloride.

Scheme 5. Conversion of 10-undecenoic acid to 10-undecenoyl chloride.



10-undecenoic acid (25.0 g, 0.1536 moles) was stirred with thionyl chloride (24.22 g, 0.204 moles) and 2 drops of N,N-dimethylformamide at room temperature for 30 minutes. The excess thionyl chloride was removed by rotary evaporation and the acid chloride was stored in a flask protected with a drying tube.

IR.(cm^{-1})

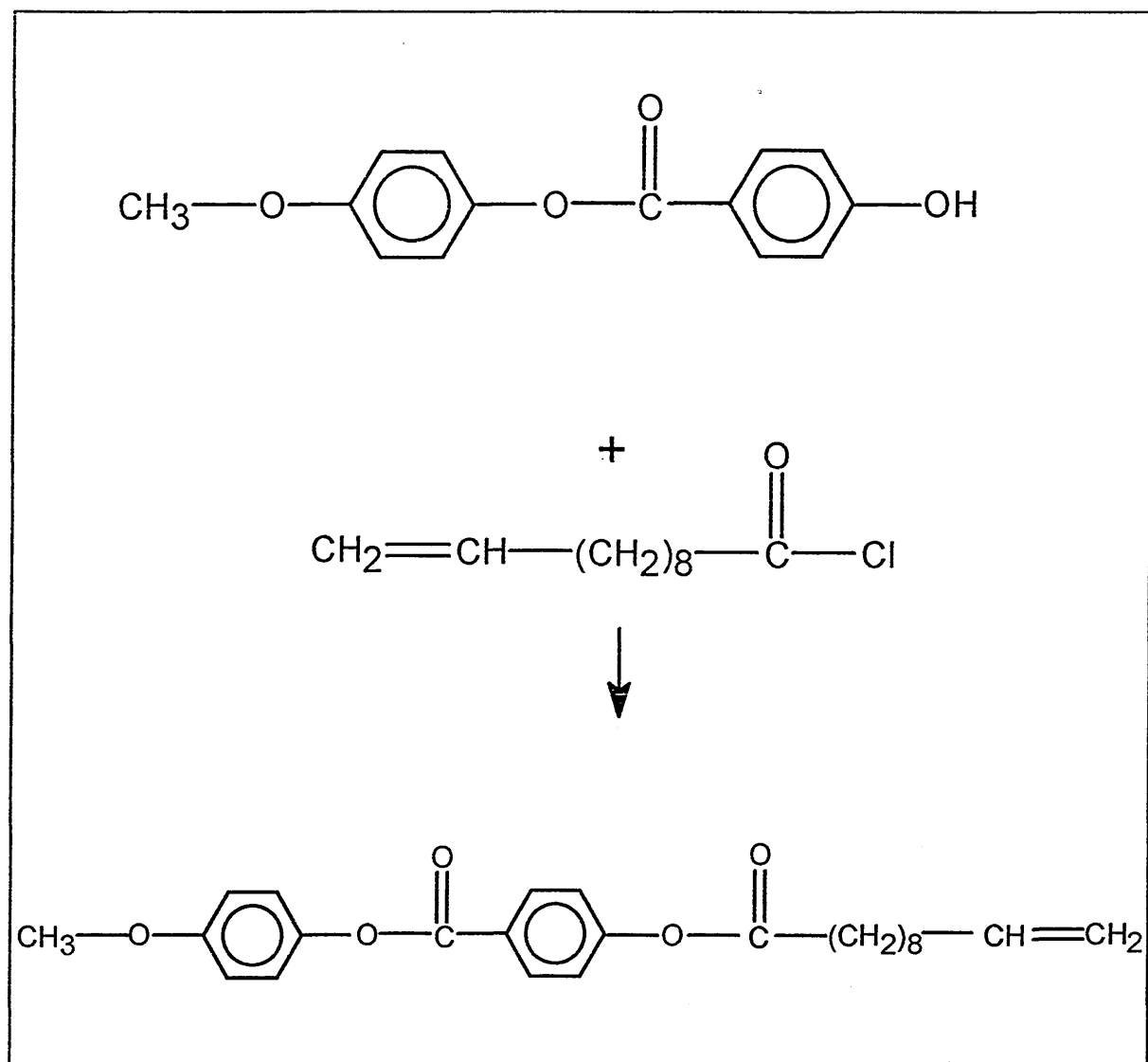
2940, 2860, 1800

¹H Nmr.

5.0(t) , 1.5(m)

2.4.9. Synthesis of mesogens based on 10-undecenoyl chloride.

Scheme 6. Synthesis of methoxy terminated mesogen.



p-Methoxyphenyl 4-hydroxybenzoate (3.0g, 0.01228 moles) and triethylamine (1.367g, 0.01228 moles) were added to a flask charged with dry THF (50 ml). The solution was cooled to less than 5 °C in an ice bath. 10-Undecenoyl chloride (2.49g, 0.01228 moles) was added slowly during four hours while maintaining the temperature below 5 °C. The mixture was diluted with dichloromethane (100 ml) and washed with water (3 x 100 ml). The dichloromethane layer was dried over anhydrous magnesium sulphate and the solvent removed under reduced pressure. Pure mesogen was obtained by column chromatography using the system silica gel / dichloromethane.

Yield = 50-55%

IR.(cm⁻¹)

2920, 2850, 1740, 1600, 1500.

¹H Nmr.

7.2(m) , 5.0(t) , 3.2(s) , 1.5 (m)

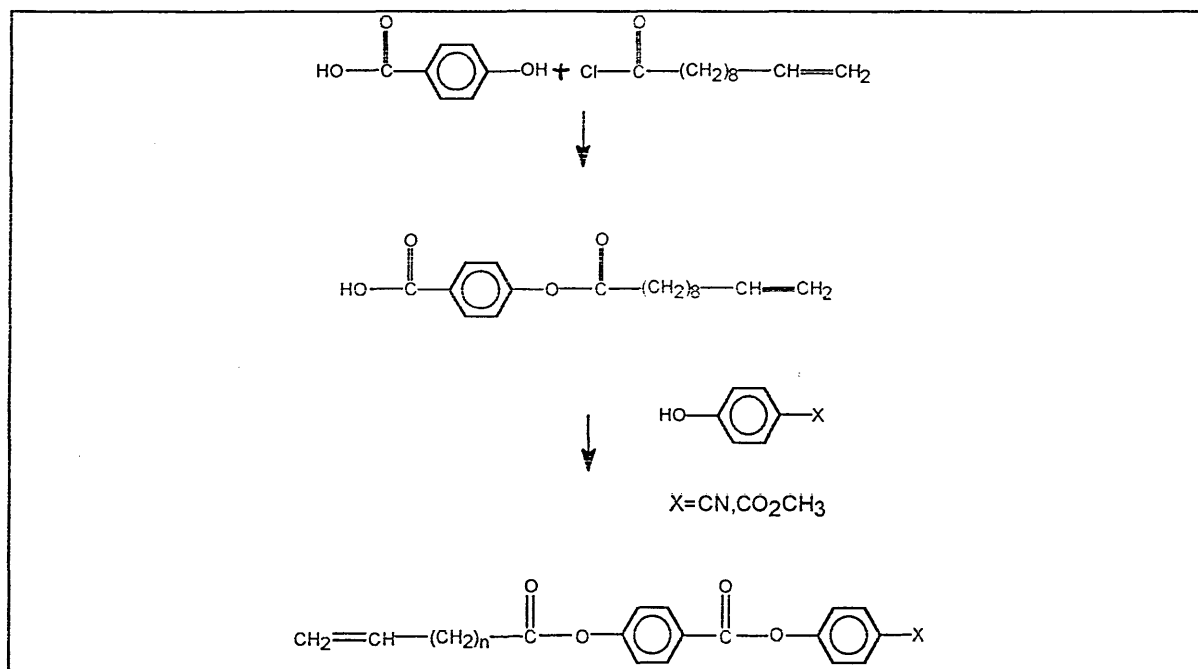
Elemental analysis.

Calculated C = 73.15% , H = 7.36%

Obtained C = 73.50% , H = 7.31%

2.4.10. Synthesis of cyano and methyl ester terminated mesogens.

Scheme 7. Synthesis of long spacer mesogens via undecenoyl chloride.



(a) Synthesis of p-10-undecenyl benzoic acid.

p-Hydroxybenzoic acid (25.0 g, 0.181 moles) and triethylamine (20.0 g, 0.200 moles) were added to a flask containing dry THF (200 ml). The solution was cooled to below 5 °C in an ice bath. Undecenoyl chloride (36.70 g, 0.181 moles) was slowly added during four hours while maintaining the temperature below 5 °C. The solution was diluted with dichloromethane (500 ml) and washed three times with water. Separation of the aqueous and organic layers could be promoted as required by salting with KCl. The dichloromethane was dried over magnesium sulphate and the solvent removed under reduced pressure. Yields of

between 20 and 55% were obtained.

¹H-Nmr. 7.1(d) , 5.1(t) , 1.4 (m)

(b) Synthesis of mesogens.

p-10-Undecenoyloxybenzoic acid (5.00 g, 0.0164 moles) was stirred with thionyl chloride (10.0 g, 0.084 moles) and two drops of N,N-dimethylformamide at room temperature for 30 minutes. The excess thionyl chloride was removed by rotary evaporation and the crude acid chloride was dissolved in dry THF (20 ml). p-Cyanophenol or methyl p-hydroxybenzoate (0.0164 moles) and triethylamine (1.825 g, 0.01804 moles) were dissolved in dry THF (25 ml). The solution was cooled to below 5 °C in an ice bath. The acid chloride was added slowly over 4 hours while maintaining the temperature below 5 °C. After addition the solution was diluted with dichloromethane (100 ml) and washed three times with water. The dichloromethane layer was dried over magnesium sulphate and the solvent removed under reduced pressure. The pure mesogens were obtained by column chromatography using the system silica gel / dichloromethane. Yields of between 45 and 55% were obtained.

¹H Nmr.

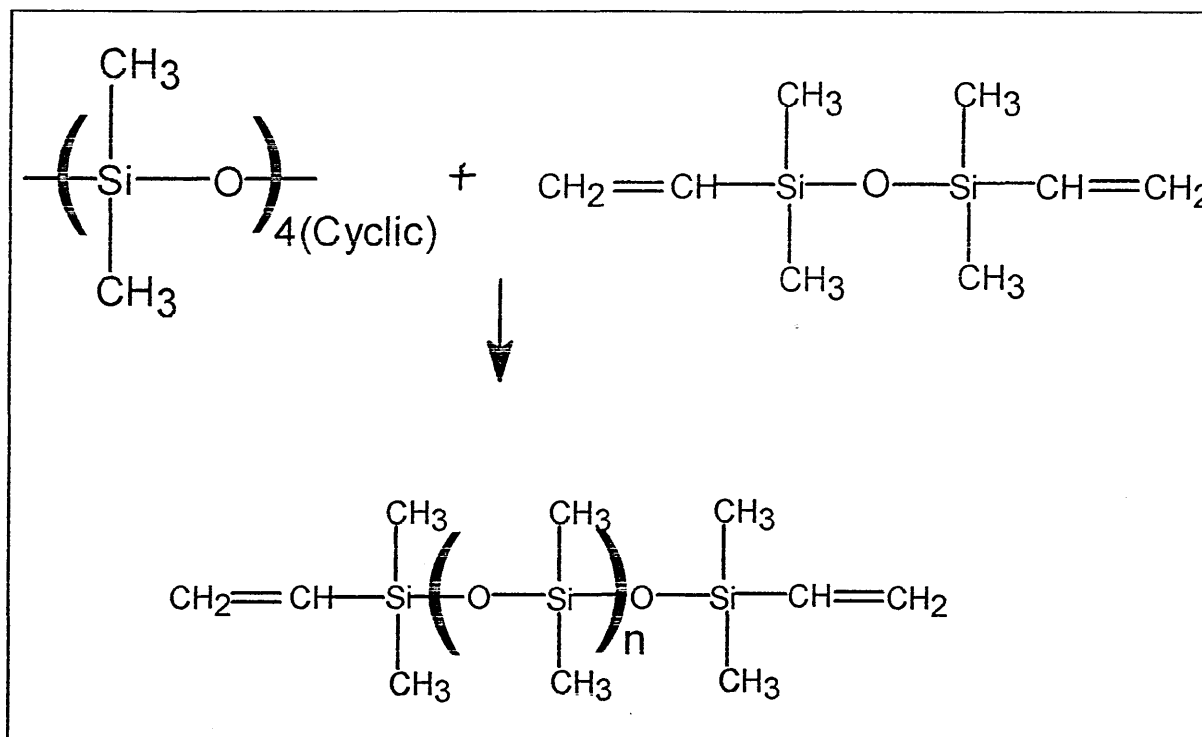
| | |
|---------------------------------|-----------------------------------|
| CN | 7.2(m) , 4.9(t) , 1.5 (m) |
| CH ₃ CO ₂ | 7.4(m) , 5.0(t) , 3.7(s) , 1.7(m) |

2.4.11. Preparation of catalyst for polysiloxane synthesis

Fullers earth (10 g) was stirred in dilute sulphuric acid (50 ml) for 12 hours, filtered, washed with distilled water until the washings were neutral and finally dried under vacuum at 100°C.

2.4.12. Synthesis of divinyl terminated polysiloxanes.

Scheme 8. Ring opening of octamethylcyclotetrasiloxane to produce divinyl terminated polysiloxanes.



Into a flame dried flask, fitted with a nitrogen balloon, was placed tetramethyldivinylsiloxane (1.5 g, 0.0080 moles) and octamethylcyclotetrasiloxane (labelled D4' from hereafter) (1.191 g, 0.0161 moles). A small amount of acid activated Fullers earth was added and the reaction mixture was stirred under nitrogen for 72 hours at 60°C. After cooling the catalyst was removed by filtration. Low molar mass rings were

removed under vacuum (150°C, 0.1 torr). The products were characterised using $^1\text{H-Nmr}$ and IR.

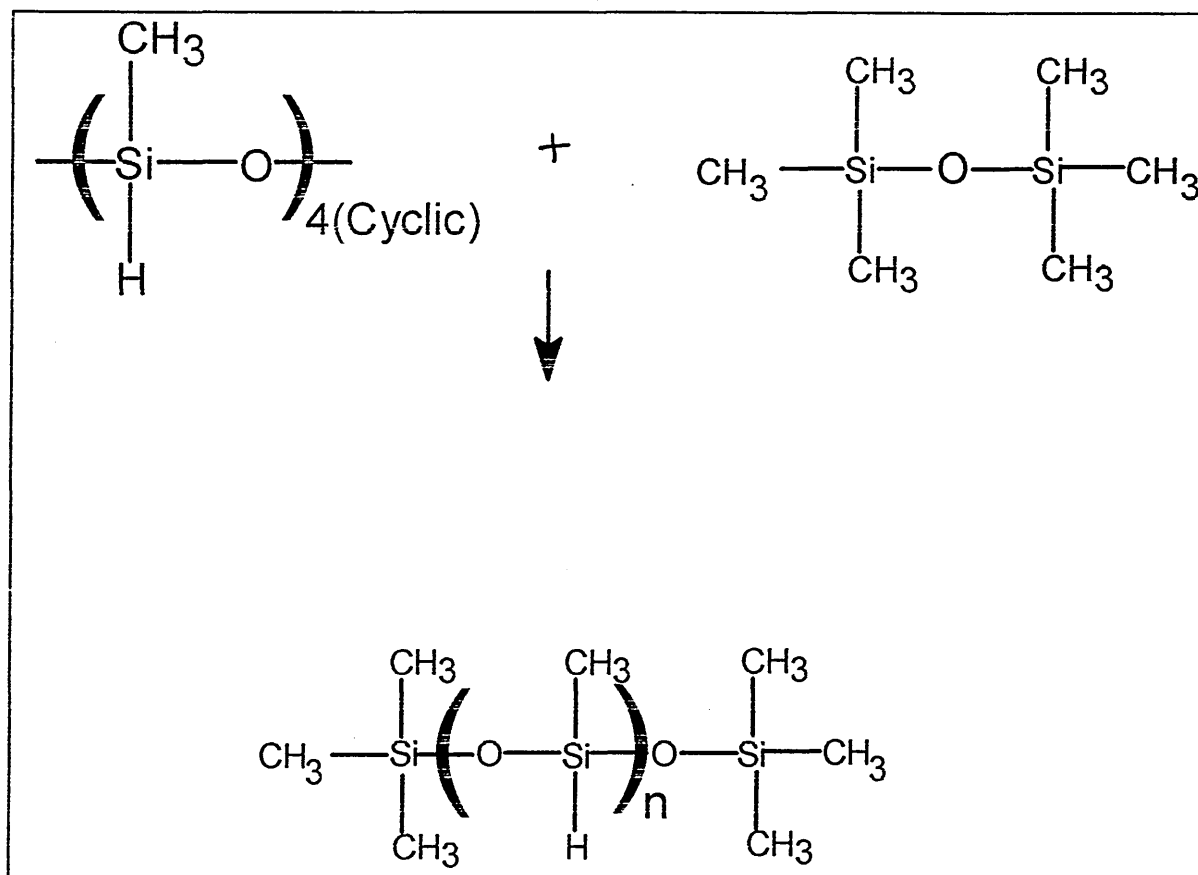
Yield = 70 %

IR (cm^{-1}) 2990, 1600, 1410, 1260, 1260, 1070

$^1\text{H-Nmr}$ 0.0(s), 4.6(broad s)

2.4.13. Synthesis of poly (hydrogen methyl siloxanes.)

Scheme 9. Ring opening of tetramethylcyclotetrasiloxane to produce poly(hydrogenmethylsiloxane)



To a flame dried flask fitted with a nitrogen balloon was added tetrahydrogenmethylcyclotetrasiloxane (29.7 g, 0.1234 moles) and hexamethyldisiloxane (1 g, 0.0062 moles). A small amount of acid activated Fullers earth was added and the mixture was stirred under nitrogen for 72 hours at 60°C. After cooling the catalyst was removed by filtration and the low molar mass rings were removed by vacuum distillation. (150°C, 0.1 torr). Products were characterised using IR and ¹H Nmr. Yield = 77%

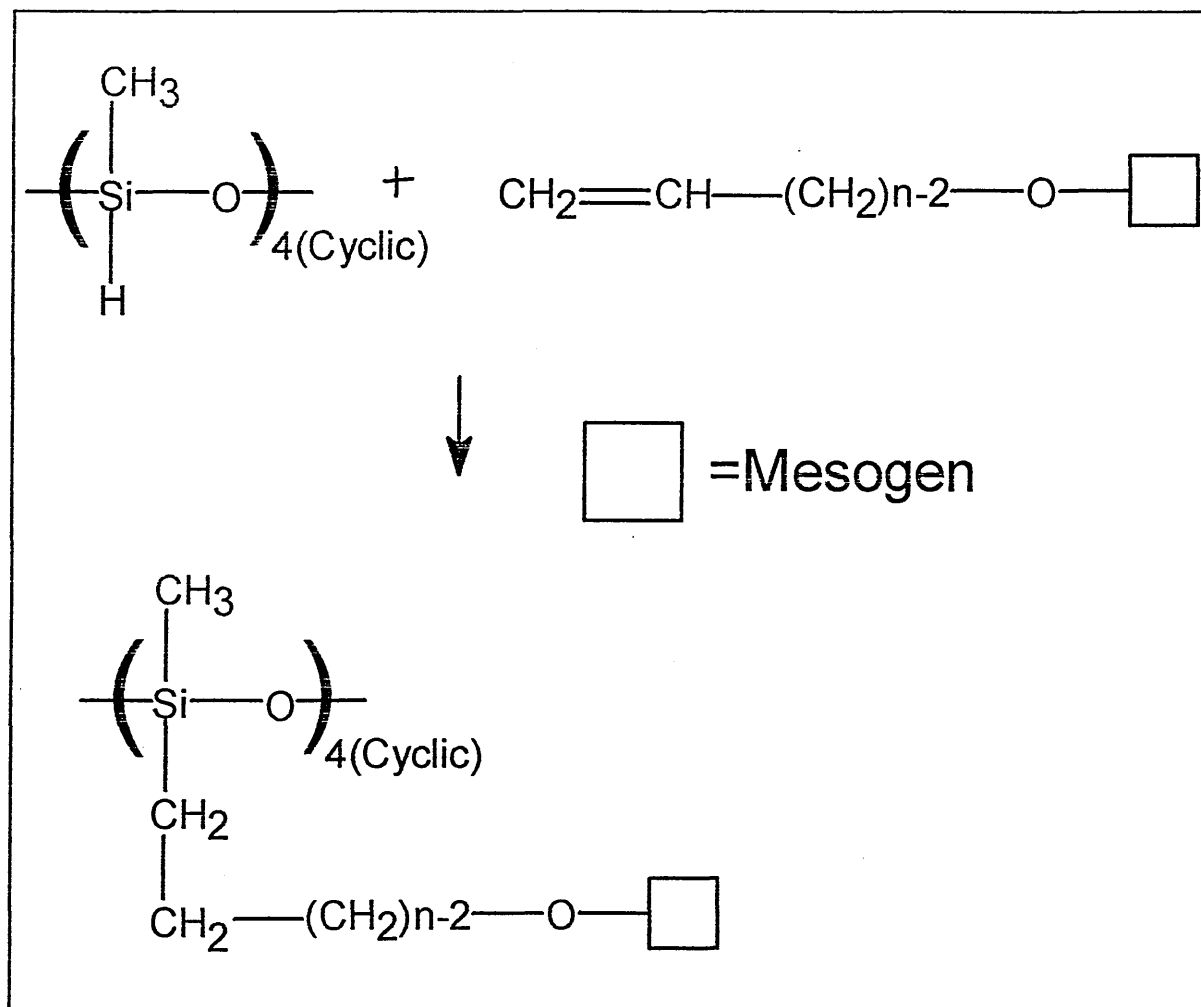
IR (cm⁻¹) 2990 , 2190 , 1410 , 1270 , 1100

¹H-Nmr. 0.0(s) , 4.5 (s)

2.4.14. Synthesis of ring systems.

Note: All polymer products were subjected to micro analysis and were monitored for Si-H disappearance.

Scheme 10. Synthesis of cyclic LC systems based on tetramethylcyclotetrasiloxane.



Route A.

Tetrahydrogenmethylcyclotetrasiloxane (0.147 g, 6.11×10^{-4} moles) was added to a flame dried two-necked flask equipped with a nitrogen balloon and a septum cap. The whole apparatus was sealed in foil to exclude light. The alkene terminated mesogen (2.68×10^{-3} moles, 10% excess) was dissolved in dry THF and added. Hexachloroplatinic acid in THF (50% solution added such that mole ratio of catalyst to alkene was 1:10), freshly prepared in a dry box, was added. The solution was stirred for five days at 50 °C, progress being monitored by the disappearance of the Si-H stretch at 2160 cm^{-1} in the IR spectrum. Pure polymers were isolated by GPC using Sephadex LH-20 gel and dry THF as the solvent. The column was monitored by TLC using 90% petroleum spirit/10% ethyl acetate. Solvent was removed by rotary evaporation and the polymer dried under vacuum as the isotropic liquid. Problems with the GPC method lead to the development of a different method for purification. As an alternative the crude product was dissolved in acetone. After standing for a few days the siloxane polymer separated as an oil and the acetone was decanted off.

Route B.

Problems with the 'dryness' of the THF led to the use of an alternative solvent. The method was as for route A except that dry toluene was used as the solvent

and propan-2-ol was used to dissolve the catalyst. The temperature could be increased to 80°C thus reducing the time for complete reaction.

2.4.15. Synthesis of linear polysiloxane liquid crystals.

To a flame-dried, three-necked round bottomed flask fitted with a nitrogen balloon and rubber septum and sealed in foil was added poly(hydrogenmethylsiloxane) (1.0 g). The mesogen (1.76×10^{-2} moles, 10% excess), dissolved in the minimum amount of dry toluene, was added. Hexachloroplatinic acid, dissolved in propan-2-ol (catalyst/ alkene = $1:1 \times 10^{-4}$) was added via the septum and the mixture was heated to 60 °C. The reaction was monitored daily (2-5 days) until the Si-H stretch had disappeared in the IR spectrum. After cooling further toluene was added dropwise to ensure complete dissolution of the polymer. The pure polymer was then reprecipitated a number of times from iced methanol until monitoring by TLC (dichloromethane) detected no free mesogen present. The methanol was removed under reduced pressure and the polymer was dried in the isotropic state under vacuum.

2.4.16. Synthesis of polysiloxane elastomers.

A range of elastomers incorporating various mesogens and cross-linking densities were produced. The general method for a system incorporating a 10 % cross-linking density is outlined below.

Method A.

Into a flame-dried three-necked round bottomed flask fitted with a nitrogen balloon and rubber septum, and sealed with foil was added poly(hydrogenmethylsiloxane) (1.0 g, 1.988×10^{-4} moles) and divinyl terminated poly(methylsiloxane) (0.611 g, 6.765×10^{-5} moles). Mesogen (1.433×10^{-2} moles) dissolved in a slight excess of dry toluene was added along with hexachloroplatinic acid in propanol (mole ratio of catalyst to alkene = $1:10^4$). The reaction mixture was then heated at 60°C until the Si-H stretch at 2160 cm^{-1} in the IR spectrum had disappeared. The solid material was then washed in a Soxhlet apparatus for two days using toluene and deswollen in methanol. Finally the products were dried under vacuum. Samples prepared as thin films could be purified by immersing in a beaker of hot toluene overnight followed by deswelling with methanol. (see table 2 over page.)

Table 2.

Reaction ratios for production of elastomers of various cross-linking density. The ratios below yield approximately 6.5 g of elastomeric material depending on the RMM of the mesogen used. The percentage of crosslinking assumes equal reactivities of mesogen and cross-linking agent.

| % Cross-linking | Moles Polymer | Moles Cross-linker | Moles Mesogen |
|-----------------|-----------------------|-----------------------|-----------------------|
| 10 | 2.00×10^{-4} | 7.96×10^{-4} | 1.43×10^{-4} |
| 15 | 2.00×10^{-4} | 1.20×10^{-3} | 1.36×10^{-4} |
| 20 | 2.00×10^{-4} | 1.60×10^{-3} | 1.28×10^{-4} |

Method B.

For elastomers with side groups having longer flexible spacers, i.e. those based on undecenoyl chloride, it was found difficult to obtain good results using method A. As an alternative it was found that the bare elastomer (without side chains) could be formed first. Once the network was formed a solution of the mesogen dissolved in dry toluene was added along with a little fresh catalyst and the method proceeds as method A.

2.4.17. Synthesis of ring elastomers.

The diagrams below illustrate the synthesis of two novel, potential liquid crystal elastomer systems. Synthetic methods were as for elastomers described previously. Table 3 at the end lists typical quantities used.

Scheme 11. Synthesis of elastomers based on tetrahydrogenmethylocyclotetrasiloxane.

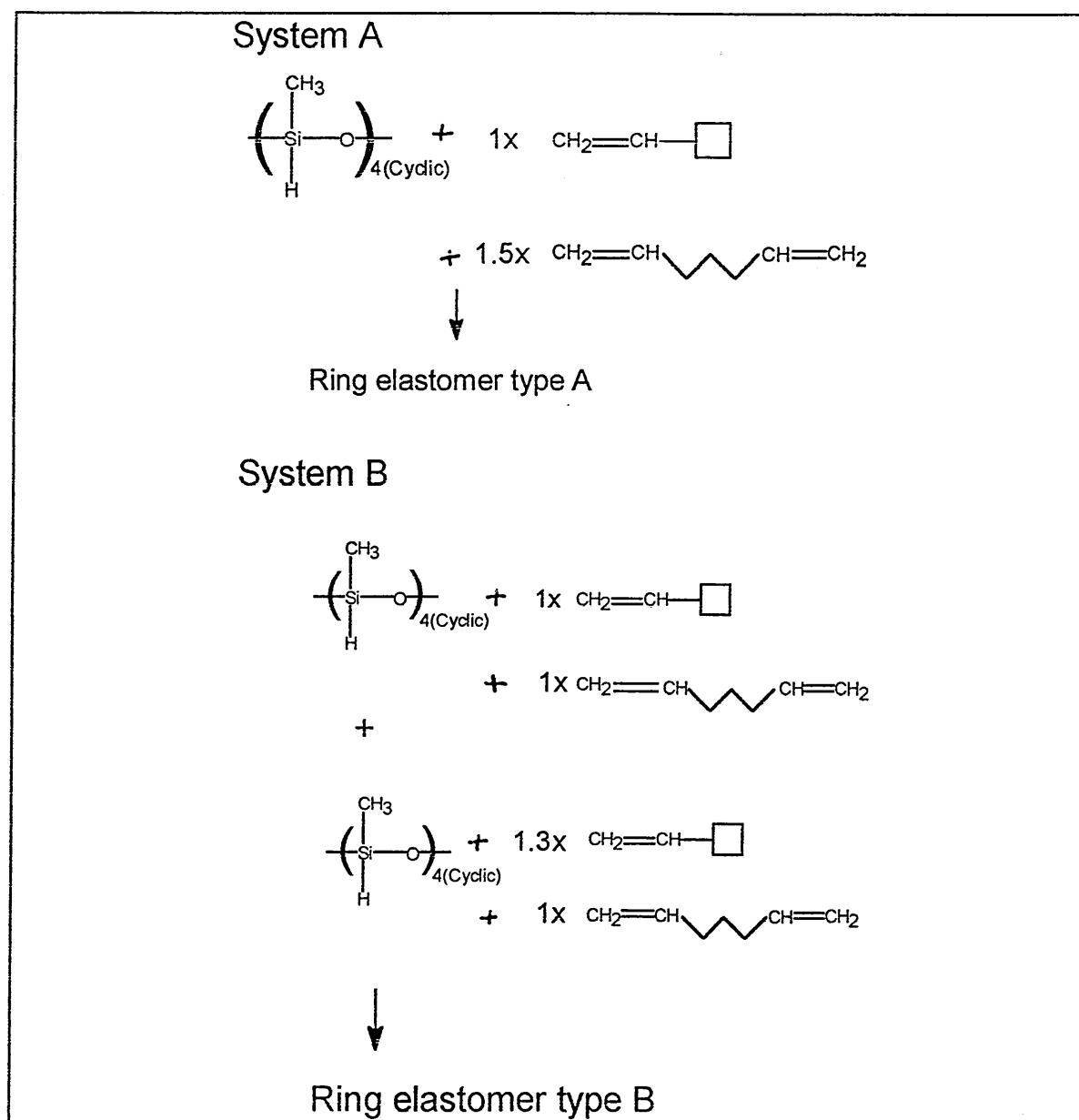


Table 3.

Reaction ratios for the production of ring elastomers based on scheme 11.

| System | Moles ring | Moles cross-linker | Moles mesogen |
|--------|-----------------------|-----------------------|-----------------------|
| A | 4.16×10^{-3} | 6.23×10^{-3} | 4.16×10^{-3} |
| B | 4.16×10^{-3} | 5.20×10^{-3} | 6.24×10^{-3} |

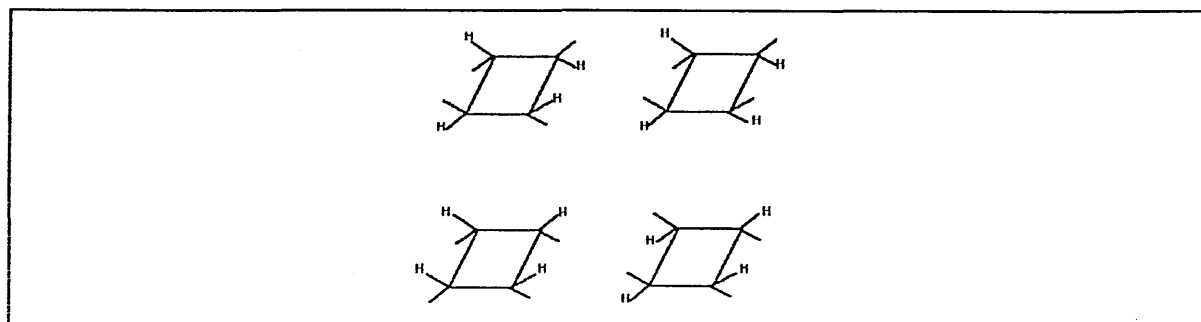
Ring = tetrahydrogenmethylcyclotetrasiloxane.

3.0 Observations on cyclic and linear systems.

3.1 Cyclic polysiloxane systems. (85,86,87)

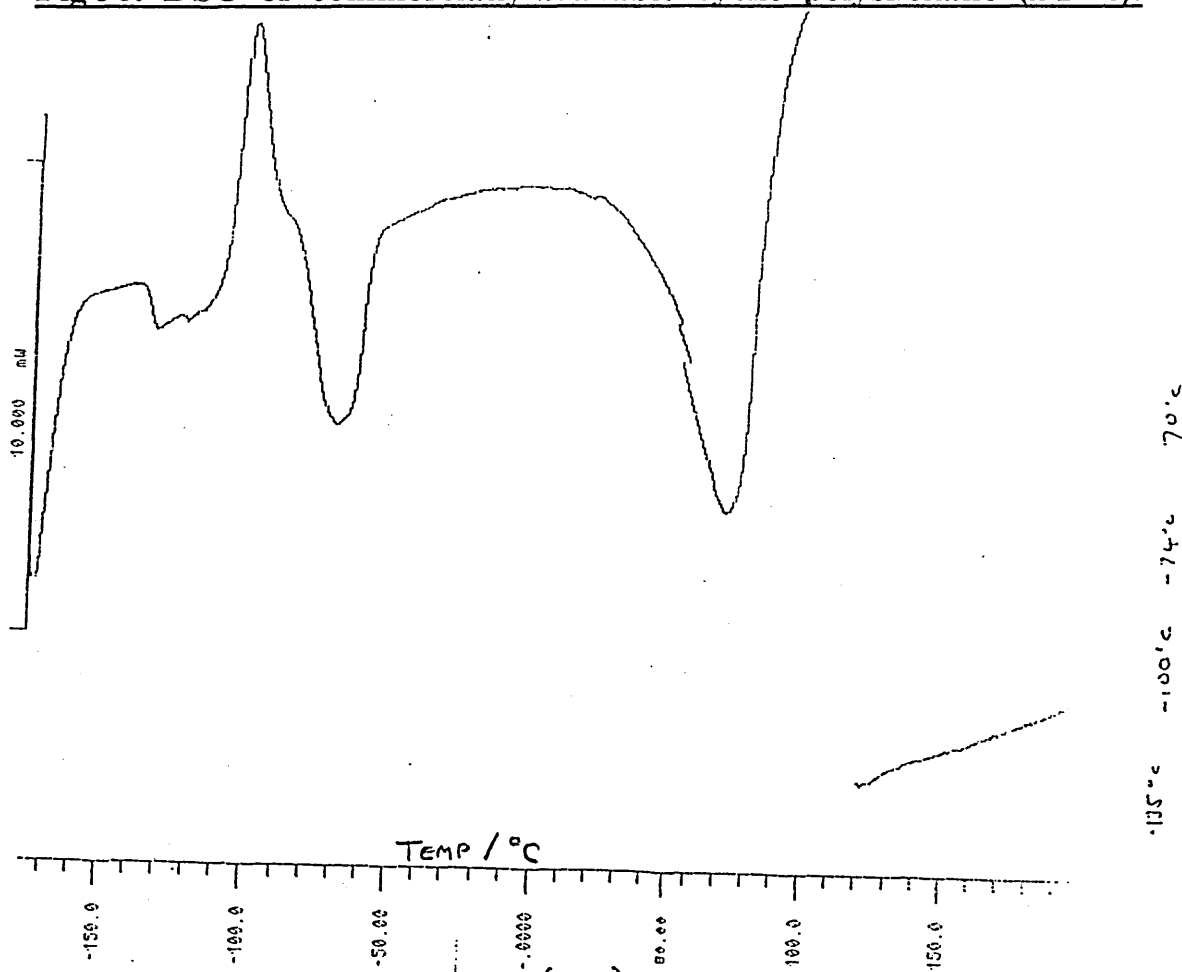
Synthesis of cyclic polysiloxanes was first achieved in 1981. These systems were described as calamitic or discotic with particular interest being shown in cholesteric derivatives. Cholesteric systems have found applications in optical and holographic storage devices (88,89). Kreuzer et al (40) have investigated a number of mesogenic systems using a variety of siloxane ring sizes. Computer modelling and synthetic work has also been previously carried out (90). We have repeated some of this earlier work and synthesised some new systems. The most commonly investigated systems are those that incorporate four siloxane units and we have used this as our cyclic oligomer. As a result we must take into account that there are four possible diastereoisomers of such a system (fig.35). Due to the system being a closed ring, free rotation about the Si-O bond is not possible and the individual isomers can only adopt other configurations allowed by ring 'flipping' (91).

Fig 35. Geometric isomers.



Each isomer is likely to have a distinct melting point. However, the result of a mixture of isomers will probably be a melting point lower than any of the individual isomers coupled with a broadening of the transition.

Fig 36. DSC of commercially available cyclic polysiloxane (DP=4).

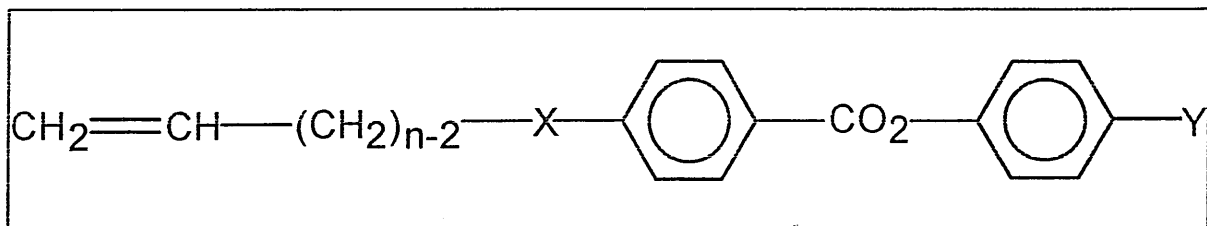


The thermogram (fig.36) appears more complex than expected. However, a broad melting transition is apparent at -100°C . The feature at higher temperature may be associated with decomposition processes, however, TGA would be needed to prove this. The effect of coupling mesogens to such a system has been investigated and compared, where possible, with data

available from the literature. The table below indicates the phase behaviour for the mesogens selected, determined from optical microscopy.

Table 4. Thermal behaviour of mesogens.

The basic mesogen structure was:



Key to table : C = Cooling H = Heating K = Crystalline

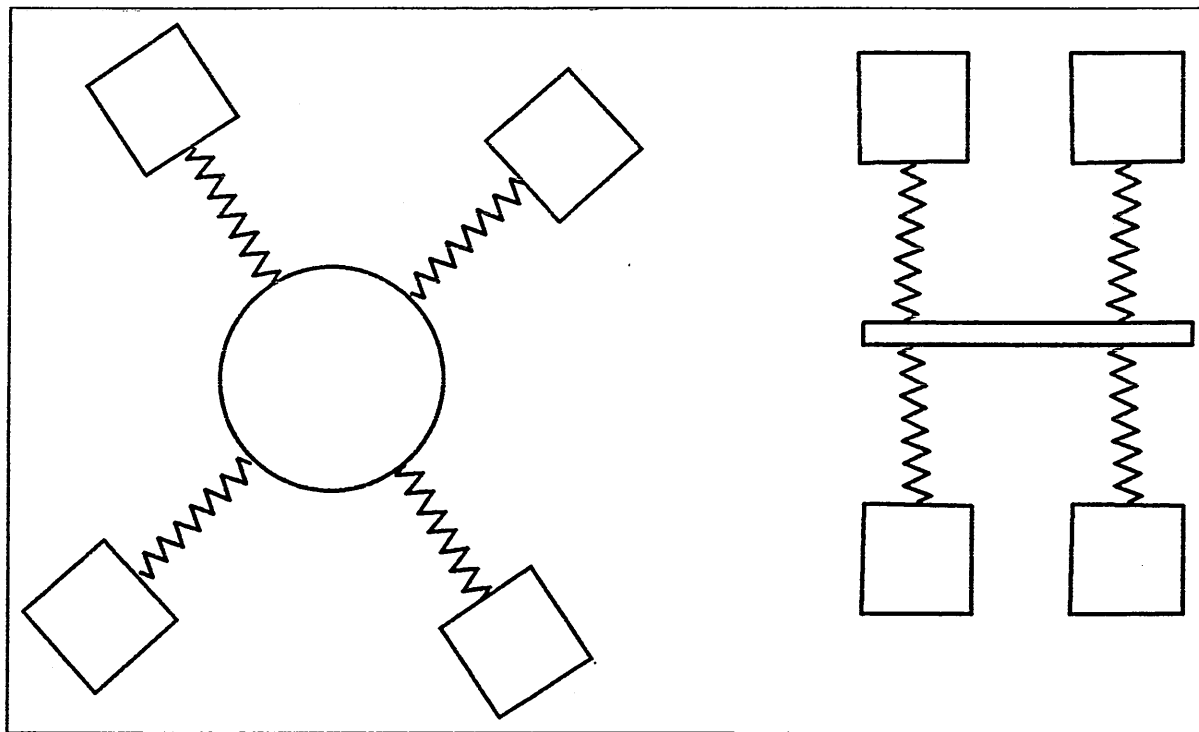
N = Nematic S = Smectic I = Isotropic

| n | X | Y | phase behaviour | Heating / Cooling |
|----|-----------------|------------------|---------------------------|----------------------|
| 3 | O | OCH ₃ | K 86.6I I 57.3N 42.0K | H C |
| 3 | O | CN | K 108.6I I 82.7S 68.9K | H C |
| 5 | O | OCH ₃ | K 82I I 52K | H C |
| 5 | O | CN | K 82I I 71.9N 58.3K | H C |
| 10 | CO ₂ | CN | K 60I I 43N 35S?K | H C |

Characters in the last column of Table 4 indicate that data is either for heating or cooling at a rate of 10 K per minute.

Following general theories we would expect the coupling of mesogens to ring systems to exhibit lc and crystalline phases since they are forced to adopt an ordered conformation. Kreuzer et al ⁽⁴⁰⁾ demonstrated that there are two possible arrangements of such structures (fig.37).

Fig 37. Possible arrangements for ring systems.



Discotic

Bundles

Monte Carlo simulations were performed by Everitt et al ⁽³⁷⁾ on such systems. The model used a ring solely as a constraint on the relative positions of the mesogens. Three dimensional ring translations, rotations and mesogen rotations were allowed in the system in a random order at high temperature. From this, two order parameters were obtained based on the symmetry axes of the rings and mesogens, both taking the form;

$$S = 0.5 (3 \cos^2 \theta - 1)$$

On reducing the temperature a transition ($S=0.3$ to 0.8) was observed at a reduced temperature of 1.4, where the reduced temperature is defined as T/T_{cb} where T is the observed temperature and T_{cb} is the clearing temperature. This general model demonstrated that such ring systems should exhibit discotic behaviour.

Figure 38, overleaf, illustrates the reaction used and Table 5, the phase behaviour for the ring systems synthesised.

Fig 38. Thermal behaviour of modified cyclic polysiloxanes.

Scheme 12: Synthesis of cyclic LC systems.

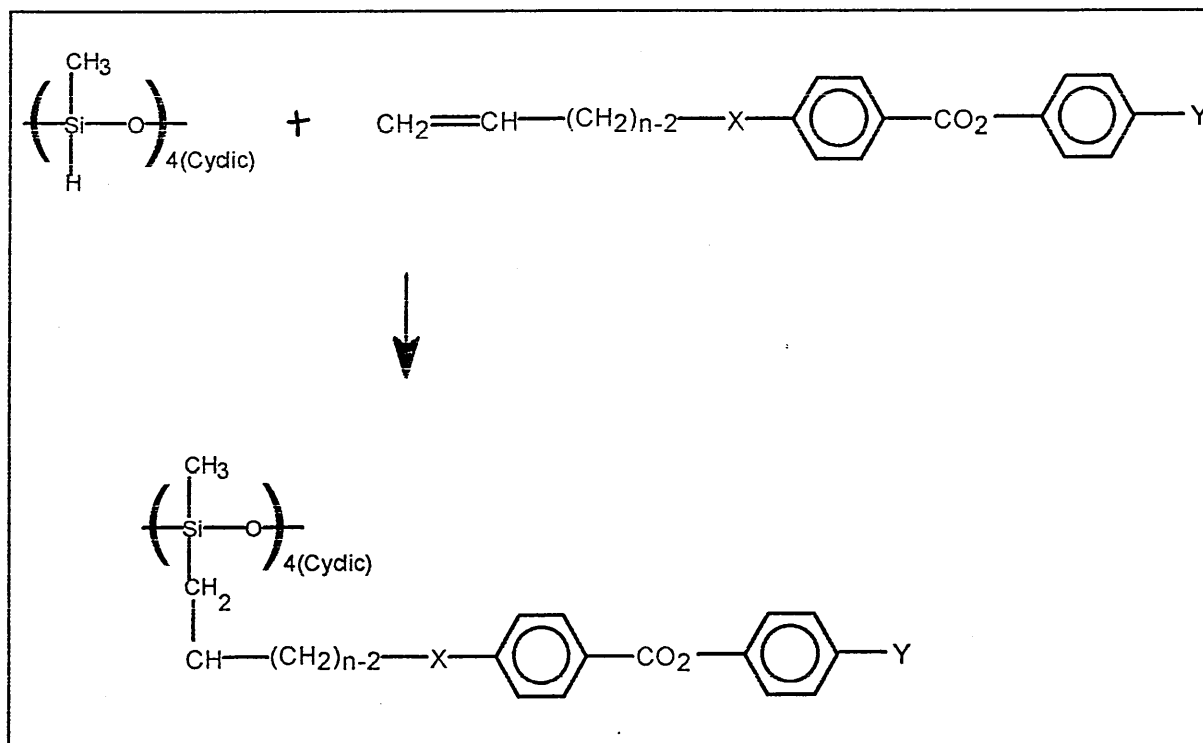


Table 5. Phase behaviour of Mesogens and Cyclic polymers in scheme 12.

| n | X | Y | Mesogen | Polymer |
|----|-----------------|------------------|-----------|---------------------------|
| 3 | O | OCH ₃ | K 86.6 I | T _g 10 I |
| 3 | O | CN | K 108.6 I | T _g 10 I |
| 5 | O | OCH ₃ | K 82 I | T _g 10 N 94 I* |
| 5 | O | CN | K 82 I | T _g -7 N 94 I |
| 10 | CO ₂ | CN | K 60 I | K 46 LC 75 I |

* Microscopy indicates a nematic phase. LC indicates nature of phase not fully known as only DSC data available.

Table 6 lists data available from other sources.

Table 6. Phase behaviour of comparable polymers from other sources.

| n | X | Y | Polymer transitions | Source |
|---|---|------------------|---------------------|----------------------|
| 3 | O | OCH ₃ | Tg 26 N 107 I | Kreuzer (see ref 40) |
| 3 | O | OCH ₃ | Tg 17 I | Cockett(see ref 67) |
| 5 | O | OCH ₃ | Tg 15 N94 I | Cockett(see ref 67) |

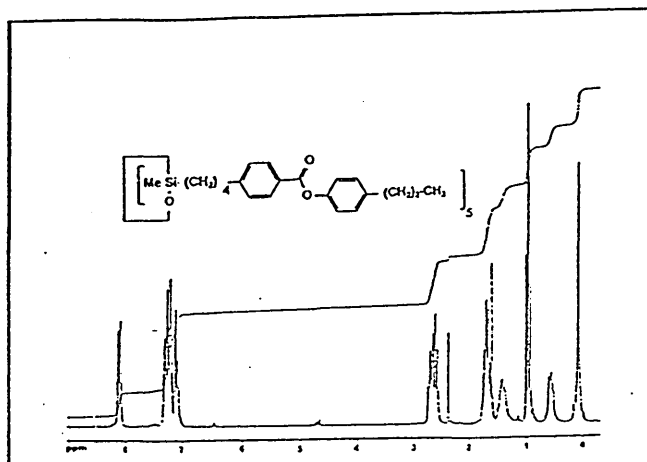
For the methoxy terminated 3 carbon spacer systems, the correlation between our data and that of Cockett is quite good with the observation of only a glass transition. Kreuzer et al⁽⁴⁰⁾ report an increased glass transition temperature and a nematic-isotropic transition. Although model considerations predict such lc behaviour, we observed no such transitions for this system.

While it is accepted that for linear polymers a 3 unit spacer is sufficient to decouple the motions of the mesogen from the backbone, we suspect that in the case of the rings this is not sufficient to overcome the conformational restraints

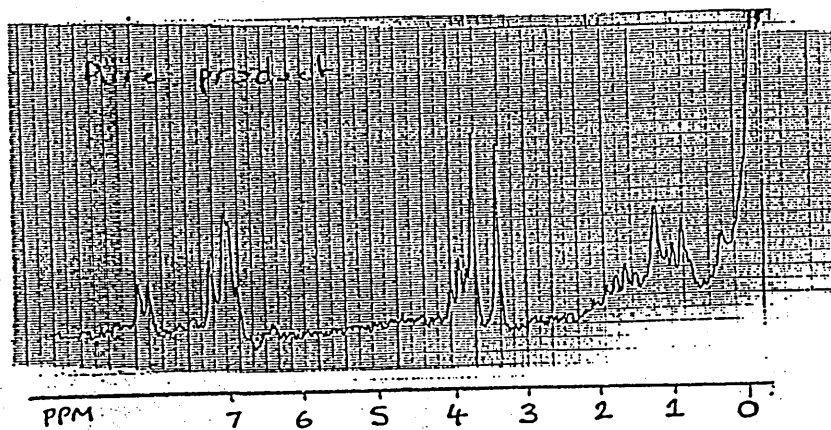
imposed by the rings. The limited degree of flexibility imparted by the spacer also seems to reduce the 'effective' disc structure and hence we observe no discotic phases. Observations on impure systems demonstrated that excess mesogen could induce lc phases in the bulk material of which it is a part. Kreuzer included ^1H nmr spectra for a selection of compounds. Figure 39 illustrates ^1H nmr spectra for one of Kreuzer's purified systems (a), one of our purified systems (b) and the same system with impurities still present at about a 5 mole % level (c). Close examination reveals that a small alkene signal around $\delta=5.0$ is still present in the Kreuzer spectra indicating the presence of unreacted alkene. Our purified sample did not exhibit this. The impure sample showed alkene peaks more prominent than Kreuzer's and exhibited a crystalline transition rather than a glass transition. This indicates that the presence of alkene impurities induced an lc phase in these systems. Nestor et al ⁽⁷⁷⁾ have demonstrated the importance of purity and this example reinforces this. Therefore we speculate that the lc phase for this system was due to the presence of mesogen impurities which could interact with the mesogens associated with ring systems.

Fig 39. ^1H nmr spectra for ring systems.

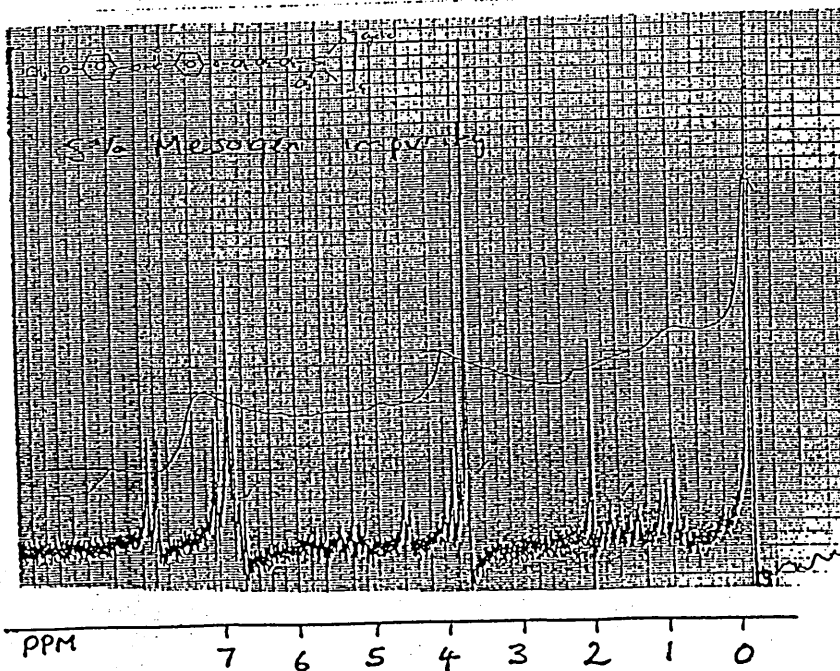
a)



b)



c)



Following this, we attempted some studies on the effect of doping the pure ring system with excess mesogen. At high proportions of excess mesogen sharp, first order thermal transitions indicating a crystalline system were observed. Microscopy indicated a nematic texture. As the system approached 50% excess mesogen the crystalline transition has broadened quite markedly. Lower proportions of excess mesogen (down to 10 mole % excess) were also observed to form crystalline materials on standing, however, these were not observable by DSC due to supercooling.

Example DSCs and a table of data are presented in Fig.42 and Table 7.

Fig 40. DSC curves for 90% and 50% excess mesogen.

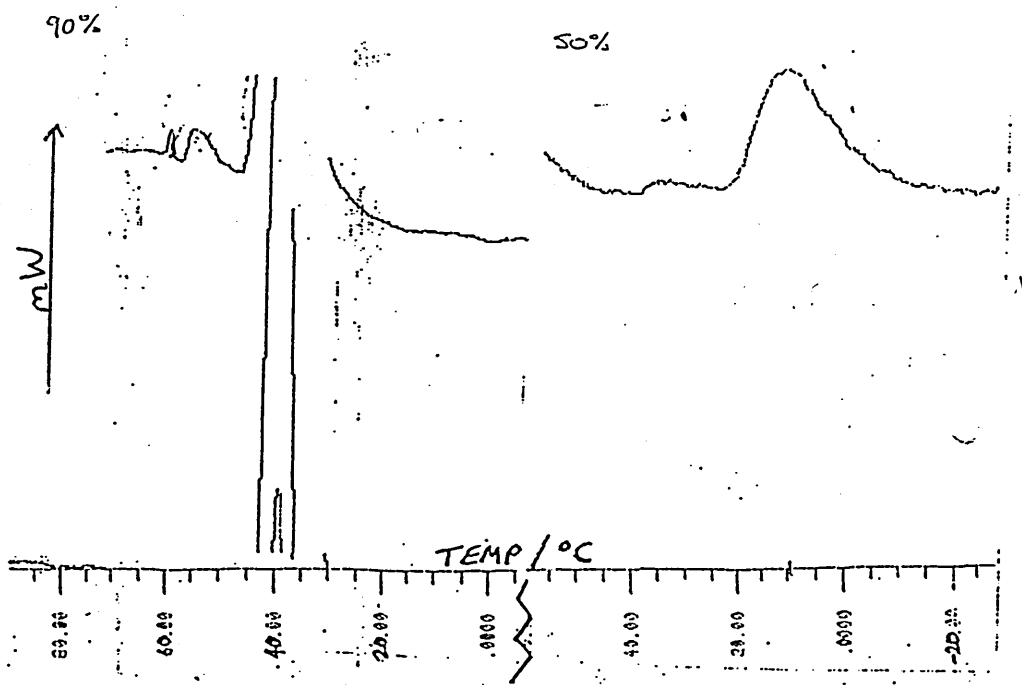


Table 7. Phase behaviour of doped cyclic polymer systems.

| % Excess mesogen | Transitions on cooling | Peak width °C |
|------------------|------------------------|---------------|
| 100 | I57.3N42K | 7 |
| 90 | I59.9LC55.4LC41K | 17 |
| 80 | I51.1LC32.7K | 25 |
| 70 | I43.5LC28.0K | 28 |
| 60 | I35.8LC18.0K | 28 |
| 50 | I35LC8.6K | 35 |
| 40 | I45.3 * 10.0K | 25 |
| 10 | -4 ** | - |
| 0 | Tg-40 | - |

* Small broad transition.

** Small broad transition.

Fig 41. Phase diagram of 'doped' ring systems.

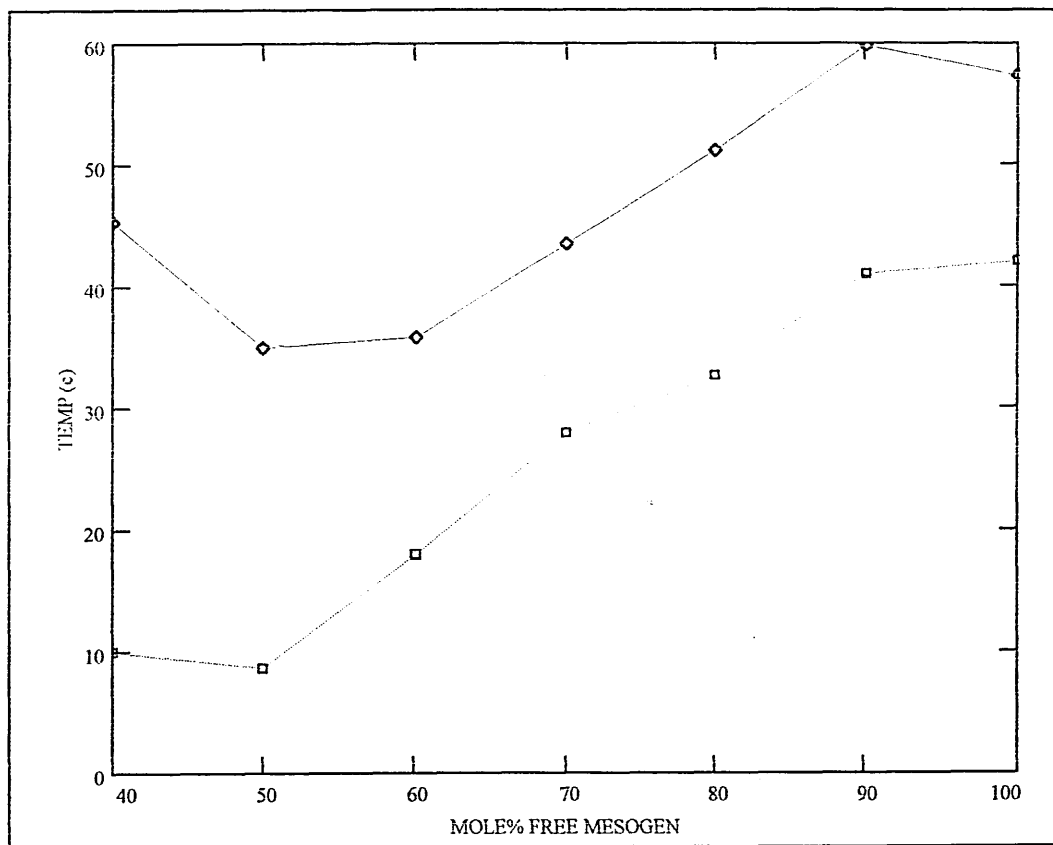
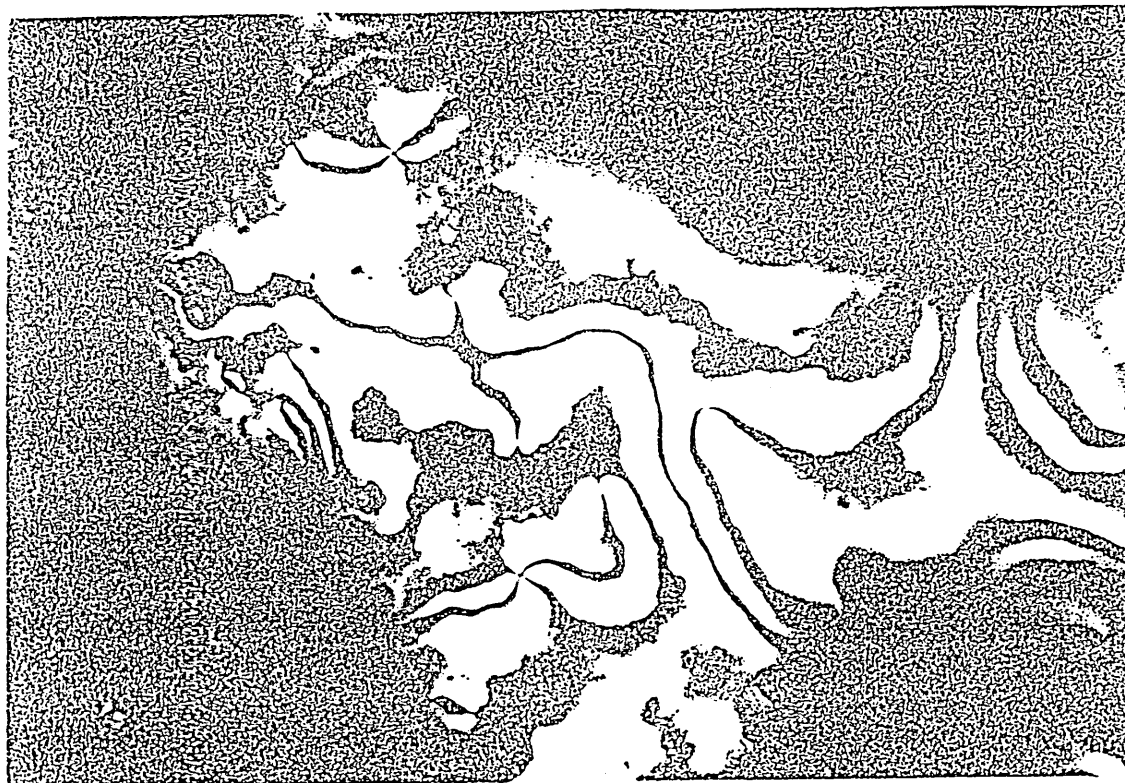
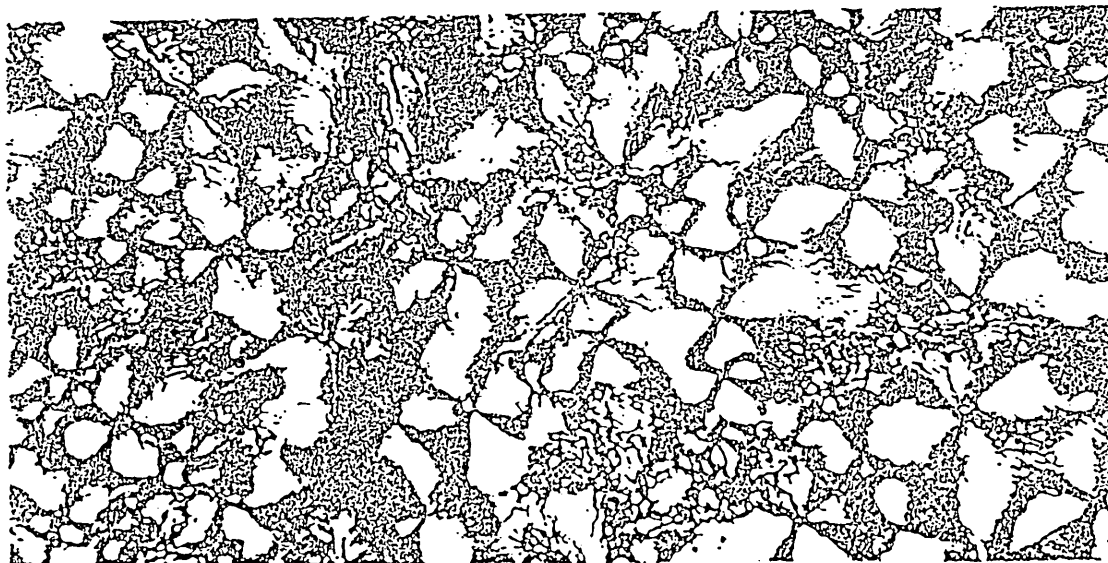


Fig 42. Optical micrographs of 7 mole% doped C3OMe ring system.

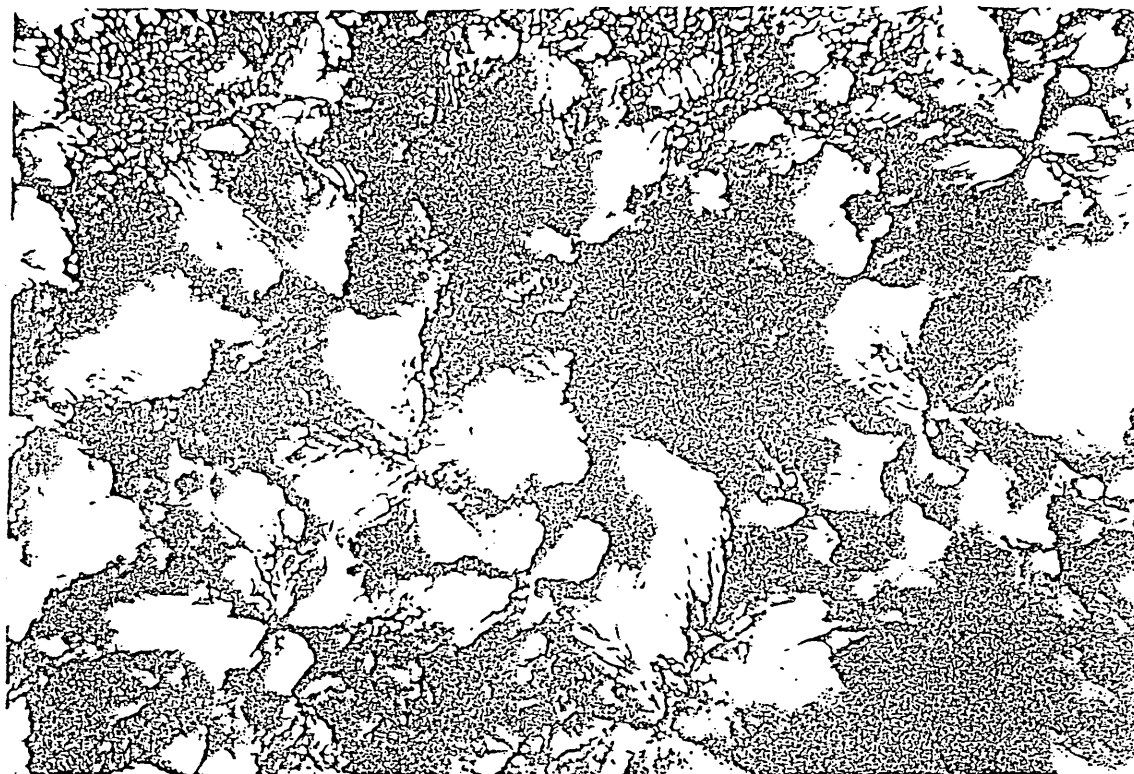
1. Pure mesogen. Nematic phase.



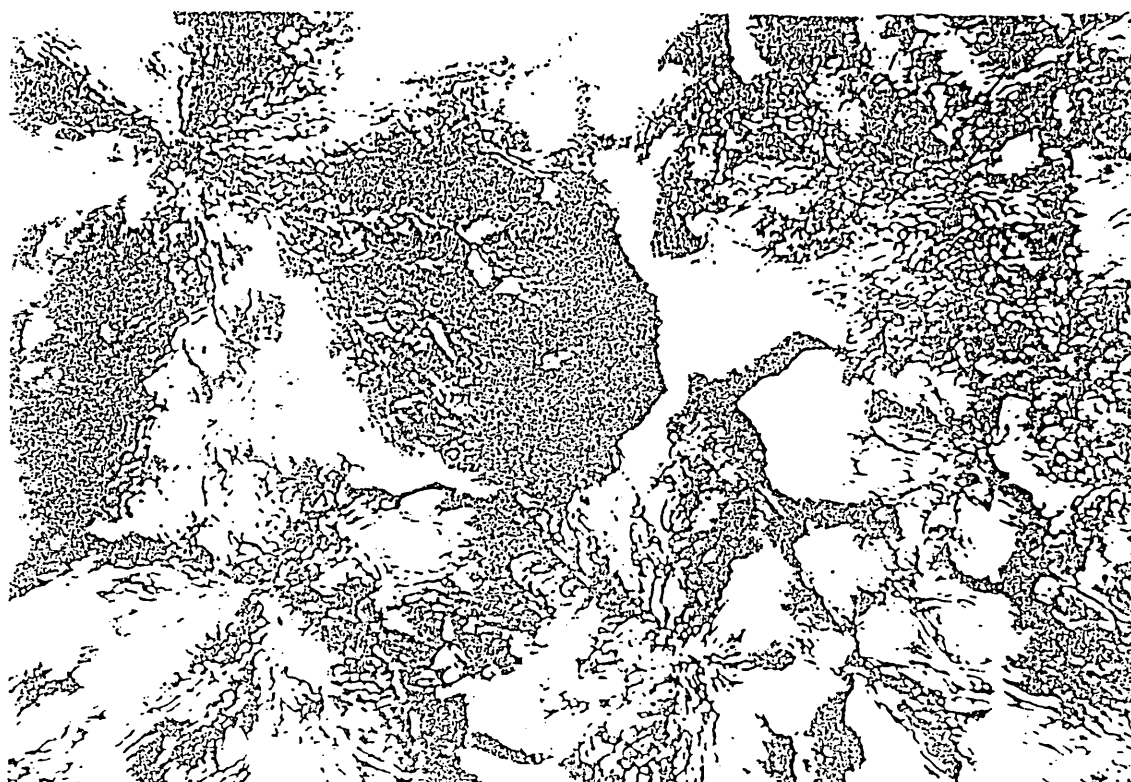
Ring system. LC phase forming from isotropic phase.



Onset of crystallisation.



Crystallisation almost complete.



The data appears to indicate that a large excess of mesogen has very little effect on the phase behaviour of the pure mesogen. An additional phase is observed at 90% mesogen possibly indicating that the ring molecule could stabilise a smectic phase not normally obtainable in the pure mesogen. As the proportion of ring increases the transition temperatures are lowered and peak widths are broadened due to the mixture of molecules. The introduction of ring material may disrupt the packing of the nematic phase thus inducing the smectic phase. As the two types of material are fully miscible a eutectic mixture is formed. For mixtures in the region 40 to 90% free mesogen, the rings disrupt the crystalline packing of the pure mesogens, hence lowering the melting point, while the free mesogen possibly forces the rings to adopt some form of ordered structure, hence the lack of a glass transition. X-ray characterisation would be required to confirm this. Below 40% free mesogen the picture becomes less clear. Crystalline transitions are completely absent. Here we speculate the mesogens are 'diluted' to such an extent that interactions are no longer possible. Ring behaviour dominates and we see evidence of the glass transition. Microscopy indicates (Fig.42) that these materials exhibit some form of lc behaviour, the exact structure of which could not be determined. Further observations made at very low mesogen impurities i.e. 5% or less would demonstrate that liquid crystal behaviour observed in these materials must be due

to free mesogen still present. Purity is normally the critical factor in obtaining reliable data for liquid crystals. Recently, Bunning et al ⁽⁸⁶⁾ demonstrated that ring systems with residual unreacted mesogen exhibited variations in thermal behaviour. However, in this case we have demonstrated that the impure material yields lc properties not normally accessible in the pure systems. Both Kreuzer and Bunning investigated systems based on five or more siloxane units. Generally such systems are found to exhibit liquid crystalline behaviour. Conformational restraints within four unit systems appear to inhibit the formation of liquid crystal phases for ring material based on short spacers. Longer spacers may allow the mesogens to decouple sufficiently from the ring to result in liquid crystal behaviour. However, it is unlikely that such materials would be discotic and we would speculate that they would behave as pseudo-linear liquid crystal polymers.

3.2. Linear polysiloxane liquid crystals.

Linear liquid crystal polysiloxanes have been investigated intensively by Finkelmann et al (92), Gray et al (93) and Nestor et al (94). Due to the flexibility of the polymer chain, pure poly(dimethylsiloxane) has a low glass transition temperature of -127 °C. We would expect that this would allow the production of substituted systems having very low glass transition temperatures in comparison to hydrocarbon analogues. While lower T_g s are indeed observed, Ringsdorf and

Schneller (95) demonstrated that they were generally in the region 0-30 °C and not nearly as low as the unsubstituted polymer. Therefore while the spacer appears to decouple the motions of the mesogen from the backbone, we can only view this process as a partial decoupling mechanism (see introduction). Figure 43 and table 8, below illustrates some data obtained by Finkelmann et al ⁽⁹²⁾.

Fig 43. System investigated by investigated by Finkelmann.

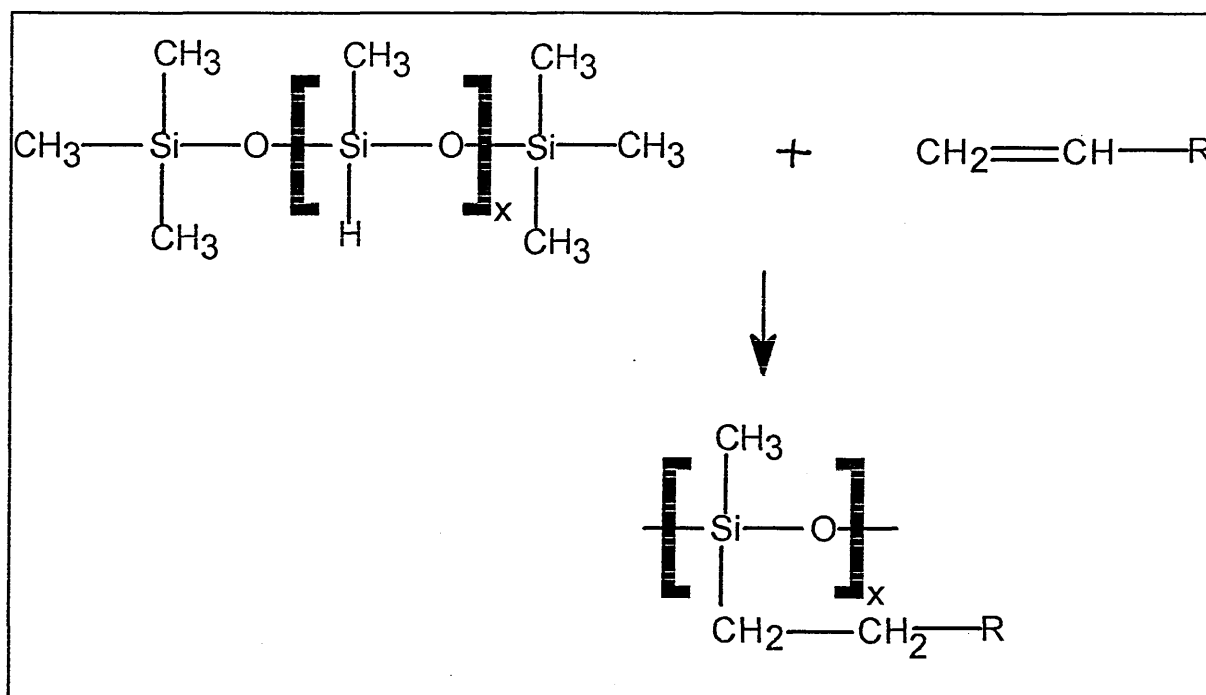
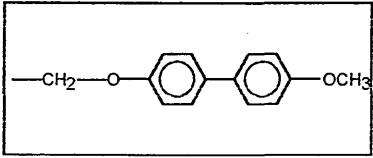
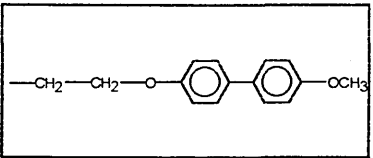
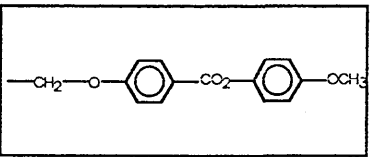


Table 8. Phase behaviour of Mesogens and linear substituted polymers.

| R | Mesogen | Polymer |
|--|---------|----------------------------|
|  | K 292 I | K 398 I |
|  | K 389 I | K 396 I |
|  | K 362 I | T _g 288 N 224 I |

We have synthesised some side chain polymers based on Finkelmann's work and on a novel system with the view to producing elastomers at a later stage. The polymers were prepared using commercially available poly(hydrogenmethylsiloxane) and a polysiloxane produced by cationic ring opening polymerisation. End group analysis by ¹H nmr and thermal analysis by

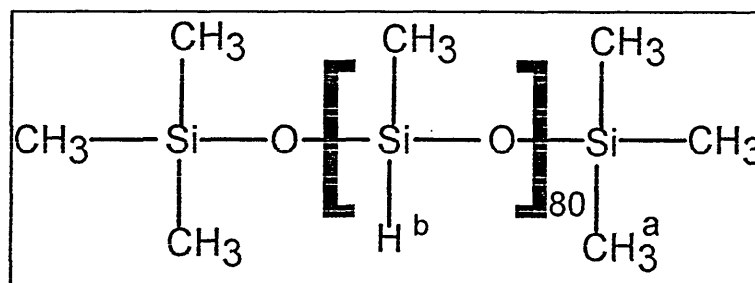
DSC allowed the two polymer backbones to be compared.

Table 9. DSC data for polysiloxane backbones.

| Sample | Glass transition temperature (°C) |
|-------------|------------------------------------|
| Commercial | -137 |
| Synthetic A | -139 |
| Synthetic B | -137 |

For a polysiloxane of DP=80 as specified by Petrach we would expect the following ¹H nmr data.

Table 10. ¹H nmr data for poly(hydrogenmethylsiloxane).



| Proton | Total count | Ratio a/b |
|--------|-------------|-----------|
| a | 258 | 3.45 |
| b | 80 | |

Table 11, below shows the experimental ratios obtained from ^1H nmr spectra.

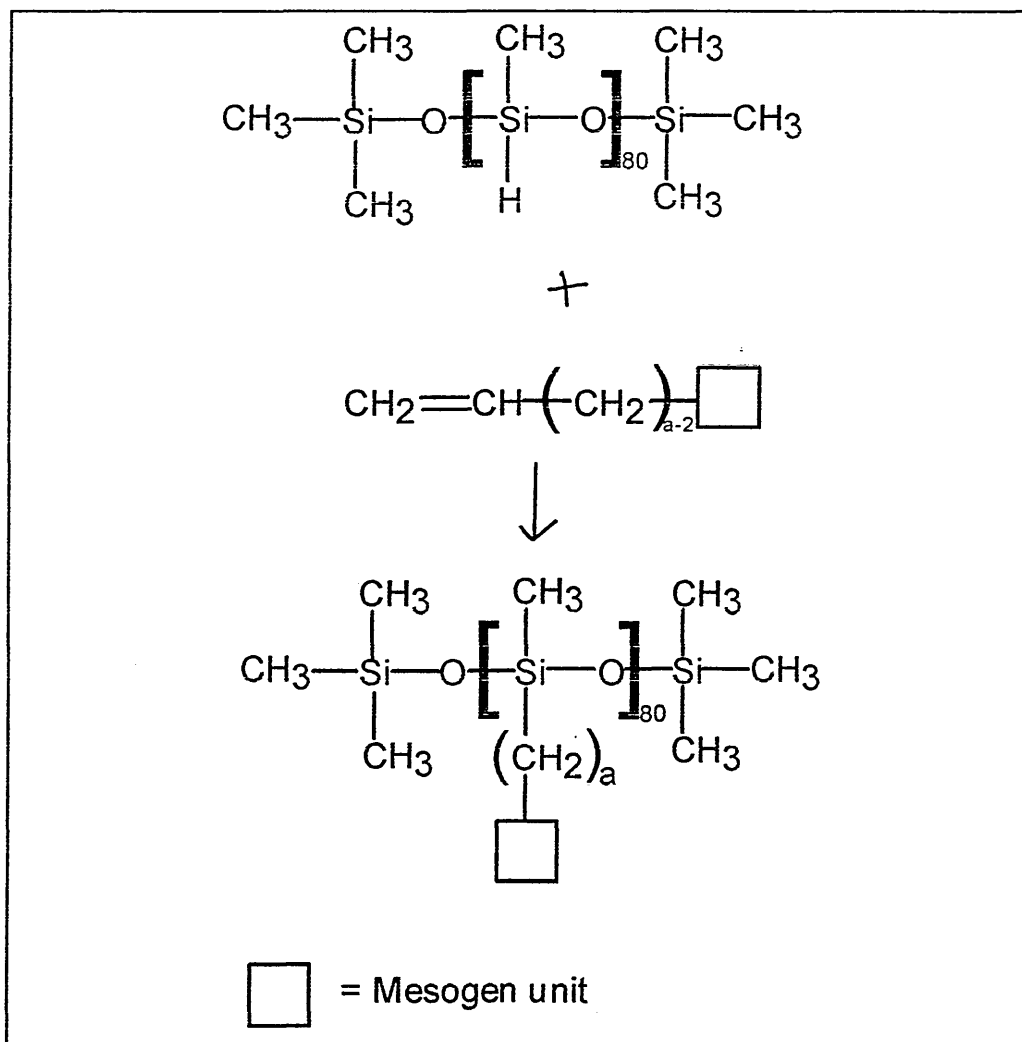
Table 11. Comparison of theoretical and measured data for

poly(hydrogenmethylosiloxane).

| Sample | Ratio a/b |
|-------------|-----------|
| Theoretical | 3.45 |
| Commercial | 3.38 |
| Synthetic B | 3.50 |

The DSC and ^1H nmr data indicate that the behaviour of our synthesised polymer backbones is comparable to that of commercial equivalent. Further comparisons will be made for the substituted polymers. Potential Ic polymers were then synthesised according to the scheme below.

Fig 44. Scheme 13: Synthesis of linear polymer liquid crystals.



The phase behaviour of the products is summarised in table 12 below.

Table 12. Phase behaviour of mesogens used in fig. 45.

| a | x | y | Phase behaviour |
|----|-----------------|---------------------------------|-------------------------|
| 3 | O | OCH ₃ | K 86.6I |
| 5 | O | OCH ₃ | K 82I |
| 5 | O | CN | K 82I |
| 10 | CO ₂ | CO ₂ CH ₃ | K 76.1S 83.4 N 91.6I |

Table 13 below represents data from polymers obtained after several heating and cooling cycles.

Table 13. Phase behaviour of modified polysiloxanes used in fig 44.

| a | x | y | Phase behaviour |
|----|-----------------|---------------------------------|-------------------------------|
| 3 | O | OCH ₃ | Tg0N58I (c) Tg- 10N60I (s) |
| 5 | O | OCH ₃ | Tg-5N58I (c) |
| 5 | O | CN | Tg5S182I (c) |
| 10 | CO ₂ | CO ₂ CH ₃ | K72S87N96I (c) |

(c) = Commercial polymer (s) = Synthesised polymer

Fig 45. DSC curve for Crystalline polymer.

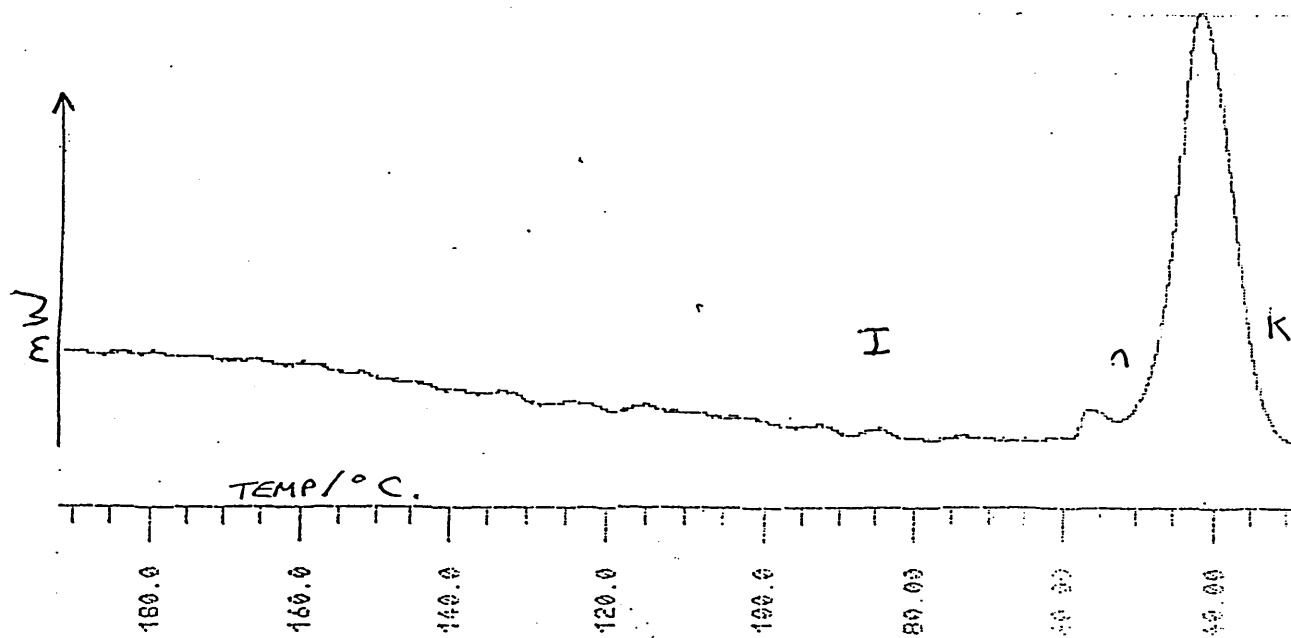


Table 14. Comparable polymer data available from the literature.

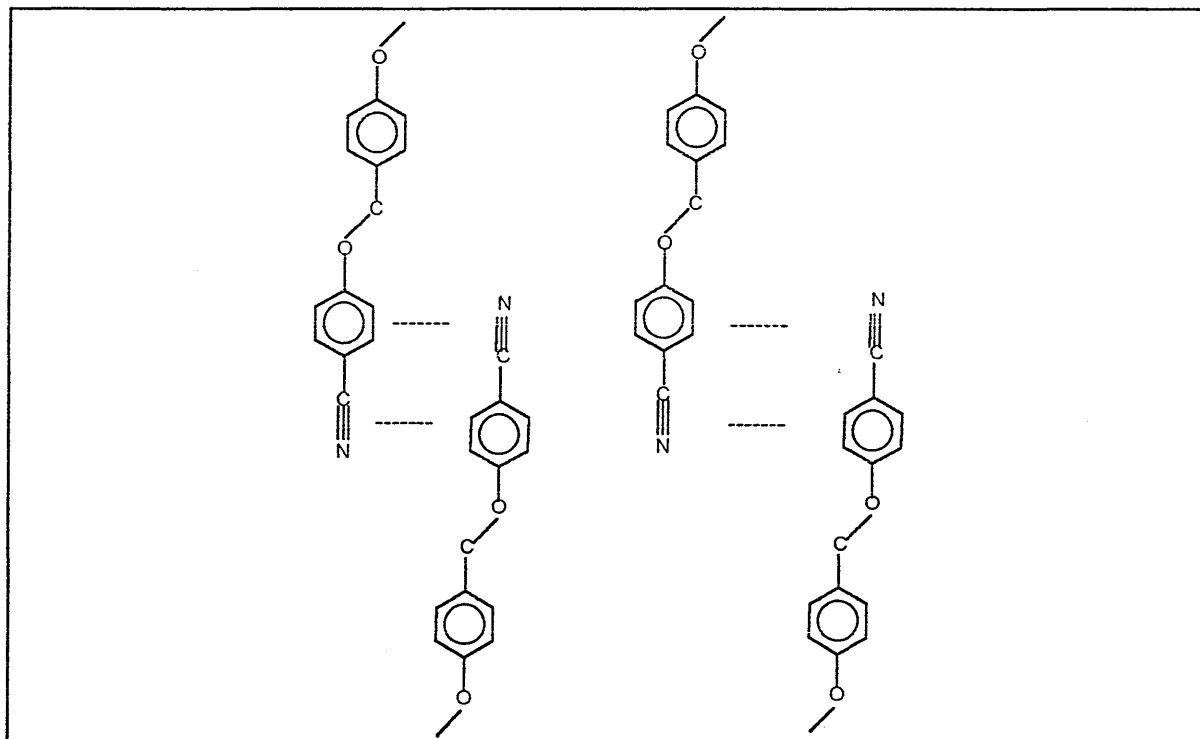
| a | x | y | Phase behaviour | Source |
|----|---|------------------|--------------------|----------------------------|
| 3 | O | OCH ₃ | Tg 15N6 II | Finkelmann (see ref 92) |
| 5 | O | CN | K 107S 183.5I | Gray (see ref 93) |
| 11 | O | OCH ₃ | K53S 133I | Ringsdorf(see ref 95) |

Comparing the data we can see that our results are in reasonable agreement with those published. Although the type of transitions match, we have to take into account certain factors. The published data contains little reference to the degree of polymerisation of the polymers, thus making comparisons difficult. Finkelmann et al ⁽⁹²⁾ quote average values of DP=120 for their polysiloxanes while our polysiloxane had a DP=80. Hence modified polymers produced from these two sources should show only small differences due to the RMM differences. An overall observation can be made: Ringsdorf and Schneller ⁽⁹⁵⁾ concluded that even though unsubstituted siloxanes have extremely low T_g s, the spacer does not give sufficient decoupling to enable very low glass transitions to be achieved. In effect the spacer imposes a restraint on the backbone. Due to the increased flexibility of the polysiloxane over their hydrocarbon analogues, we observe a lowering of the glass transition temperature. The lack of polymer characterisation in much of the literature makes comparison with published data difficult. Direct comparison can only be made with Finkelmann et al ⁽⁹⁴⁾ for the 3-carbon spacer methoxy-terminated polymer. Here we see that our transition temperatures are lower. This is in agreement with observations on the effect of degree of polymerisation on transition

temperature (96).

The T_g values of our samples seem low (especially for the synthetic polymer) compared to Finkelmann's. Initially it was thought that this was due to incomplete substitution. However, no residual Si-H stretching was detected by IR and the difference is most likely attributable to the differences in the degree of polymerisation of the polysiloxanes used. On changing from a 3-carbon spacer to a 5-carbon spacer we observe a slight lowering of the transition temperatures. Again this is in agreement with published data (97). Increasing the spacer length enhances the decoupling of backbone and mesogen. In comparison, the 5-carbon spacer cyano-terminated polymer has a smectic phase with a much larger temperature range. (177 °C range compared to 57 °C). This is an effect of the terminal substituent. The cyano unit produces a greater dipole moment than a methoxy substituent and hence the dipolar interaction between neighbouring molecules is stronger. As a result of this increase in dipole moment, we can visualise an interdigitation effect between neighbouring molecules, the result being a smectic phase. (See Fig. 46).

Fig 46. Possible interdigitation due to enhanced dipole moment.



This also agrees with the general observation that increasing the spacer length tends to induce smectic mesophases.

The final polymer contains effectively an 11 carbon spacer although we must take into account that this includes a carbonyl unit. The terminal unit is now a methyl ester. Data for the most closely related compound in the literature is provided by Ringsdorf and Schneller⁽⁹⁵⁾. Here a true 11 carbon spacer is used coupled with a

methoxy terminal unit, so we can only make tentative comparisons. Both polymers are crystalline at room temperature, agreeing with observations that spacers longer than eight carbon units allow sufficient decoupling to induce side chain crystallisation. Again both polymers exhibited a smectic mesophase as expected with longer spacers. However, the methyl ester-terminated polymer also exhibited a nematic phase. This is consistent with low molar mass lc observations. The terminal group is not only greater in size but also induces a greater dipole moment. The size increase disrupts the packing of the smectic layers thus favouring the nematic phase and lowering the isotropisation temperature. The effect of the carbonyl unit appears to be negligible. Due to the increased spacer length, the effect of the linking unit on the geometry of the mesogen relative to the backbone has been greatly diminished. The 3-carbon spacer methoxy terminated unit is common to both the linear and cyclic systems. While the cyclic system exhibits no lc phases, it is of interest to note that the glass transition temperature of this system is almost identical to that of the linear polymer. Hahn and Percec⁽³⁸⁾ also observed similar behaviour for a cyclic system that did exhibit lc behaviour. Here they also noted that the nature of the lc transitions was also almost identical to that of the linear polymer. Considering the differences in RMM this is unexpected and no theoretical basis has been found for this observation.

4. Observations on elastomeric material.

4.1. Polysiloxane elastomers.

Liquid crystalline elastomers were first prepared by Finkelmann et al (98). These early elastomers were based on polysiloxane networks but, since then, liquid crystal elastomers based on both siloxane and hydrocarbon backbones have been made and characterised. A number of synthetic routes to elastomers have been described. Finkelmann et al describe the one step process where mesogens and cross-linking units are coupled to a polysiloxane backbone in a 'one-pot' approach. This tends to yield elastomers with relatively low glass transition temperatures ^(95 and 98). Elastomers based on hydrocarbon backbones have also been produced from monomer and cross-linking units in a single step process, e.g. Barnes et al (99). Legge et al (100) demonstrated a two step process. Initially a copolymer was produced from monomer units. Elastomers were then produced by casting a film of the copolymer in dichloromethane with diisocyanatohexane onto a Kapton sheet. Solvent was removed under reduced pressure and the sample was heated in a uniform magnetic field of 0.6 T at 108 °C for 72 hours to ensure complete cross-linking. Effectively cross-linking is occurring in the nematic melt. The characteristics of the elastomers based on the first two methods are very similar. As expected, due to the differences in backbone architecture, the siloxane based systems have

glass transitions about 10 °C lower than corresponding hydrocarbon analogues. Transitions in both types can be induced either thermally or mechanically. The third system is different in that it exhibits a memory effect (see later) even after holding the sample in the isotropic state for 17 days. On cooling the same direction of orientation always occurs unlike the monomer, which exhibits local alignment. Liquid crystal elastomers present several unusual properties including stress induced molecular switching (101), shifts in phase transition (102), piezoelectricity and electrically induced shape changes (103) and electro-optical properties. We have been concerned with the synthesis and characterisation of some known and novel liquid crystal elastomers, adopting the approach of Finkelmann. The majority of the work involved methoxy-terminated phenyl benzoate esters. (See fig. 47.)

Fig 47. Scheme 14: Typical synthetic route for production of elastomers incorporating methoxy terminated phenylbenzoate ester.

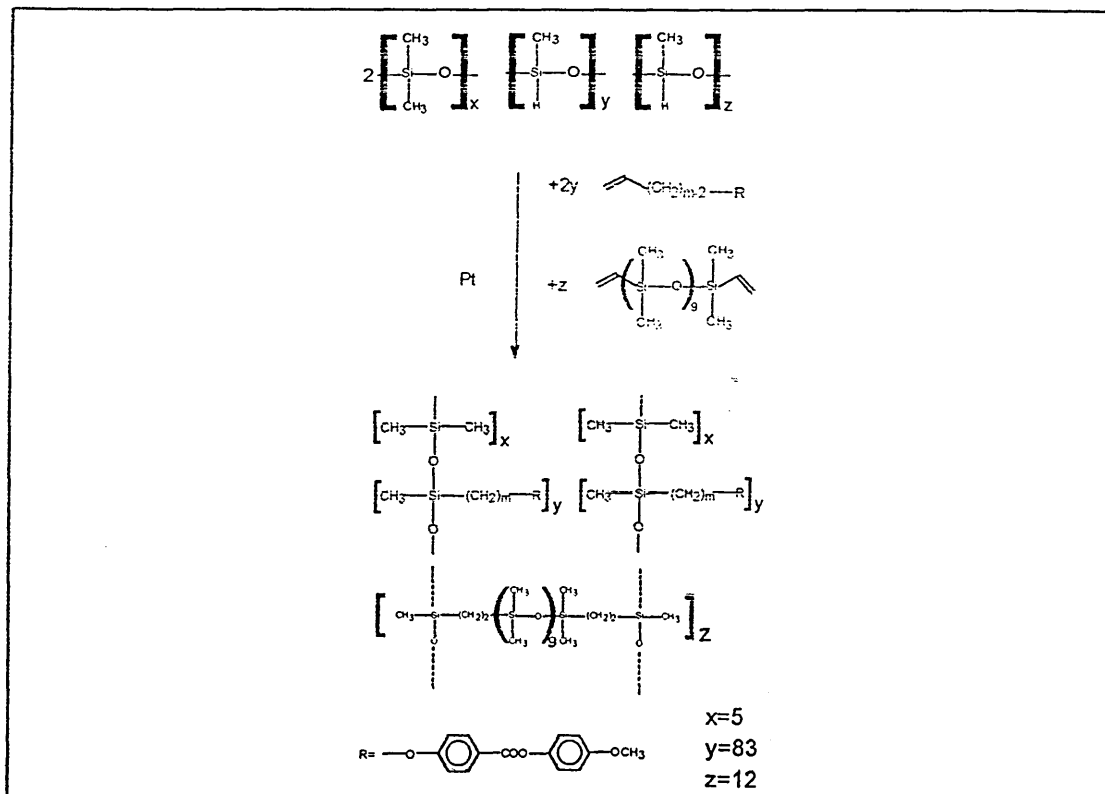


Table 15 below represents the phase behaviour previously observed for elastomers and linear polymers incorporating similar structural units.

Table 15. Thermal behaviour for linear polymers and elastomers produced via scheme 14.

Elastomer: $x=5$ $y=83$ $z=12$

Linear: $x=5$ $y=95$ $z=0$

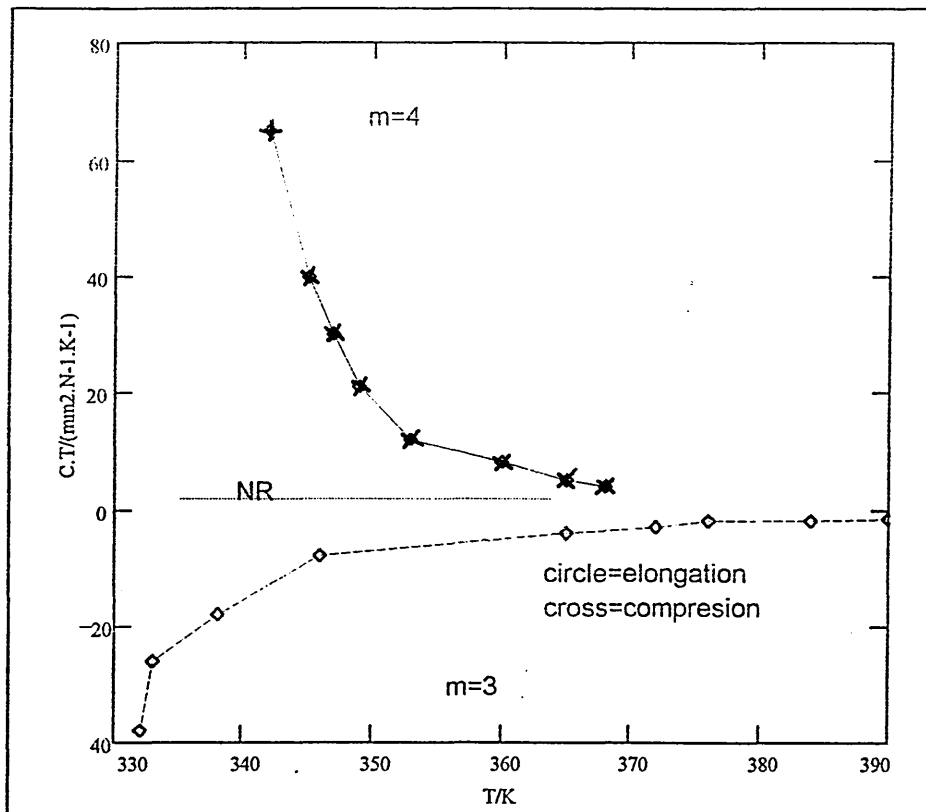
| m | Phase behavior | Type |
|---|----------------|-----------|
| 3 | T_g 285N332I | Elastomer |
| 3 | T_g 288N334I | Linear |
| 4 | T_g 275N343I | Elastomer |
| 4 | T_g 288N368I | Linear |

Here, Finkelmann clearly demonstrated that network and lc properties could be combined to yield an lc elastomer. Later Legge et al ⁽¹⁰⁰⁾ demonstrated that lc elastomers could display memory effects, by which the elastomer 'remembers' the orientational configuration at the time of cross-linking, the degree of this effect being dependent on the density of cross-linking. It is useful to review some of Finkelmann's work on siloxane systems. Liquid crystal elastomers can be obtained by cross-linking lc side chain polymers. In these systems the translational motion of the entire 'molecule', i.e. macro Brownian motions, is prevented. Motions of the chain segments, i.e. micro Brownian motions, remain unhindered. Hence, while lc elastomers exhibit properties characteristic of lc polymers, they also have novel properties such as rubber elasticity (104).

Therefore, above the glass transition temperature the side groups have almost the same degree of freedom as in the analogous linear polymers. Due to their elasticity, the influence of mechanical stress on liquid crystal behaviour is of interest. High birefringence in the lc state leads to these studies being performed at temperatures high enough to induce the isotropic state. Obviously then, stress-optical measurements in this region yield information on the lc units in the isotropic state. The stress-optical coefficient, C , which is a quotient of the birefringence, Δn , is proportional to the optical anisotropy of a chain segment, where $\Delta\alpha$ is the difference between the polarisabilities parallel and perpendicular to the axis of the statistical segment. The sign of Δn tells us about the orientation of the liquid crystal side units. A theory proposed by Kuhn (105) suggests that the product CT , where C is the stress optical coefficient, should not vary with T . This is indeed observed for natural rubber, although strong deviations are observed for liquid crystal elastomers.

Fig 48. CT v T for natural rubbers and lc siloxane elastomers.

(m = side chain spacer length)

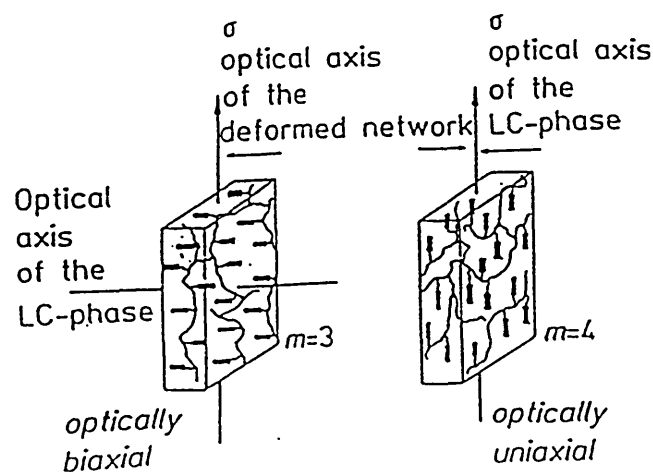


The difference between the m=3 and m=4 curves is explained by the different orientations of the side groups. For m=3, Δn is negative, and hence the refractive index perpendicular to the chain segment is the greatest. The rapid increase in CT as temperature decreases to T_c (clearing temperature) is explained by the formation of pre-transitional clusters. For m=4, the preferred alignment is

parallel to the chain segment. We therefore have two optically different samples. When $m=3$, the sample is biaxial, the optical axis of the mesogen being perpendicular to the anisotropically deformed network. When $m=4$, the sample is uniaxial, i.e. network and liquid crystal optical axis coincide.

Thermomechanical measurements, involving changes in specific volume, can be made on liquid crystal elastomers in a manner analogous to anisotropic solids. Specific volume changes can be obtained over temperature ranges while the sample is macroscopically aligned in the lc state by mechanical deformation. For $m=3$, it was shown that alignment for stretched samples was perpendicular to deformation. As a result we might expect compression measurements to yield an optically uniaxial sample with liquid crystal segments orientated parallel to the axis of deformation. Figure 49, below demonstrates this.

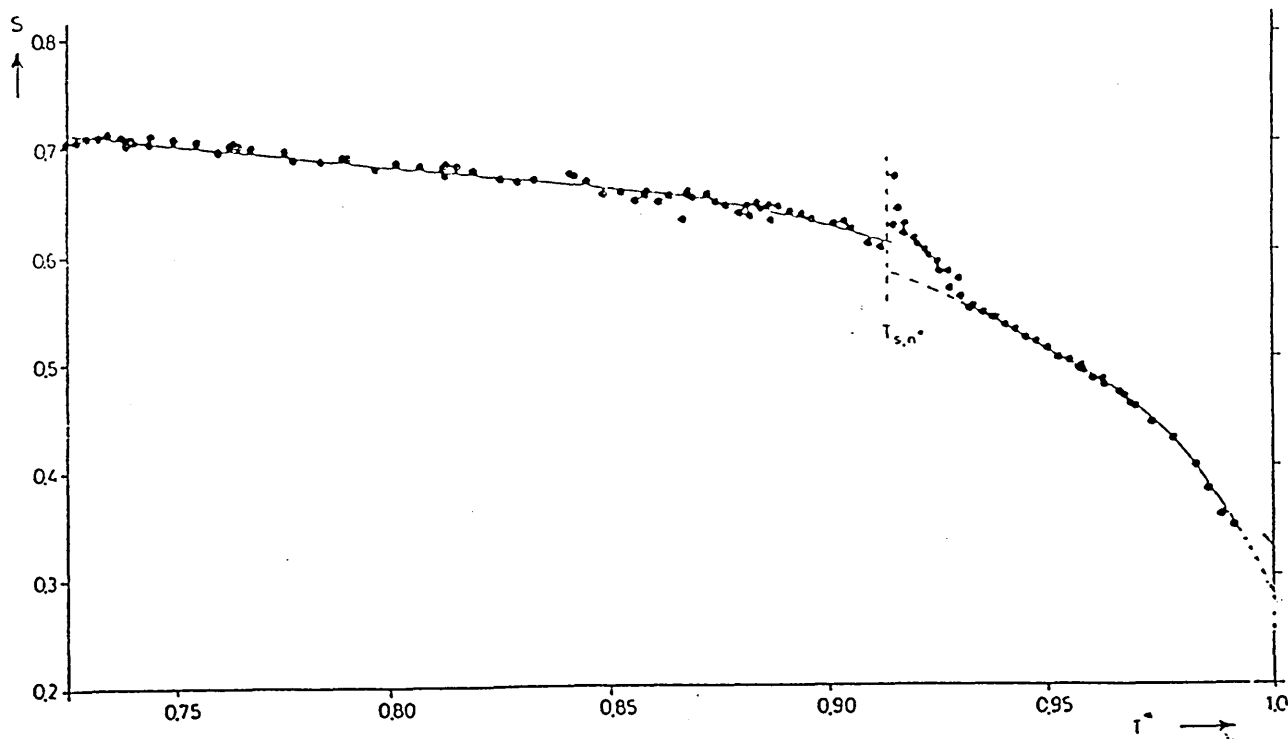
Fig 49. Uniaxial/biaxial systems.



In the isotropic state, the elastomer behaves like a conventional rubber. As the temperature is lowered to T_c an anisotropic deformation of the sample occurs leading to decreases in length. Below T_g the system behaves as a conventional glass. It is clear that mechanical deformation of elastomers causes a macroscopic orientation of the mesogenic groups in a manner analogous to electric or magnetic field-induced effects in conventional low molar mass liquid crystals. As in low molar mass and linear polymer lcs, the order parameter of elastomers can be determined (106). Elastomers that incorporate an IR active unit in the mesogen can either be stressed or heated and the resultant changes in the absorption parallel and perpendicular to a direction within the sample e.g. direction of stretching, can be determined. Schatzle and Finkelmann (107) investigated heating effects using an elastomer incorporating a small proportion of cyano terminated mesogens. The order parameter can be calculated using the formula detailed in section 1.1.6.

The results are shown in figure 50.

Fig 50. Example of the order parameter for an elastomer.



4.1.1. Elastomers incorporating short spacers.

We have repeated some of Finkelmann's work. The results are shown in the table 16 below. The system is based on $m=3$ as in fig 47.

Table 16. Thermal data for elastomers analogous to Finkelmann's elastomers.

| Sample No. | % Cross-linking | Phase behaviour |
|------------|-----------------|----------------------|
| 1 | 20 | T _g 0N53I |
| 2 | 20 | T _g 0N43I |
| 3 | 20 | T _g 0N52I |
| 4 | 20 | T _g 5N52I |
| 5 | 12 | T _g 0N62I |

Samples 1-4 are different samples obtained by the same synthetic route.

Sample 5 is reported by Finkelmann.

Our results are based upon a polymer of DP=80 while Finkelmann's polymers have DP=100. This should be in the region where polymer RMM has little effect on phase behaviour or transition temperatures. In addition, the presence of a cross-linking agent effectively makes the molecular mass the same as the sample mass (assuming a single, network structure) and hence the differences in phase behaviour should now be attributable to variations in cross-linking density. Barnes et al. ⁽⁹⁹⁾ demonstrated that as the degree of cross-linking is increased the glass transition temperature is raised, while the nematic to isotropic transition temperature is generally reduced. This is to be expected as an increase in cross-linking density has two effects. The first is to restrict the

motions of the chain segments between cross-linking units which affects the glass transition temperature, while the second factor is the reduction in liquid crystal density, i.e. fewer mesogens per unit volume, within the sample which will reduce the interactions between mesogens thus lowering the temperature of the Ic transitions. This work was based on polyacrylates which are much stiffer than polysiloxanes. Their observations indicate a relatively large increase in T_g up to 10% cross-linking density after which the effect becomes smaller. Nematic to isotropic transition temperatures generally fall linearly.

4.1.2. Effect of cross-linking density on phase transitions.

For siloxane elastomers we would expect this effect to be less dramatic due to the increased flexibility of the backbone. A comparison of our data and Finkelmann's does show an increase in T_g and a reduction in the nematic to isotropic transition temperature. (See table 17).

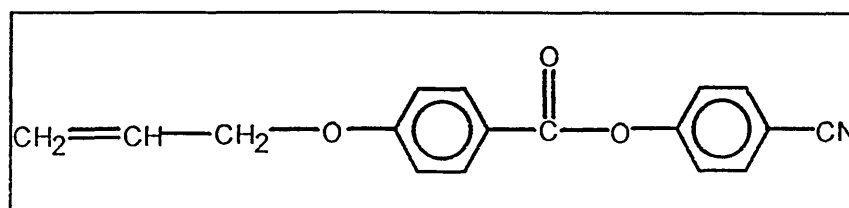
Table 17. Effect of cross-linking density.

| % cross-linking | Elastomer | Linear polymer |
|-----------------|----------------|------------------|
| 20 | T_g 0 N 52 I | T_g 0 N 58 I |
| 20 | T_g 0 N 43 I | T_g -10 N 60 I |
| 20 | T_g 0 N 53 I | ----- |
| 10 | T_g 0 N 60 I | ----- |
| 20 | T_g 5 N 49 I | T_g 15 N 62 I |
| 10 | T_g 0 N 62 I | T_g 3 N 61 I |

Lines 1-3 are different samples (20% cross-linking) synthesised in the same way. 4 is 20% cross-linking while 5 and 6 are taken from Finkelmann's data.

The results for linear polymers represent the range of data observed for materials produced from the same backbone as the elastomers and do not relate directly to elastomers on the same line. From the data we see that at 10% cross-linking both Finkelmann and ourselves observe nematic to isotropic temperatures very similar to the linear polymers. Finkelmann observes a reduction in glass transition temperature on cross-linking while our elastomers exhibit similar or slightly higher glass transition temperatures. This seems more consistent with Barnes' observations on the effects of cross-linking density. We should note that it would be difficult to obtain exactly matching transition temperatures due to differences in the starting polymer. Also consistent with Barnes, both Finkelmann and ourselves observe a reduction in the nematic to isotropic transition temperature on increasing cross-linking density. An elastomer based on a cyano terminated mesogen was also produced.

Fig 51. Cyano terminated elastomers.



Mesogen =

Table 18. Phase behaviour of 'Cyano' and 'Methoxy' terminated elastomers.

| | |
|--------------|---|
| C3CN | Tg 0 LC 52 I (20% cross linked elastomer) |
| Free mesogen | K 108.6 I (heating) I 82.7 LC 68.9 K (cooling) |
| C3OME | Tg 0 LC 52 I (20% cross linked elastomer) |
| Free mesogen | K 86.6 I (heating) I 57.3 LC 42.0 k (cooling) |

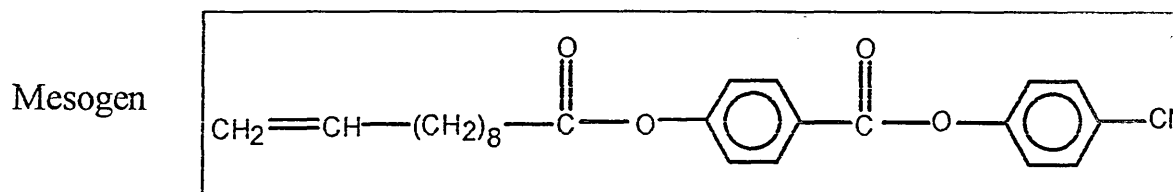
It is surprising that mesogens with such varying thermal transition temperatures yield elastomers of such similar ones. No explanation of this effect has been found in the literature and we assume that the network properties restrict the ordering properties of the mesogen independent of the strength of mesogen interactions.

4.1.3. Elastomers incorporating long spacers.

Attention was then switched to mesogens containing longer spacers. It is well known that in side chain liquid crystalline polymers, long spacer groups induce side chain crystallisation in preference to a glass transition. Initial studies were performed on samples containing 30% cross-linking agent. The results are shown

in figure 52 and table 19.

Fig 52. Elastomers incorporating long spacers and high cross-linking density.



K 60 I (heating) I 42 N 31 S 27 (cooling)

Table 19. Repeat sample elastomers. 30% cross-linking.

| Sample | Heating run | Cooling run |
|--------|----------------|-------------|
| A | 1 K 43 lc 58 I | - |
| B | 1 K 39 lc 56 I | 1 I 25 K |
| | 2 K 36 I | 2 I 25 K |

Here we have an interesting effect. Both samples exhibit an I_c phase on initial heating which is lost on successive heating/cooling runs. This is similar to the memory effect observed by other researchers⁽¹⁰²⁾. Work by Barnes et al⁽⁹⁹⁾ indicates that high cross-linking densities (above 20%) lead to a loss of I_c phases. We initially chose a density of 30% in an attempt to restrict the effects

of side chain crystallisation. Hence, in effect, we appear to be observing an initial memory effect, namely an lc state locked in by the polymerisation process. Heating the sample destroys the lc structure. Cross-linking density was then reduced to 10% with the following observations.

Table 20. Phase behaviour of samples incorporating 10% cross-linking.

| Sample | Phase transitions | |
|--------|-------------------|---------------|
| | Heating | Cooling |
| A | K 45 lc 130 I | - |
| B | K 39 lc 130 I | I 110 lc 18 K |

Hawthorne (108) has demonstrated that for side chain liquid crystal polymers with short spacers and exhibiting a glass transition, a reduction in mesogen density lowers the observed thermal transition temperatures and vice-versa. Our samples exhibit side chain crystallisation temperatures which, unlike glass transition temperatures, we would expect to remain constant (mesogen behaviour should be independent of the backbone) down to the point where the mesogen density is insufficient to induce the liquid crystal state. At this point further reductions would affect the glass transition temperature as we reduce the restrictions on the polymer backbone motion. Hence we observe similar crystalline transition temperatures for both the 10 and 30% cross-linked elastomers. However, we

note that the liquid crystal to isotropic temperature has dramatically increased and is reproducible. The free mesogen (C10CN) exhibits both a nematic and a smectic phase while the elastomer exhibits only a single liquid crystal state. In line with similar liquid crystal polymers we expect this to be a smectic state although X-ray work is required to confirm this. Synthesis of other elastomers, based on long spacer mesogens, was now attempted.

Fig 53. Mesogens incorporating longer spacers.

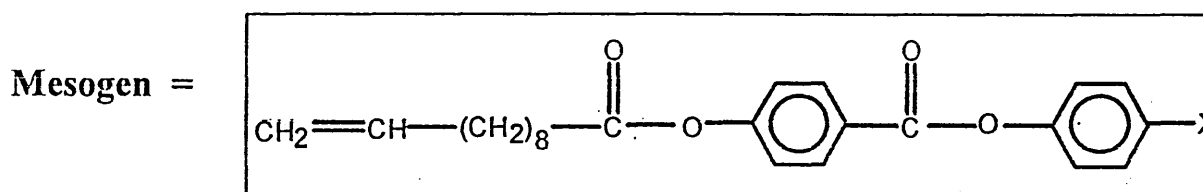


Table 21. phase transitions for mesogens in figure 53.

| | X = OMe (C10OMe) | X = CO ₂ Me (C10CO ₂ Me) |
|---------|------------------|--|
| Heating | K 59 lc 72 I | K 76 lc 83.4 lc 91.6 I |
| Cooling | I 66 lc 40 K | I 91.3 lc 79 lc 52 K |

Attempts at one stage synthesis using these mesogens proved unsuccessful. Two possible reasons arise:

1. The increase in mesogen length, due to the change in the terminal group, prevents the cross-linking process occurring.

2. The C10CN sample achieves cross-linking through a reaction involving the terminal CN group.

The second of these is easily ruled out for three reasons:

a. The conditions of the polymerisation were exactly the same as for previous elastomers involving CN terminated molecules. Effects of catalyst ageing, that can promote cross-linking through CN units, were taken into account and hence fresh catalyst was always used.

b. FTIR measurements on samples clearly indicated the presence of unreacted CN units. Cross-linking effects would reduce the number of CN triple bonds.

c. The results of experiments involving C10CN units were always repeatable. CN is always observed in the resulting elastomer.

The residue from a C10CO₂Me cross-linking experiment was recovered and precipitated from methanol to yield a white crystalline solid with the following transitions (°C).

C10CO₂Me residue K 53.7 lc 70.9 lc 83.6 I

C10CO₂Me Free mesogen K 76.1 lc 83.4 lc 91.6 I
(for comparison)

The lowering of the transition temperatures indicates that a linear polymer species has been formed, possibly a side-chain co-polymer with non-mesogenic

sites being occupied by vinyl terminated cross-linking agent. Following this, a different route was attempted. Unsubstituted networks were swollen and mesogens were allowed to diffuse through them, followed by deswelling and drying under vacuum. In this way it was hoped to produce elastomers based on C10COMe and C10CO₂Me units. The following results were obtained.

Table 22. Phase behaviour for polymers obtained from swelling experiments.

| Mesogen | %Cross-linking | Phase behaviour |
|-----------------------|----------------|-----------------|
| C10OMe | 10 | K 55 I |
| C10OMe | 15 | K 59 I |
| C10CO ₂ Me | 10 | K 72 I |
| C10CO ₂ Me | 10 | K 65 I |

For comparison:

| | |
|-------------------------|--------------------------|
| C10OMe free mesogen | K 59 lc 72 I |
| C10CO ₂ Me " | K 76.1 lc 83.4 lc 91.6 I |
| Unsubstituted elastomer | T _g -102 |

It is unclear what occurred in these experiments. Initially substitution appears to have occurred to some extent. However two factors argue against this:

1. The crystalline transition temperatures of the materials are very high compared to the C10CN derivatives.

2. For the C10CN derivatives we noticed a large drop in transition temperatures compared to the free mesogen. For the C10OMe and C10CO Me samples we observe that the crystalline transition temperature is almost identical to that of the free mesogen.

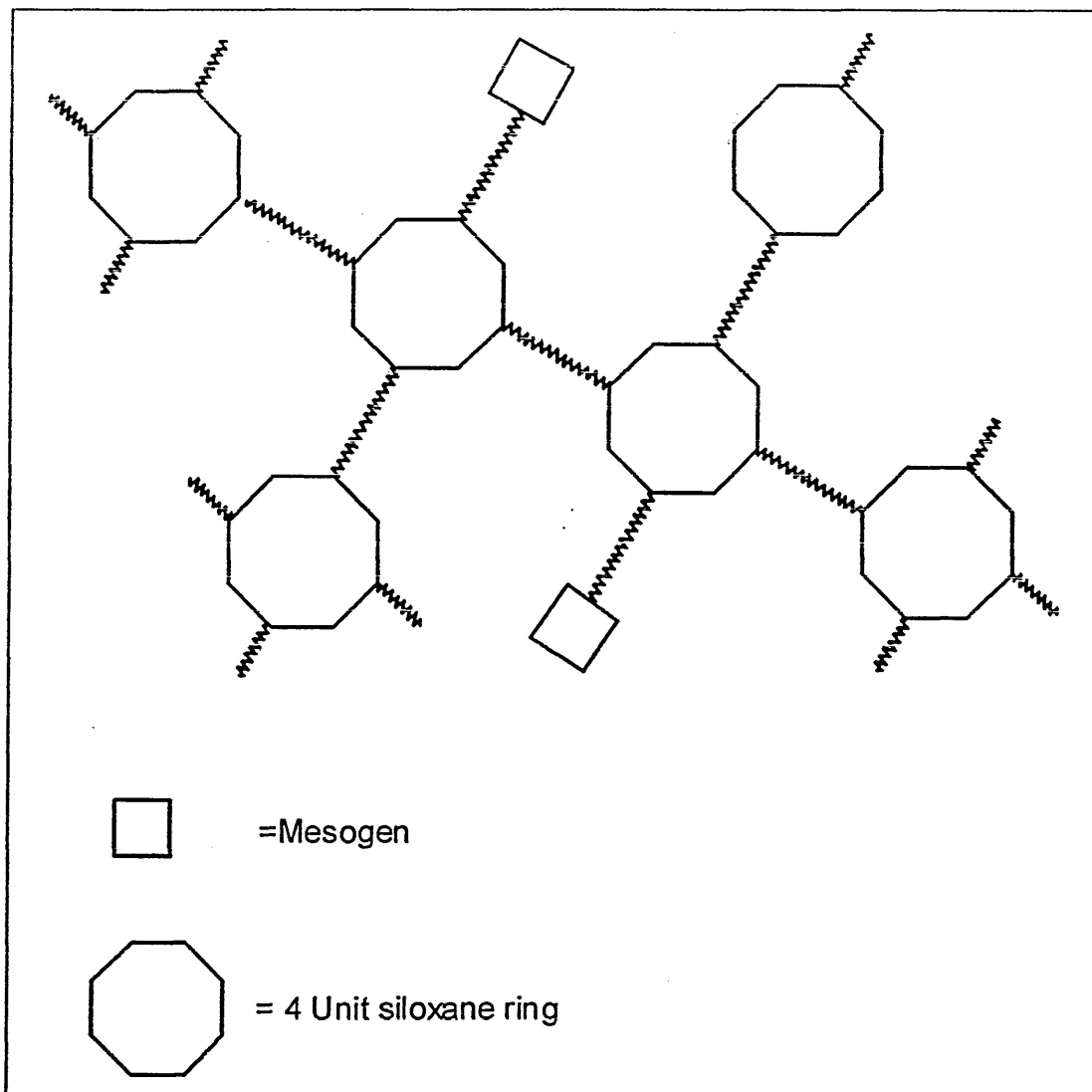
We also note that no liquid crystal transitions were observed for the C10OMe and C10CO₂ Me materials. For these reasons it is likely that the mesogens have simply diffused into the networks without reacting and we have a polymer network 'doped' with free mesogen. The crystalline transition temperature is characteristic of the free mesogen with the liquid crystal transition temperatures probably not detected by the DSC due to poor signal/noise ratios.

4.2. Novel networks.

So far we have studied the effects of cross-linking linear polymer species to produce networks. In addition we have devised and investigated a new route to produce novel networks from cyclic oligomers. Earlier we investigated polymer modification reactions involving four membered siloxane rings to produce disc-like molecules. It follows that it should be possible to link these rings together to produce a network of rings. It turns out that three out of the four sites are required to be involved in the cross-linking process to produce a

network. This means we have a very high cross-linking density of 75% on the rings which leaves 25% substitution by the mesogenic units.

Fig 54. Potential Ic ring network.

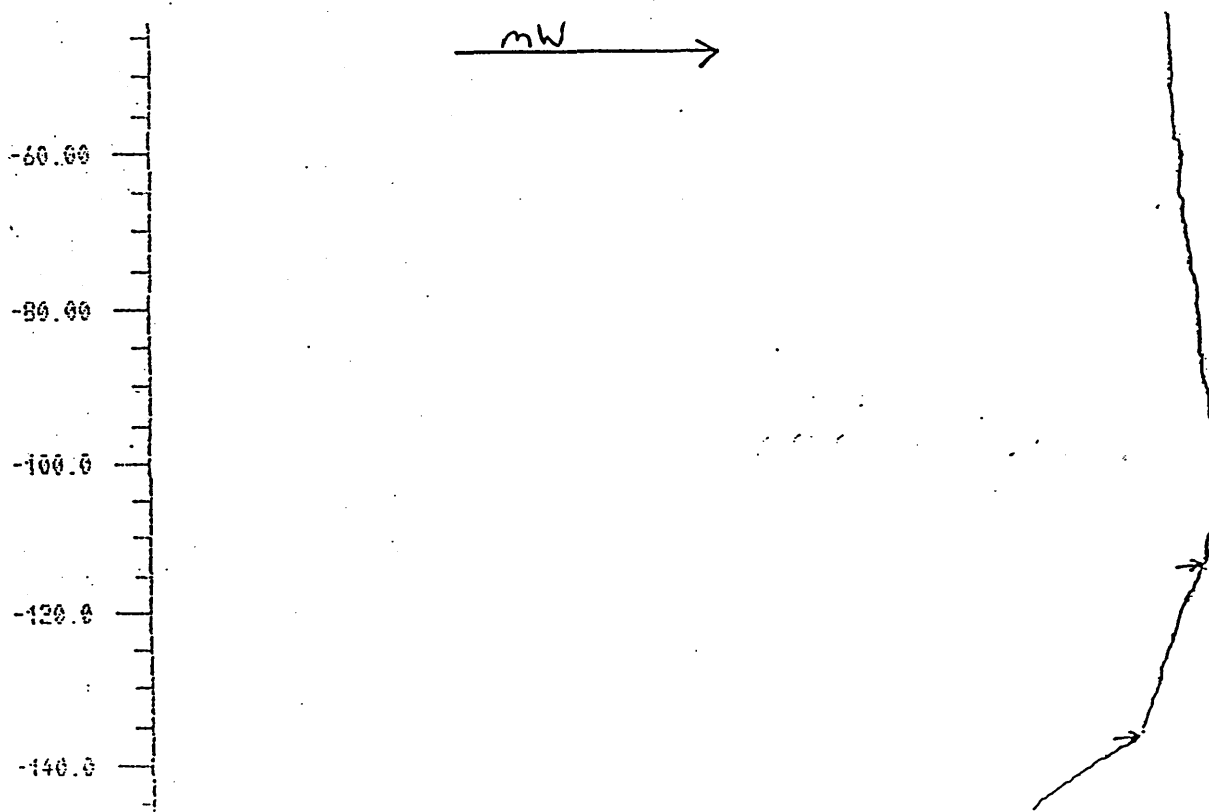


The process was carried out for the mesogens C3CN and C3OMe. The DSC results are indicated below.

Table 23. Thermal data for ring elastomers.

| <u>Mesogen</u> | <u>Transition temperatures</u> |
|-----------------------|---------------------------------|
| C3OMe | T_g -110 T_g -140 |
| C3CN | T_g -115 T_g -135 |
| Typical unsubstituted | T_g -102 linear type network. |

Fig 55. DSC curve for cyclic network C3CN.



It was observed that these ring elastomers were brittle. Their extensibility was limited and yet they were highly compressible, to such an extent that they behaved in ways similar to a rubber ball! A number of interesting points arise from these results. No liquid crystal transitions were observed for these polymers. This is not surprising if we compare them to the disc systems produced earlier. Even with all four sites occupied with mesogenic units, we observed no liquid crystal structure for these materials. With only one site per ring occupied by mesogens in this ring network it would be highly unlikely that a liquid crystal structure would result, unless the polymerisation process orders the rings into layers. If this occurred it might be possible for weak interactions to occur between mesogens in neighbouring layers. However, considering that the layer separation must be of the order of the cross-linker length, this is very unlikely.

Three ways appear possible to overcome this:

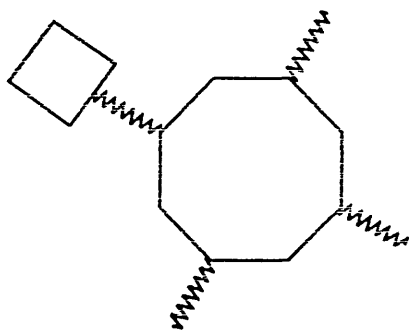
1. Mesogens with longer spacer units could be used. Here we would try to decouple the mesogens from the ring network. However, unlike conventional networks where the chains are held loosely together and the network can easily deform to accommodate larger units, here we have a much more constrained system and it is unlikely that larger units could be successfully incorporated. Indeed, an attempt was made to incorporate the C10CN unit into such a system, the result being a lack of network properties.

2. Larger ring systems could be used. In this way the percentage of sites being occupied by mesogens on the ring could be significantly increased. If a twenty unit ring system were used we could increase this figure from 25 to 85%. The larger ring systems would now resemble a conventional network. As well as predicting a liquid crystal phase, due to the increased mesogen density, we would expect better network properties. Not only should the network deform in more traditional ways, through the cross-links, but also deformation and relaxation properties would be available by ring deformation. We would expect these systems to show enhanced elasticity. Unfortunately such rings were not available to investigate this possibility.

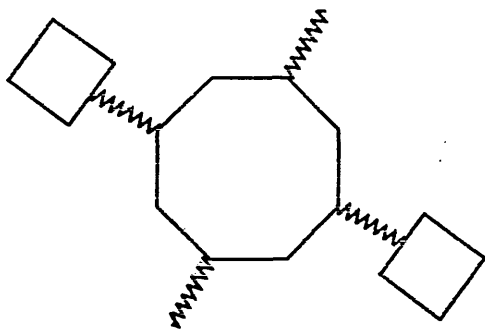
3. It is possible to increase the mesogen density on the four-unit ring system. We now consider a system to be composed of two types of rings, the first the normal type with one mesogen and three cross-linkers per ring and the second containing two mesogens and two cross linkers per ring. By using only two cross-linkers, these rings can only link together as a chain. This process effectively increases the mesogen density from 25% to 37.5% (see Fig. 56). This approach was attempted using the C3CN unit, the result being a single glass transition temperature of -100°C .

Fig 56. Novel 'two ring type' network.

Mixture of following ring structures in network.



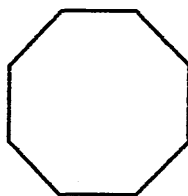
1 Mesogen
per ring



2 Mesogens
per ring



=Mesogen



=Ring

~~~~~ =Cross-linker

## 5. Observations on deformation of elastomers.

### 5.1 Orientation by mechanical deformation.

Classical elastic behaviour, as described by Hooke's law, is characterised by a stress within a material directly proportional to the strain applied to it. A thin metal strip will stretch to a permanent deformation if a force is applied to it. Heating this strip at constant force will cause further deformation. In contrast, an elastomer does not obey Hooke's law and heating will cause the material to shrink. The difference is simply that stretching the elastomer causes elongation of the chains thus reducing their entropy. The retractive effect is caused by the tendency of the system to increase its entropy towards the value it had when undeformed. Gaussian chain statistics (109) can be used to predict the average orientation of the chains. The probability of two cross-links, on a chain of length  $L$ , being separated by a distance  $R$  is found to be;

$$P(R) = \exp(-3R^2/2l_0L)$$

where  $l_0$  is the effective step length at the temperature of network formation.

The free energy due to elastic effects is the average over  $P$  of this phase space weight:

$$F = -k T (\ln P)$$

$$T = \text{Temperature}$$

$$k = \text{Boltzmann's constant}$$

Thus, rubber elasticity and Hookian elasticity depend on different effects. Hookian elasticity is based upon increased energy due to greater molecular separation while rubber elasticity is a result of entropy effects due to chain elongation and cross-linking density. Deviations from a classical stress-strain curve will arise due to the limited extensibility of the chains. Studies into the orientation of mesogenic side groups by mechanical deformation have been carried out by a number of people (110,111,112,113,114). Generally these have involved experiments using X-ray or polarising microscope techniques. Recently, Brauchler et al (115) have investigated the effects of deformation using FTIR techniques. For such studies, a window in the IR spectrum of the elastomeric network is required through which the vibrations of a suitable side group can be observed. The most suitable side group is the cyano-unit. With its fundamental stretching frequency around  $2300\text{ cm}^{-1}$ , it is generally isolated from the typical hydrocarbon frequencies. Brauchler included a cyano-containing side unit at 5% levels as a label quantifiable using FTIR. By polarising the light passing through the sample it is possible to determine the preferred orientation of the sample on stretching at constant temperature or heating at constant draw ratio.

## **5.2. Effects of heating undrawn samples.**

Samples that exist in the glassy state at room temperature can be held at constant length in a frame. The sample can then be heated to its isotropic state. Absorbance measurements using polarisation directions parallel and perpendicular to the beam can be made while the sample cools. Two possibilities arise. If the mesogens align parallel to the stretching direction we would expect the absorbance of the CN stretching vibration parallel to the stretching direction to increase and the perpendicular component to decrease. The opposite would be true for mesogens aligning perpendicular to the stretching direction. However, we also have to consider if the system is biaxial or uniaxial. For the case of perpendicular alignment, uniaxial systems would have a random distribution of the mesogen long molecular axes perpendicular to the stretching direction thus demonstrating rotational symmetry.

## **5.3. Effect of stretching at constant temperature.**

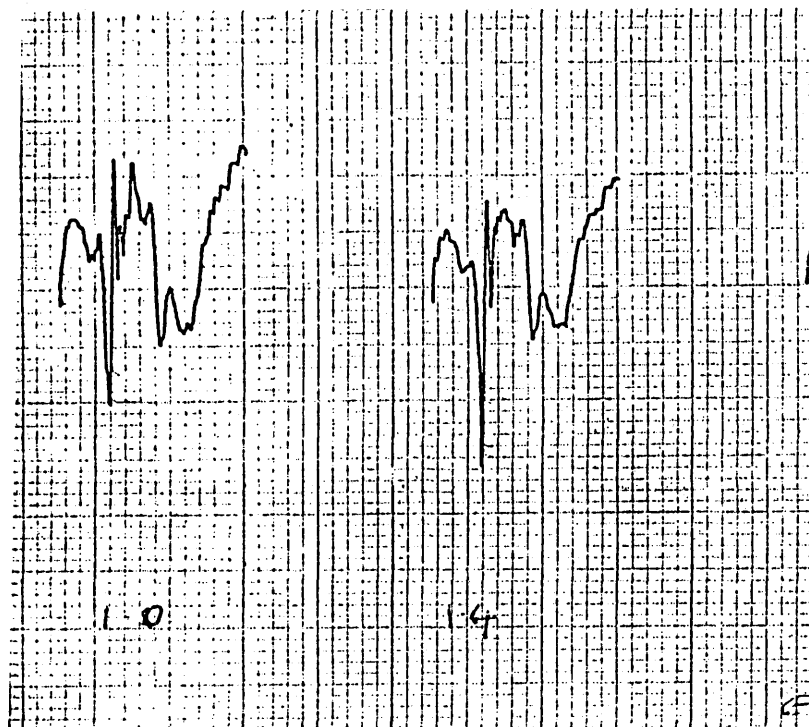
In order to determine whether phase changes can be induced mechanically rather than thermally, we can use a similar method. One further factor can be investigated by this procedure: careful study of absorbance data enables the film thickness to be monitored. By assuming constant volume, changing the length will change the film thickness and width proportionately

and hence the absorbance for a fixed beam area will also change.

#### **5.4. Absorbance measurements.**

Absorbance data was obtained from a Galaxy 6021 FTIR spectrometer equipped with a liquid nitrogen cooled Mercury Cadmium Telluride (MCT) detector and a dry air-purged sample compartment. Samples were held in a stretching frame constructed such that the thread of the screw had a 1 mm pitch. The sample chosen for measurements was the elastomer based on C3CN. The C10CN sample proved too brittle to work with, while the ring elastomer demonstrated no interesting phase behaviour besides being brittle. The C3CN elastomer has a glass transition at 0 °C and an lc to isotropic transition at 52 °C. It was hoped to measure the improvement in order on stretching. The CN stretching vibration at around 2200 cm<sup>-1</sup> was used to detect the change in orientation of the mesogens. Initially it was hoped to compare this with the Si-CH modes involving the polysiloxane which occur in the regions of 1260 , 850 and 755 cm<sup>-1</sup>. These proved to have large background absorbances making measurement errors unreasonably large. The spectra in Fig.57 relate to a sample that is unstretched followed by a sample with an extension ratio of 1.4

Fig 57. Sample unpolarised spectra for C3CN system.



The IR beam was unpolarised as at this stage we were trying to observe whether the CN and Si-CH absorbances could be clearly observed and to determine the effect of reducing the film thickness on absorption. It was anticipated that the introduction of the polariser would yield less sensitive results. Table 24 gives the data for these frequencies and extension ratios.

Table 24. Deformation data for C3CN system.

Sample : C3CN 20% cross-linked.

| Extension ratio | Peak absorbance |           | Absorbance Ratio |
|-----------------|-----------------|-----------|------------------|
|                 | CN Str          | Si-CH Str | CN/Si-CH         |
| 1.0             | 0.56            | 0.55      | 1.03             |
| 1.4             | 0.54            | 0.53      | 1.02             |
| 1.8             | 0.48            | 0.47      | 1.03             |

The main problem is the small peak amplitude for the Si-CH vibration against the high background absorption which makes accurate measurements difficult in comparison to the strong CN stretching absorption which is easily distinguishable. Also, we must consider the lack of beam polarisation at this stage. Signals that are difficult to detect without polarisation would lead us to predict difficulties with a reduced beam intensity. We therefore anticipate low signal/noise ratios for the Si-CH units which would reduce the accuracy of any measurements. Secondly, as would be expected, we observe no real change in the ratios of the absorbances as we are measuring the total rather than parallel or perpendicular polarisations (see later). We also observe that increasing the extension ratios does reduce the absorbance values and hence we can obtain information on film thickness assuming that absorption is not

sensitive to orientation. Film thickness can be analysed in an approximate way as follows. Beer's law (116) states that the absorption is proportional to the sample thickness, i.e.

$$A = E \times C \times L$$

A = Measured absorbance

E = Molar absorbance coefficient

C = Sample concentration

L = Path length

If we consider that on stretching the sample retains constant volume, then it can be shown that the new sample thickness will be proportional to the inverse square root of the new length or extension ratio.

### **5.5. Partially substituted polysiloxanes.**

In order to obtain more reliable data a new approach was needed. Ideally we would like to compare two frequencies in the same region of the spectrum. One should be associated with the mesogen and one with the network. Using samples produced so far this is not possible. However, if we have a sample where some of the backbone sites are left vacant then we can compare the CN and Si-H stretching frequencies. A sample was produced where 50% of the site were occupied by mesogens and 50% were left blank. This was found to exhibit a similar DSC to the 'normal' C3CN type elastomer with slight changes in the

transition temperatures ( $T_g - 10$  to  $50$  I). Absorbances parallel and perpendicular to the beam were then determined, using a polarised input beam, for a sample during the stretching experiment. Again it should be stressed that as the sample already exists in the liquid crystalline state at room temperature, we are only trying to detect small improvements in the ordering of the mesogens.

An example spectrum is shown in fig.58.

**Fig 58. C3CN spectrum exhibiting Si-H and CN stretching frequencies.**

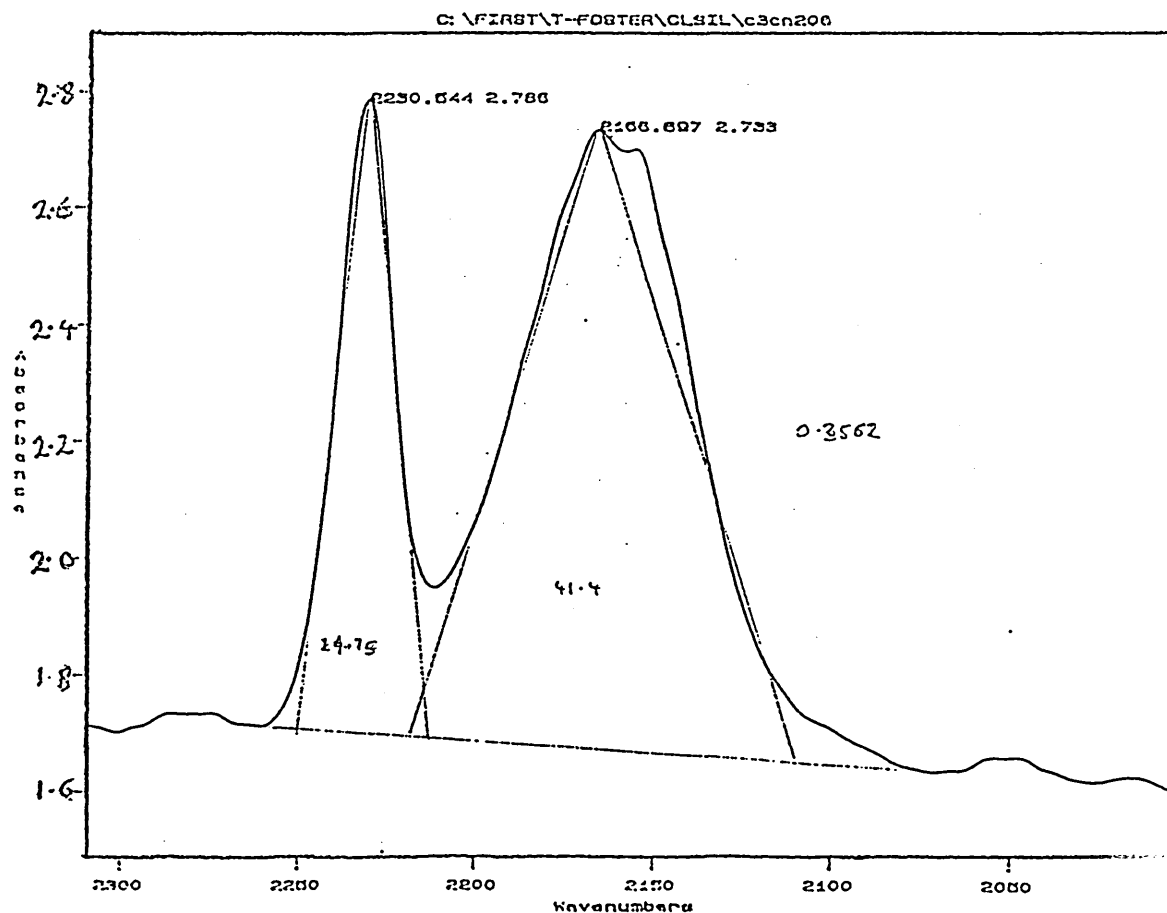


Table 25. Absorbance values for C3CN sample determined perpendicular and parallel to stretching direction.

**1. Results measured perpendicular to stretching direction**

| Extension ratio | Peak absorbance |      | Peak Area (Arbitrary units) |       |
|-----------------|-----------------|------|-----------------------------|-------|
|                 | CN              | Si-H | CN                          | Si-H  |
| 1.00            | 2.98            | 2.91 | 21.70                       | 64.07 |
| 1.26            | 2.79            | 2.74 | 19.98                       | 59.54 |
| 1.53            | 2.77            | 2.63 | 19.41                       | 58.22 |
| 1.80            | 2.83            | 2.67 | 19.42                       | 58.86 |

**2. Results measured parallel to the stretching direction.**

| Extension ratio | Peak absorbance |      | Peak area (Arbitrary units) |       |
|-----------------|-----------------|------|-----------------------------|-------|
|                 | CN              | Si-H | CN                          | Si-H  |
| 1.00            | 1.17            | 1.14 | 8.80                        | 26.21 |
| 1.26            | 1.18            | 1.15 | 11.06                       | 32.04 |
| 1.53            | 1.17            | 1.12 | 11.94                       | 33.68 |
| 1.80            | 1.12            | 1.08 | 11.78                       | 32.72 |
| 2.06            | 1.09            | 1.03 | 11.99                       | 32.64 |
| 2.34            | 1.08            | 1.01 | 12.12                       | 32.45 |
| 2.60            | 1.06            | 0.96 | 11.88                       | 31.59 |

Areas for the peaks were obtained using a curve fitting package.

The figures in Table 25 indicate small decreases in the absorption of both peaks parallel to the stretching direction accompanied by small increases in that perpendicular to the stretching direction for the cyano-unit. Assuming the Si-H units simply move with the backbone, their absorbance should only vary as a function of sample thickness and with the alignment of the backbone. We should see a small decrease in the Si-H absorbance in one direction and possibly an increase in the other direction, due to thickness / backbone alignment effects, i.e. reduced sample thickness coupled with backbone alignment in the direction observed. If stretching induces enhanced mesogen alignment in a preferred direction, we would observe larger changes in the CN absorbance relative to the Si-H absorbance. Therefore it is useful to look at the ratio of CN / Si-H measurements. (See table 26).

**Table 26. Ratio of absorbances and areas of CN/Si-H**

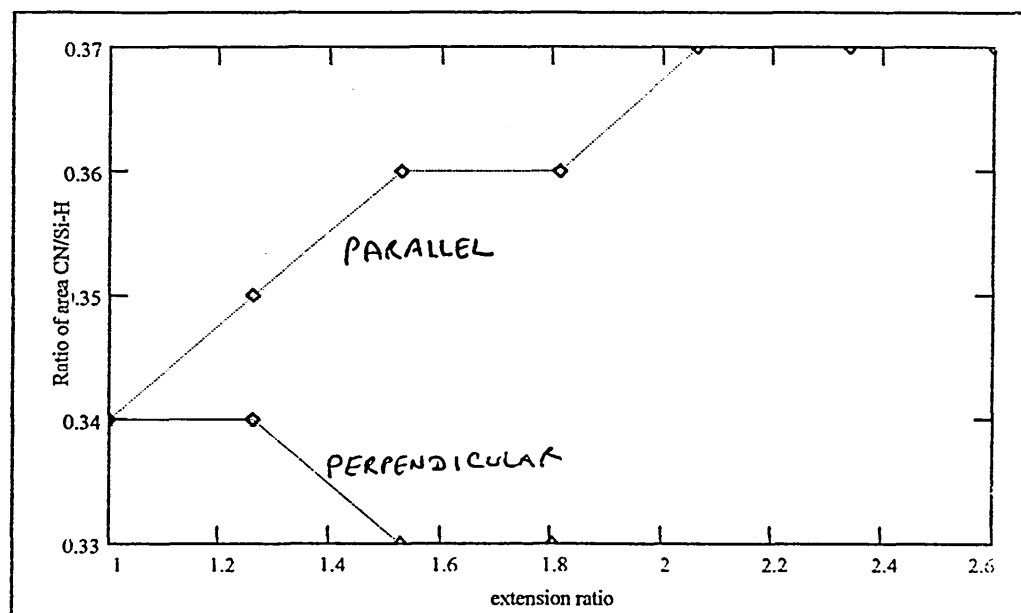
PERPENDICULAR

| Extension ratio | Ratio CN/Si-H peaks |      |
|-----------------|---------------------|------|
|                 | Absorbance          | Area |
| 1.00            | 1.02                | 0.34 |
| 1.26            | 1.02                | 0.34 |
| 1.26            | 1.05                | 0.33 |
| 1.80            | 1.06                | 0.33 |

PARALLEL

| Extension ratio | Ratio CN / Si-H Peaks |      |
|-----------------|-----------------------|------|
|                 | Absorbance            | Area |
| 1.00            | 1.02                  | 0.34 |
| 1.26            | 1.03                  | 0.35 |
| 1.53            | 1.04                  | 0.36 |
| 1.81            | 1.04                  | 0.36 |
| 2.06            | 1.06                  | 0.37 |
| 2.34            | 1.07                  | 0.37 |
| 2.60            | 1.07                  | 0.37 |

**Fig 59. Plot of Area ratios versus extension ratio for CN/Si-H stretching modes using data from table 26.**



The ratio of absorbances indicates that the alignment both parallel and perpendicular to the stretching direction is increasing slightly which is unlikely. However, if we compare areas (which yield smaller errors), we see that those parallel to the stretching direction demonstrate a small increase while those perpendicular show a small decrease. This is as expected. We predict small changes as we are studying a system that is already ordered and the increases in one direction must be compensated by decreases in a perpendicular direction.

The plot (see figure 59) clearly indicates that stretching increases the alignment of the mesogens parallel to the stretching direction. On reaching an extension ratios of 1 to 1.8 we observe a 7.4 % increase in the ratio of CN/Si-H absorbance areas for that parallel, while a drop of 2.7% is recorded for that perpendicular. Thus we are observing an enhancement of the liquid crystal alignment induced by mechanical force.

### **5.6. Observations on sample thickness.**

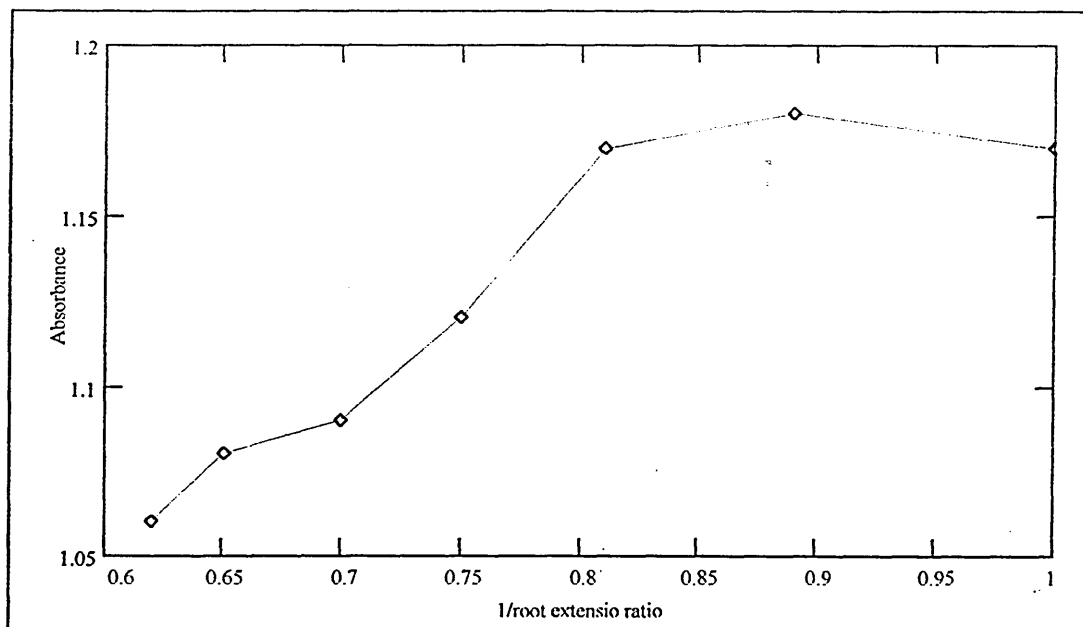
The variation in thickness as the sample is stretched is expected to be proportional to the inverse square root of the length, providing that deformation is equal in all directions and that there is no volume change. As absorbance is proportional to the thickness of the sample, it follows that this must also be proportional to the inverse square root of the sample length. Therefore, if the absorbance changes are simply a result of change in the sample dimensions,

a plot of inverse square root of extension ratio versus absorption should be a straight line, providing the sample deforms ideally. Obtaining an ideal sample is difficult due to the synthetic approach, clamping restrictions etc. Therefore we would expect our results to deviate from this. Furthermore, due to its initial ordered state, we expect our sample to exhibit signs of further ordering in the initial stages of elongation and hence we expect larger deviations at the lower extension ratios. Therefore, at the point where side chain ordering has ceased, we expect a change in the slope of the plot. The results are shown below in table 27.

**Table 27. Results for parallel absorbances of cyano units.**

| 1/root extension ratio | Absorbance |
|------------------------|------------|
| 1.00                   | 1.17       |
| 0.89                   | 1.18       |
| 0.81                   | 1.17       |
| 0.75                   | 1.12       |
| 0.70                   | 1.09       |
| 0.65                   | 1.08       |
| 0.62                   | 1.06       |

Fig 60. Plot of Absorbance v inverse root extension ratio for elastomer C3CN at 20% cross-linking. Data taken from table 27.



The plot demonstrates two separate regions. At extension ratios greater than 1.6 (relates to an inverse root extension ratio of 0.8) we observe a proportional behaviour between absorbance and inverse root extension ratio, indicating that this region corresponds to changes in sample dimensions on stretching, whilst maintaining a constant volume. For the region of extension ratios between 1.0 and 1.6 (relates to 1 and 0.8 in terms of inverse root extension ratio) the absorbance remains roughly constant. We speculate that a small ordering effect is taking

place. Mesogen alignment is improving due to the constraints imposed by the network and hence the sample volume will have to change to adopt these new conformations. Further studies would be needed to prove this unambiguously.

### Cyclic polysiloxane systems.

These systems proved difficult to isolate in high purity. While the use of Sephadex gel will separate monomers from cyclics, the choice of pore size appears to be critical. Theoretical models predicted such systems should exhibit liquid crystal behaviour due to the systems behaving essentially as a solid disc. We would therefore expect the systems with the shortest spacer group to exhibit the strongest discotic behaviour. Short spacer units will couple the motion of the mesogens and rings by limiting the number of possible conformations. For the system  $n=3$ , no liquid crystal behaviour was observed. Cyclics incorporating side chains with longer spacer units ( $n=5$ ,  $n=10$ ) did exhibit liquid crystal behaviour, although this is probably due to decoupling of the mesogen from the ring. In effect we have a unit similar to linear material with low degrees of polymerisation. Doping of pure cyclic material with excess mesogen resulted in liquid crystal behaviour, however, its exact nature was not fully determined. Further work on doped cyclic material could result in systems of extended thermal stability.

### Linear polysiloxane liquid crystals.

These materials generally behaved in accordance with published data. Short spacer units resulted in nematic types while the introduction of a longer spacer unit

resulted in smectic systems. Terminal groups with large dipole moments (i.e. CN) also yielded smectic behaviour. For materials with very long spacers ( $n = 10$ ), side chain crystallisation dominates and the observed liquid crystal behaviour is almost identical to the pure liquid crystal unit. Differences in phase behaviour between samples produced from commercially available polysiloxane and laboratory synthesised material demonstrate the need for careful polymer characterisation. Further differences due to the number of polymer precipitations during purification, highlighted the need for a larger number of precipitations than was previously thought, the accepted value now being 8 - 10 rather than 3.

### **Elastomeric material.**

Short spacer material ( $n=3$ ) behaved as predicted by Finkelmann et al (48), in that glass transitions around  $0^{\circ}\text{C}$  were generally observed for methoxy terminated mesogens. Variations in cross linking density produced conflicting evidence. We observed two effects. For high cross linking densities (around 30%), a memory effect was observed. The liquid crystal structure is locked in on initial polymerisation and subsequently lost on heating. This is generally consistent with published data. For lower cross linking densities (around 10-12%) slight increases in cross-linking appear to yield increases in the glass transition temperature. This conflicts with Finkelmann et al's work (98) on

polysiloxanes, while matching the trends observed by Barnes et al (99) on hydrocarbon species. While some error can be apportioned to the DSC instrument, this does not explain the overall trend. Further work would be required to determine the exact nature of this effect, although the most likely reasons appear to be competition between the restriction of the backbone mobility and the reduction in mesogen density. Elastomers produced incorporating long chain spacers ( $n$  is larger than 10) generally exhibited side chain crystallisation as expected. Materials produced from cyclic siloxanes appeared to yield elastomeric materials, although these were brittle in nature. Synthesis of these proved very variable and the exact conditions required could not be determined. Although these elastomers were analogous to the C3CN and C3OMe linear polymers, their phase behaviour was remarkably different. Neither of the cyclics exhibited liquid crystal behaviour, while both demonstrated remarkably low glass transition temperatures, less than  $-100^{\circ}\text{C}$ . Lack of liquid crystal behaviour was probably due to the low mesogen density, around 25%, although this is generally taken as the lower limit for polymer substitution before mesogenic behaviour is observed. The increased backbone restriction probably restricts the conformational mobility of the mesogen, thus limiting their ability to adopt a liquid crystal structure in such a dilute environment. Each sample exhibits two very low glass transitions, one due to the ring and the other due to the cross-linking unit.

The low temperature of these transitions is the surprising aspect of this work. This would imply that it may be possible, through combinations of different mesogens and/or larger rings, to produce liquid crystalline materials with very low glass transition temperatures. Investigations on sample deformation provided evidence of enhanced order. Samples used already existed in the liquid crystal state. The application of force to the sample appeared to yield increased mesogen alignment up to extension ratios of about 1.8. Further extensions produced observations consistent with simple variations in sample thickness.

1. Reinitzer, F. *Monatsh. chem.*, 9, 421 (1888)
2. Lehmann. O.Z., *Phys. Chem.*, 4, 462 (1889)
3. Chandrasekar. S, 'Liquid Crystals' , Cambridge University Press, Chapter 1, (1980)
4. Chandrasekar. S, 'Liquid Crystals' , Cambridge University Press, Chapter 2, (1980)
5. Gray, G.W., Winsor, P.A., in 'Liquid Crystals and Plastic Crystals', eds. Gray and Winsor, 1, Ellis Horwood, Chichester, England, (1974).
6. Barrow, G.M., *Physical Chemistry*, McGraw-Hill , Chapter 5, (1988).
7. Gray, G.W., Goodby, J.W., *Smectic Liquid Crystals*, Leonard Hill, (Blackie) Glasgow and London, Chapter 1, (1984.)
8. Gray, G.W., Goodby, J.W., *Smectic Liquid Crystals*, Leonard Hill, (Blackie) Glasgow and London, Chapter 2, (1984.)
9. Finkelmann, H., Benthack, H., Rehage, G., *Journal de Chimie Physique.*, 1, 80, (1983).
10. Kreuder, W. and Ringsdorf, H., *Makromol. Chem. Rapid Commun.*, 4, 807, (1983).
11. Gresham, K.D., McHugh, C.M., Bunning, T.J., Crane, R.L., Klei, H.E., Samulski, E.T., *J. Polym. Sci., Polym. Chem.* 32, 2039, (1994).
12. Wilfong, R.E., Zimmerman, J., J, *Appl. Polm. Sci.*, 17, 2039, (1973)
13. Doty, P., Bradbury, J.H., Holtzer, A.M., *J. Am. Chem. Soc.*, 78, 947, (1956).
14. Wilkes, G.L., *Mol. Cryst. Liq. Cryst.* 18, 165, (1972).

15. Cherdron, H., Makromol. Chem., Macromol. Symp. 33, 85-89, (1989).
16. Jackson, W. J. Kuhfuss, H. F., J. Polym. Sci., Polym. Chem, 14, 2043, (1976).
17. Chung, T., Calundann, G. W., East, A. J., 'Liquid Crystal Polymers and their Applications' in 'Handbook of Polymer Science and Technology', 3, 83, Marcel Dekker, New York and Basel, (1989).
18. Blumstein. A, (ed). Mesomorphic order in polymers and polymerisation in liquid crystal media, asc, Symp. Ser. 74. American Chemical Society, Washington D.C. (1980).
19. Shibaev, V. P, Plate, N. A., Polym. Sci. USSR, 19, 1065. (1977).
20. Finkelmann. H, Luhmann, B., Rehage, G. and Stevens. H, in Liquid Crystals and Ordered Fluids, Vol 14. eds Griffin, A. C. and Johnson, J. F., Plenum, New York, 715. (1984)
21. West, R., J. Chem. Edu., Organosilicon Chemistry, Parts 1 and 2, 57, 165, 334. (1980)
22. Gray, G. W. , Side Chain Liquid Crystal Polymers., Blackie, Glasgow, Chapter 4, 106, (1989).
23. Stevens, H., Rehage, G. and Finkelmann, H., Macromolecules, 17, 85, 1. (1984)
24. Hawthorne, W. (1986), PhD thesis, University of York, U.K. From Side Chain Liquid Crystal polymers., Blackie, Glasgow, Chapter 4, 118, (1989)
25. Shibaev et al from Finkelmann, H., Rehage, G., Advances in Polymer Science, 60/61, 99-192, (1984).
26. Gemmell, P. A., Gray , G. W., Lacey, D., Alimoglu, A. K. and Ledwith, A., Polymer, 26, 615. (1985)

27. Hartmann, F.L, Finkelmann, H., Makromol. Chem. 191, 2707-2715 (1990).
28. Keller, P., Hardouin, F., Mauzac, M., Achard, M.F., Mol. Cryst. Liq. Cryst., 155, 171-178. (1988).
29. Keller, P; Int. Conf. On Liquid Crystal Polymers, Bordeaux, Abstr 20P I.
30. Hassel. F, Merr, R.P., and Finkelmann, H., Makromol. Chem., 188, 1597. (1987)
31. Zhou, Q.F., Li.H.M. and Fing, X.D., Macromolecules, 20, 233. (1987)
32. Diele, S., Oelsner, S., Kuschel, F., Mol. Cryst. Liq. Cryst, 155, 399-408. (1988)
33. Talroze, R.V., Shibaev, V.P., Sinitzyn, V.V., and Plate, N.A., Polymeric Liquid Crystals, Edited by Alexandre Blumstein, Vol 28, 331. (1985)
34. Bunning, T.J, Kreuzer, F-H, TRIP, Vol 3, 10, 318 (1995)
35. Richards, R.D.C et al. J. Chem. Soc., Chem. Commun., 95. (1990)
36. Edwards, C.J.C., Rigby, D., Stepto, R.F.T., Dodgson, K., Semlyen, J.A., Polymer, 24, 391. (1983)
37. Everitt, B.R.D, Care, C.M., and Wood R., Mol Cryst. Liq. Cryst., 153, 55. (1987)
38. Hahn, B. and Percec, V., Macromolecules 20, 2961. (1987)
39. Richards, H. Mauzac., Tinh, N., Sigaud, G., Achard, M. Hardovin, F. and Gasparove, H. Mol. Cryst. Liq. Cryst., 1155, 141. (1988)
40. Kreuzer, F.H., Andrejewski, D., Huss, W., Haberle, N., Riepl, G., and Spes, P., Mol. Cryst. Liq. Cryst., 199, 345-378. (1991)

41. Mark, J.E., *J.Chem.Educ.*, 58, 898. (1981)
42. Mark, J.E., *Makromol.Chem.*, Suppl.2, 87-97 (1979)
43. Flory, P.J., 'Principles of Polymer Chemistry', Cornell University, Ithaca, New York, (1953).
44. Warner, M., Wang, X.J., *Macromolecules*, 24, 4932-4941, (1991).
45. Mark, J.E., *Matter. Sci. Monogr.*, 26, 336-62, (1985).
46. Mooney, M., *J.Appl.Phys.*, 19, 434, (1948).
47. Rivlin, R.S., *Phil.Trans.R.Soc.London, Ser.A*, 241, 379, (1948).
48. Finkelmann, H., Kock, H.J. and Rehage, G., *Makromol. Chem. Rapid Commun.*, 2, 317. (1983)
49. Mandelkern, L., *Crystallisation of Polymers*, McGraw-Hill, New York. (1964)
50. Treloar, L.R.G., 'The Physics of Rubber Elasticity', 3rd ed., Clarendon, Oxford, (1975).
51. Ronca, G. and Allegra, G., *J.Chem.Phys.*, 63, 4990. (1975)
52. Langley, N.R. and Ferry, J.D., *Makromolecules*, 1, 353. (1968)
53. deGennes, P.G., in *Polymer Liquid Crystals*, Academic Press, New York. (1982)
54. Finkelmann, H., Kock, H.J., Gleim, W., Rehage, G., *Makromol.Chem., Rapid Commun.*, 5, 287-293 (1984).
55. Finkelmann, H., Gleim, W., Hammerschmidt, K., Schatzle, J., *Makromol.Chem., Macromol.Symp* 26, 67, (1989).
56. Finkelmann, H., *Side Chain Liquid Crystal Polymers.*, Chapter 10, 287. Blackie, Glasgow, (1989).

57. Finkelmann, H., Gleim, W., Kock, H.J., Proc Intunpac, Macromol. Symp., 28, 556, (1982).
58. Mandelkern, L., Crystallisation of Polymers. McGraw-Hill, New York. (1964)
59. Treloar, L.R.G., 'The Physics of Rubber Elasticity', 3rd ed., Clarendon, Oxford, (1975).
60. Ronca, G. and Allegra, G., J.Chem.Phys., 63, 4990. (1975)
61. Langley, N.R. and Ferry, J.D., Makromolekules, 1, 353. (1968)
62. deGennes, P.G., in Polymer Liquid Crystals, Academic Press, New York. (1982)
63. Schatzle, J., Finkelmann, H., Mol.Cryst.Liq.Cryst., 1987, 142, 85-100. (1987)
64. Pinsl, J., Brauchle, Chr., Kreuzer, F., Journal of Molecular Electronics, 3, 9-13 (1987)
65. Wendorf, J.H., Eich, M., Mol.Cryst.Liq.Cryst., 169, 133-166, (1989).
66. Shibaev, V.P., Kostromin, S.G., Plate, N.A., Ivanov, S.A., Vetrov, Yu.V., Yakovlev, I.A., Polym. Commun. 24, 364 (1983)
67. Cockett, S. PhD Thesis, Sheffield Hallam University. (1992)
68. Finkelmann, H., Rehage, G., Makromol. Chem., Rapid Commun. 1, 31-34 (1980).
69. U.S. Pat. 2491843., Gen. Electric (1946).
70. Dow Chemical Company, U.S. Pat 2,46XX (1945).
71. Crivello, J.V., Conlon, D.A., and Lee, J.E., J.Polymer Sci., Part A: Polym Chem, 24, 1197-1215 (1986).

72. Hurd, D.T., J. Am. Chem. Soc., 77, 2998-3001 (1955).
73. Gemmell, P., Gray, G., Lacey, D., Mol. Cryst. Liq. Cryst. 94, 343 (1985)
74. Ringsdorf, H., Scheller, A., Makromol. Chem. Rapid Commun. 3, 557. (1982)
75. Ringsdorf, H., Schmidt, H-W., Eilingsfeld, H., Eitzbach, K.H. Makromol. Chem. 188, 1355. (1987)
76. Spier, J., Webster, J., Barnes, G., J. Amer. Chem. Soc. 69, 188. (1957)
77. Nestor, G., White, M., Gray, G., Lacey, D., Toyne, K., Makromol. Chem. 188, 2759-2767 (1987).
78. Apfel, M.A., Finkelmann, H., Janini, G.M., La, R.J., Lukmann, B.H., Price, A., Roberts, W.L., Shaw, T.J., Smith, C.A., Anal. Chem. 57, 651 (1985).
79. Spier, J.L., Zimmermann, R., and Webster, J.A., J. Am. Chem. Soc., 78, 2278, (1956).
80. Spier, J.L., Webster, J.A., and Barnes, G.H., J. Am. Chem. Soc., 79, 974, (1957).
81. Finkelmann, H., Rehage, G., Makromol. Chem., Rapid Commun. 1, 32-34 (1980).
82. Lipowitz, J., Bowman, S.A., J. Org. Chem., 38, 162 (1973).
83. Akhrem, I.S., Christovalova, N.M., Vol'pin, M.E., Russ. Chem. Rev. (Engl. Transl.), 52, 542 (1983).
84. Finkelmann, H., Kiechle, U., Rehage, G., Mol. Cryst. 94, 343 (1983).

85. Gemmell,P.A., Gray,G.W., Lacey,D., Mol.Cryst. Liq Cryst. 102,43 (1984).
86. Bunning,T.J.,Samulski,E.T.,Adams,W.W.,Crane,L., Mol. Cryst. Liq. Cryst., 231, 163-174.(1993)
87. Hahn,B.,Percec,V.,Mol.Cryst.Liq.Cryst.Inc.Nonlin.Opt. 157, 125. (1988)
88. Pinsi,J.,Brauchle,C.,Kreuzer,F.H., Journal of Molecular Electronics, 3 , 9-13 (1987)
89. Birecki,H.,Naberhuis,S., Kahn,F.J., SPIE Proc.420, 194 (1983).
90. Luckhurst,G.R., Romano,S., Proc. R. Soc. London, A, 373, 111-130, (1980).
91. Wright,P.V., Semlyen,J.A., Polymer, 11, 462 (1970).
92. Finkelmann,H.,Rehage,G.,Makromol.Chem., Rapid Commun.1,733-740(1980)
93. Gray,G.W., Hawthorne,W.D., Hill,J.S., Lacey,D.,Lee,M.S.K., Nestor,G., White,M.S., Polymer,30, June (conference issue), 1989.(applications)
94. Nestor,G., White,M.S., Gray,G.W., Lacey,D.,Toyne, K.J., Makromol.Chem.,188,2767 (1987).
95. Ringsdorf,H.,Schneller,A., Makromol.Chem., Rapid Commun. 3, 557-562 (1982).
96. Coles,H.J.,Physics and Chemistry of Polymeric Liquid Crystals, R.Soc.Chem.-Spec Publ,60,97-115,(1986).
97. Percec,V.,Pugh,C.,Side Chain Liquid Crystal Polymers,Chapter 3,

98. H.Finkelmann , H.J. Kock, G. Rehage., Makromol. Chem., Rapid Commun. 2, 317-322, (1981).
99. Barnes,N.R.,Davis,F.J.,Mitchell,G.R., Mol.Cryst.,168, 13-25, (1989).
100. Legge,C.H.,Davis,F.J.,Mitchell,G.R.,J.Phys.II France, 1253-1261, (1991).
101. Davis, F.J., Mitchell, G.R., Polymer Commun. 28,8, (1987).
102. J., Kaufhold W., Finkelmann H., Makromol.Chem. 190, 3269 (1989).
103. Zentel R.,Liquid Crystal 1, 589, (1986).
104. Finkelmann,H., from 'Side chain Liquid Crystal Polymers', Ed C.B McArdle,Blackie , chapter 10.(Glasgow 1989)
105. Kuhn,W.,Grun,F.,Kolloid Z. 101,248,(1942).
106. Zentel,R., Reckert,G., Makromol. Chem. 187, 1915-1926 (1986).
107. Schatzle,J., Finkelmann, H.,Mol.Cryst.Liq.Cryst., 1987, 142, 85-100. (1987)
108. Hawthorne,W., Trends in Polymer Science,3,No.5., 173-174, (1995).
109. Warner, M., Gelling,K.P.,J.Chem.Phys.,88,(6),4008-4113, (1988).
110. Hammerschmidt,K.,Hinkelmann,H.,Makromol.Chem. 190, 1089-1101,(1989).
111. Zentel,R.,Angew.Chem.Int.Ed.28, 1407,(1989).

112. Davis, F. J., *J. Mater. Chem.*, 3(6), 551-562, (1993).
113. Zentel, R., Benalia, M., *Makromol. Chem.*, 188, 665, (1987).
114. Kaufhold, W., Finkelmann, H., Brand, H. R., *Makromol. Chem.*, 192, 2555, (1991).
115. Brauchler, M., Oeffel, C., Speiss, H. W., *Macromol. Chem.* 192, 1153-1176, (1991).
116. Spectroscopic Methods in Organic Chemistry, Williams, D. H., Flemming, I., McGraw-Hill, London, Chapter 2, 7, (1966)
117. Finkelmann, H., Ringsdorf, H., Wendorf, J. H., *Makromol. Chem.* 179, 273, (1978)
118. Puhknarevich, V. B., Trofimov, B. A., Kopylova, L. I., Voronkov, M. G., *Zh. Obshch. Kim.* 43, 2691 (1973). (From Gray, G. W., Lacey, D., Nestor, G., White, M., *Makromol. Chem., Rapid Commun.* 7, 71-76 (1986))